eman ta zabal zazu
Universidad del País Vasco
Euskal Herriko Unibertsitatea

Distribution of stem cells inside induced gliomas by Ethyl-nitrosurea

Front page image: Immunofluoresce of Nestin (green), GFAP (red) and Hoechst (blue) of cells with different morphologies in ENU-induced gliomas

Doctoral Thesis

Álvaro García Blanco

2014

Que difícil es resumir en un par de páginas todo lo que me gustaría expresar y agradecer sobre estos últimos cinco años de mi vida que además coincide que he estado trabajando en esta tesis…

En primer lugar dar las gracias al departamento de Neurociencias por haberme permitido haber llevado a cabo esta tesis. Gracias a José Vicente por darme la oportunidad de empezar lo que ahora es este trabajo y haberme enseñado todo lo que significa la ciencia.

Agradecer a todos los miembros de mi grupo (tanto la parte doctora; Susana, Harkaitz, Enrike) como los compañeros que empezaron como becarios (Cata, Naiara, Irantzu, Hodei) todo lo que me han enseñado y todos los momentos que hemos pasado.

A lo largo de estos años se comparten muchas cosas con la gente que te rodea en el trabajo, y yo empecé con el "minigrupo" del Master (Fatima, Ianire y Fede… que momentos en esas clases de Master!). Por supuesto agradecer también a todos los integrantes de los otros grupos del departamento con los que he compartido todos los días lo bueno y lo malo de trabajar juntos haciendo una tesis. Gracias a todos por estar ahí y haber hecho de este trabajo algo mucho, mucho más ameno (sin ningún orden en particular Belen, Barbara, Laura, Anita, Ana, Saioa, Silvia, Manu, Nuria, Asier, Joana, todos los "zamudianos" y todas las nuevas incorporaciones…).

Un recuerdo también para todos los compañeros (y ante todo amigos) de Farmacia y mi estancia en Vitoria durante la carrera (Xabi, Joserra, Alvarito, Amaia…).

Ein grosser Grüsse und vielen Danken an Michel, Patrick und das ganze AG Mittelbronn (Klaus, Lukas, Conny, und alle andere…) die mich ein verschiedenes Blick über die Onkologie und die Förschung beigebracht haben. Danke für die viele Plauderei über das Gehirn, Gliomas, Fussball, Politik, Musik usw. Vielen Dank auch an alle andere deutsche Kumpels die

so gemacht haben, dass meine 3 Monaten in Frankfurt so schnell geschehen haben.

Durante estos años han sucedido un montón de cosas buenas y otras no tanto (tanto laboralmente como fuera del trabajo), pero en todo momento he estado rodeado por un grupo de amigos que me ha ayudado en los malos momentos y con los que he celebrado los buenos (tanto propios como ajenos). En estos momentos es imposible no acordarse de mi "cuadrilla" de ex-nadadores (Ale Fadura!) Bilbo, Santa, Pani, Lete, Kurtis y Largo. Cuando empecé esta tesis muchos estabais todavía en la carrera, y mirad todo lo que nos ha pasado desde entonces!! A pesar de que no reconozcan que una tesis es un trabajo tan bueno como cualquiera, (y mucho mejor que algunos!!) a partir de ahora tendrán que llamarme Doctor Bárbaro (juajua).

Y llegando al final, la familia. Mi familia que me ha ayudado tanto y me ha enseñado a ser como soy y de la que estoy súper orgulloso. Mis abuelas Nati y Juani, mis ti@s, prim@s... (no pongo todos los nombres para no hacer una lista muy larga, pero daros TOD@S por aludidos) y sobre todo mi madre, mi padre y mi hermano. Este trabajo es en parte resultado suyo, por haberme educado, enseñado, soportado, aliviado y alegrado en tantas ocasiones. Así que parte de esta tesis es obra vuestra, disfrutadla.

Y por ultimo agradecer a la persona que más ha hecho posible esto y que ha estado a mi lado durante todo este tiempo. Esti, que me has acompañado a lo largo de estos años y has estado conmigo en los buenos momentos y en los malos. Gracias por haberme ayudado tanto y por haberme animado, alegrado y distraído cuando era necesario. Muchas gracias por ser como eres.

“Nothing in life is to be feared, it is only to be understood. Now is the time to understand more, so that we may fear less"

Marie Curie

The most exciting phrase to hear in science, the one that heralds new discoveries, is not “Eureka"', but “That's funny …"

Isaac Asimov

Index

Abbreviators

ABC	Avidin-biotin complex
BBB	Blood-brain-barrier
BSA	Bovine serum albumin
BrdU	Bromodeoxyuridine
CI	Confidence interval
CNS	Central nervous system
CSC	Cancer stem cell
DAB	Diaminobenzidine
DNA	Deoxyribonucleic acid
EBA	Endothelial barrier antigen
ENU	Ethyl-nitrosourea
EPC	Endothelial precursor cell
EPO	Erythropoietin
GAS	General adaptation syndrome
GBM	Glioblastoma multiforme
GluT	Gluocose transporter
GFAP	Glial fibrilary acidic protein
H/E	Haematoxylin/eosin
HIF	Hypoxya-inducible factor
HO	Heme oxygenase
iNOS	Inducible nitric oxide synthase
GFAP	Glial fibrillary acídica protein
GSC	Glioma stem cell
LEA	Lycopersicon esculentum agglutinin
MAP	Microtubule-associated protein
MPNST	Malignant peripheral nerve stealth tumours
MRI	Magnetic resonance imaging
NF	Neurofilament
NSC	Neural stem cell
OPN	Osteopontin
PDGF	Plaquetet derived growth factor

PDGFR	Plaquetet derived growth factor receptor
PBS	Phosphate saline buffer
PFA	Paraformaldehyde
SVZ	Subventricular zone
TGF	Transforming growth factor
VEGF	Vascular endothelial growth factor
VEGFR	Vascular endothelial growth factor receptor
WHO	World health organisation

I.-Introduction

1.1-Gliomas and stem cells

1.1.1-Gliomas

Gliomas are primary diffuse infiltrating tumours of the Central Nervous System (CNS) that originate from glial cells. They are classified depending on their histological appearance and on their malignancy degree.

Based on their origin they are classified into: astrocytomas when they arise from astrocytic cells; oligodendrogliomas when they originate from oligodendroglial cells; they can also have a mixed component of oligodendrocytes and astrocytes which are known as oligoastrocytomas; and finally there are ependydomas, constituting another type of glioma, most probably deriving from ependymal cells and radial glial cells (Taylor et al., 2005).

Based on their degree of malignancy there are low-grade gliomas and high-grade gliomas (astrocytomas, oligodendrogliomas or mixed gliomas). Low-grade gliomas are tumours with few malignant characteristics, but the majority of them develop with the time (between 2 and 5 years on average) and end as more malignant tumours. They are classified as World Health Organization (WHO) grade II tumours and are diffuse infiltrating gliomas with a predominance of either astrocytic cells or cells resembling oligodendrocytes. Mixed low-grade gliomas are called oligoastrocytoma (WHO grade II), and in these tumours there is a mixture of cells and histopathological features resembling oligodendrogliomas and astrocytomas.

High grade gliomas are the most frequent form of gliomas and are classified as anaplastic astrocytoma, anaplastic oligodendroglioma or anaplastic oligoastrocytoma (all of them with WHO grade III). The highest grade of gliomas, knowns as glioblastomas multiforme (GBM), is the most frequent form of them (>60%) and is called (Lantos et al., 2002, Ohgaki and Kleihues, 2005). They are assigned to WHO grade IV. Glioblastomas are frequently located in the subcortical white matter of the cerebral hemispheres. They can develop as “de novo” or “secondary” tumours

depending on their biological origin and clinical features. The “de novo" GBMs manifest in short time (less than three months) (Ohgaki et al., 2004) without precursor lesions, while “secondary GBMs" develop from lower grade gliomas. “De novo" glioblastomas account approximately for 90% of all GBM and these patients are usually older than those who develop “secondary glioblastomas" (Ohgaki and Kleihues, 2007).

Histologically, GBMs are anaplastic tumours with pleomorphic cells, nuclear atypias, multiple mitoses (sometimes aberrant), prominent microvascular proliferation and necrotic zones. Glioblastomas are among the most vascularised tumours and their vasculature is one of the most important subjects in the study of gliomas (Hardee and Zagzag, 2012). Microvascular proliferations are a typical hallmark of glioblastomas. They consist of multilayered endothelial cells, even though recent research suggest that they consist more likely of pericyte proliferations (Girolamo et al., 2013), that can appear as glomeruloid tufts.

Glioblastomas represent one of the most treatment-refractory primary brain tumours. Even though they are not very numerous, averaging just between 3-5 cases per 100.000 per year in the most developed countries (Lantos et al., 2002; Jovcezka et al., 2013), their mortality and mean survival time are indicators of this devastating disease (Ostrom et al., 2014). The mean patient age at first glioblastoma occurrence is between 62-64 years (Ostrom et al., 2013), but the range of incidence is between 45 and 75 years (Ohgaki et al., 2004). Regardless of advances in surgical and imaging techniques, GBM remains as one of the most lethal types of tumour, due to their invasive growth behaviour into normal brain parenchyma and their resistance to standard therapies

The treatment for GBM is surgical resection, radiotherapy and/or chemotherapy. Despite progress in these fields, only 20% of patients survive longer than one year (according to studies by Ohgaki et al., 2004; Ohgaki and Kleihues, 2005), even though some modern series have reported 29% survival rate over 2 years (Ho et al., 2014). In clinical trials the

mean survival time of glioblastomas is around 14 months (Ahmed, 2014) with radiotherapy and concomitant temozolomide. Nowadays, clinical trials with anti-angiogenic factors like bevacizumab (alone or in combination with other treatments like irinotecan) show good response in patients (Jovcevska et al., 2013) and improve the progression-free survival time (Omuro and DeAngelis, 2013), but this could be partially due to the fact that clinical trials tend to recruit younger patients with good quality of life (indicated by the Karnofsky index).

1.1.2-Stem cells

The first indications of the existence of stem cells in the brain were found during de 60s (Altman and Das, 1966). The distribution of stem cells was observed by tritiated thymidine in neonate rats in the hippocampus and olfactory bulb, and they were named neural stem cells. Nowadays it is well accepted that there are three areas in the adult brain of mammals which contain neural stem cells: the gyrus dentatus of the hippocampus, the subventricular zone (SVZ) (Eriksson et al., 1998; Doetsch et al., 1999) and the olfactory bulb (Lois and Alvarez-Buylla, 1994; Whitman and Greer, 2009).

Neural stem cells (NSC) are characterised by being undifferentiated cells, having the capacity to differentiate to neurons, astrocytes and oligodendrocytes (Alvarez-Buylla and García-Verdugo, 2002) and to proliferate for an extended time period. Neural stem cells also have the ability of self-renewal (Stem Cells: Scientific Progress and Future Research Directions. Department of Health and Human Services. June 2001) and can form neurospheres in vitro (Reynolds and Weiss, 1992).

NSCs have the ability to infiltrate and migrate to different brain areas after injection in nude mice brains (Tamaki et al., 2002), and due to this, stem cells are being investigated for use as the basis of a therapy to regenerate tissue in pathologies like neurodegenerative diseases. Besides their promising potential to become an important tool in regenerative

therapy, they are also associated with tumourigenesis and invasiveness (Nadig, 2009).

The concept of cancer stem cell (CSC) was firs reported in 1977 by Fidler and Kripke in melanomas. Cells of this type were experimentally described for the first time in leukaemia patients' blood and isolated for the first time in 1997 by Bonnet and Dick (Bonnet and Dick, 1997). Tumour stem cells, later also called tumour initiating cells because of their tumourigenic potential, have been defined as a subpopulation of neoplastic cells with characteristics typical of somatic stem cells (self-renewal as well as the capacity to generate all the tumour cell types). It is hypothesised that tumour stem cells gain these characteristics as an adaptation to the tumoural microenvironment, but their origin remains unclear. Recent research has demonstrated the relation between stem cells and cancer stem cells; Holland (2001) suggested that cancer stem cells could develop from altered stem cells. Both cellular types share the previously-mentioned characteristics, as well as many cell signalling pathways such as the Bcl-2, Sonic hedgehog (Shh) and Wnt signalling cascade (Reya et al., 2001). Both types of stem cells also share common markers like CD133, Nestin (Dahlstrand et al., 1992) and Sox2 transcription factor (Gangemi et al., 2009).

Despite all the similarities between stem cells and tumour stem cells, there are also differences between them, such as expression of differentiation markers, chromosomic alterations and higher tumourigenic capacity of the tumour stem cells (Hadjiypanis and Van Meir, 2009). Many alterations that have been described can lead stem cells to cancer stem cell formation such as overexpresion of Notch and Akt (Takebe and Ivy, 2010) and activation of p53 (Germano et al., 2010), among others.

Before thediscovery of CSCs, tumour development was explained by the "stochastic theory". This theory assests that all neoplastic cells are clones from a single cell and all of them have the same genetic alterations

(Hadjiypanis and Van Meir, 2009). With the discovery of the cancer stem cells, new hypotheses were developed such as the "hierarchical model", where the stem cell status is irreversible and CSCs sustain the tumour growth, just like their normal tissue stem cell counterparts. Another difference is that in the "stochastic theory", all the tumoural cells have the same tumourigenesis capacity, whereas in the "hierarchical model", only a small subset of tumour cells (the cancer stem cells) are able to reproduce the tumour.

Nowadays, another model is gaining traction, the "plasticity model". This model assumes that only a few cancer cells have adapted to the tumour environment and are capable of starting the tumourigenic process and guide the tumoural growth (Shen et al., 2008), that is, of behaving as CSCs. The difference with the "stochastic model" is that the characteristics of stemness gained by the CSCs and the inheritability of these characteristics do not remain constant in the same cell population. The CSCs can differentiate and dedifferentiate depending on the stimuli produced by the tumoural microenvironment.

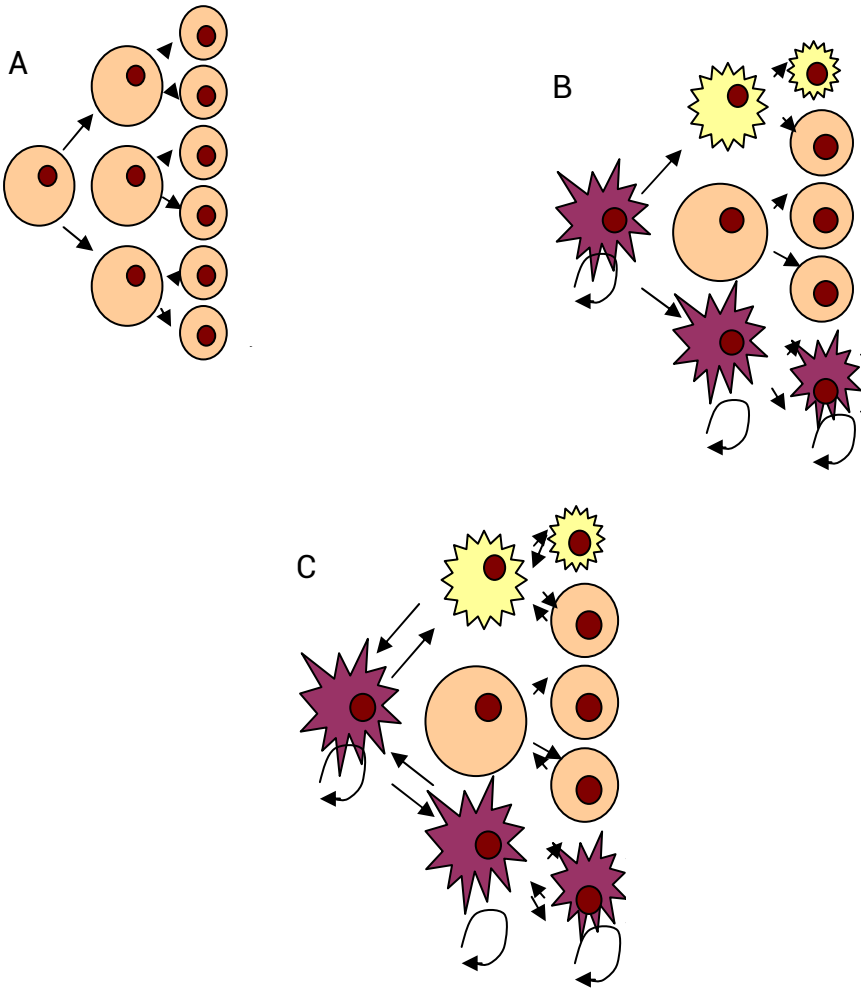

Figure 1: Different schemes showing different theories that could explain the cancer growth.
A) Stochastic theory; all the tumoural cells are clones of an original cancer cell. **B)** Hierarchical theory; one subpopulation of cells lead the tumour growth. The tumoural cells status is irreversible. **C)** Plasticity theory; the stemness status of the tumoural cells is reversible and depends on the microenvironment.

1.1.3-Cancer stem cells and glioma

In oncology, and especially in brain gliomas, the presence of stem cells has been linked to bad patient prognosis. It was not until 1992 that Dahlstrand and collaborators (Dahlstrand et al., 1992) identified cancer

stem cells in glial tumours. As previously described, CSCs and neural stem cells share many characteristics, but they also show different surface marker expression and tumourigenic capacity. These cells could generate a glial tumour when injected into nude mice brains (Galli et al., 2004).

Recent reports show that CSCs have enhanced resistance to radiation, thanks to more efficient DNA repair machinery via protein kinase phosphorilation Chk1 and Chk2. On the other hand, CSCs show resistance to chemotherapeutic drugs through overexpression of membrane transporters that pump the drugs out of the cell (Donnenberg and Donnenberg, 2005).

Due to their chemo and radio resistance and their high invasiveness capacity, it is known that they play a pivotal role in the recurrence of glial tumours after therapy and they are also believed to be responsible for the infiltration and recurrence of glioblastomas (Schiffer et al., 2014). As a result, CSCs are now viewed as possible therapeutic targets.

1.1.4-Cancer stem cells markers and distribution

Despite recent efforts trying to identify the tumour stem cells, no specific marker has been identified so far for this cellula subtype. However, a wide variety of markers have been proposed to identify these cells:

-Nestin, a protein found in neural stem cells in the SVZ, is a marker of neuroepithelial stemness (Jang et al., 2004). Nestin is an intermediate filament that is expressed in progenitor neural cells during neural development. In adults, Nestin is expressed mainly in the SVZ. Many pathologic conditions can induce Nestin to be overexpressed, like ischemia, inflammation or neoplasias (Holmin et al., 1997, Jang et al., 2004). Nestin has been described as a marker of CSCs in astroglial tumours (Singh et al., 2003), indicating undifferentiated states and degree of malignancy (Schiffer et al., 2010), but it is not specific for cancer stem cells (Hadjipanayis and Van Meir, 2009). Nestin expression has been described as appearing from the first stages in glioma models (Jang et al.,

2004) and its expression is linked to the glioma grade and has been observed in tumour endothelial cells, as stated in previous reports (Ehrmann et al., 2005). However, Nestin expression has also been reported in CNS after different types of injure, such as seizure, traumatic injure or ischemia (Schmidt-Kastner and Humpel, 2002).

-CD133 is a transmembrane glycoprotein marker for NSCs that is expressed in undifferentiated cells in the early postnatal stage, and is also present in glioma stem cells (Dell'Albani, 2008). CD133 positive cells have also been observed in different types of tumour (Schiffer et al., 2010) and it is currently the most reliable marker for CSCs, even though there are still controversies about it. In gliomas, it has been described in the malignant stages (Christensen et al., 2008). CD133+ cells have tumourigenic capacity (Schiffer et al., 2010) and its expression has been related to bad prognosis (Zeppernick et al., 2008).

Other markers that are not specific for stem cells but are used for the study of stem-like cells (in CNS tumours) are:

-**Osteopontin (OPN)** is a member of the SIBLING family (Small Integrin-Binding LIgand N-linked Glycoprotein) and is a phosphoprotein related to the proliferation and migration of neural stem cells (Yan et al., 2009, Kalluri and Dempsey, 2012). It has been associated in gliomas to a bad prognosis (Jang et al., 2006) and its overexpression has also been related with angiogenesis and parenchyma invasion (Jan et al., 2010).

-The **Notch** family of transmembrane receptors comprises Notch-1, -2, -3 and -4. Notch signalling is essential for the maintenance of neural stem cells and Notch genes are widely expressed during embryonic development (Dell'Albani, 2008). Notch signalling has also been referred to as a ''gatekeeper against differentiation" (Artavanis-Tsakonas, 1999). Notch expression has been described in human tumours and tumour models (Jang et al., 2000) and specifically Notch-1 seems to play a critical role in tumourigenesis, besides of being overexpressed in human gliomas (Purow et al., 2005, Shih and Holland, 2006).

There are other markers like GFAP, Neural-tubulin, Neurofilament O4 or Noggin that have been linked to CSCs (Dell'Albani, 2008), but none of them is a specific marker.

CSCs in tissues have been reported as being located around the tumoural vasculature. Calabrese and collaborators described in 2007 a subpopulation of Nestin positive-cells in association with the vascular endothelium. They also observed that cancer stem cells were found to secrete elevated levels of VEGF (vascular endothelial growth factor), which was induced by hypoxia (Calabrese et al., 2007) as it will be explained in paragraph *1.1.6 CSCs and hypoxia.* Later, Christensen and collaborators in 2008 described the existence of CD133+ cells around tumoural vasculature of human gliomas. It has been proposed that CSCs are located in "niches" that allow them to survive and maintain their undifferentiated status (Denysenko et al., 2010). Niches are defined as a limited area where stem cells grow, with a complex and dynamic microenvironment that regulates their stem cell properties (Seidel et al., 2010).

Studies have linked this location to the chemo- and radio-resistance of CSCs (Denysenko et al., 2010), so the paper of these niches would be to provide a convenient microenvironment where the CSCs can survive and proliferate. The niches could serve as reservoirs where they can expand prior to a subsequent tissue invasion. There lies the importance of defining and locating these niches.

1.1.5-Tumourspheres from GBM

As there is no specific marker to identify the CSCs, the gold standard to identify them is the *in vitro* growth of tumourspheres. These appear *in vitro* under restrictive conditions, when the majority of tumour cells suffer apoptosis and the surviving cells grow as spheroid arrangements in suspension, with a rich extra-cellular matrix surrounding them. By definition, stem cells have the capacity to give rise to spheres when grown in specific conditions. If the neurospheres are then dissociated into single

cells, these cells can give rise to secondary neurospheres, and soproducing neurospheres in a serial fashion and hence demonstrating their self-renewal properties (Das et al., 2008). It is also known that tumourspheres are formed from various statuses of differentiated and undifferentiated cells (Ahmed, 2009); the stem cells and their different status differentiated progeny. This fact complicates even more the identification of cancer stem cells. Cells from the tumourspheres show positivity for many stem cell markers such as CD133, Nestin, GFAP, Sox-2 etc. (Pastrana et al., 2011) (Fig. 2).

Nowadays the sphere-assay is considered as an experiment that evaluates the potential to behave like a stem cell.

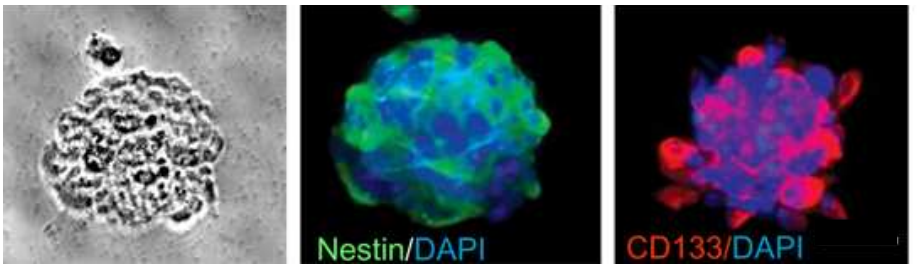

Figure 2: Morphology of neurospheres and immunocharacterization with stemness markers. Adapted from Scully et al., 2012.

1.1.6-CSCs and hypoxia

It has been reported that the tumour microenvironment is essential for the survival and genesis of the cancer stem cells. Cancer stem cells have also been described as the cellular subpopulation with the capacity to regenerate the tumour inside a suitable environment (Fan et al., 2007).

When gliomas become malignant, neoplastic cells increase metabolic requirements, being supplied by microvascular adjustments. However, at some point, tumoural requirements exceed the metabolic support of these adaptive changes of the pre-existed microvasculature and the genesis of new vessels is induced to supply oxygen and nutrients. When the

microvascular network is not able to provide enough oxygen, tissues suffer hypoxia. Microvascular alterations develop in malignant tumours as a result of an adaptive process to the referred relative tissue hypoxia. One of the most important consequences is the compromise of the Blood-Brain Barrier (BBB) function.

Hypoxia is a typical feature of GBM. It has been reported that hypoxia induces the selection of clones of tumoural cells. Some of these cells would suffer adaptations in order to survive, transforming themselves into tumoural stem cells (Heddelston et al., 2009). When hypoxia appears, hypoxia-induced factor (HIF) is activated and its expression induces the up-regulation of different molecules like VEGF (linked to angiogenesis), iNOS (Inducible nitric oxide synthase; related to vasodilation), EPO (Erythropoietin; a key molecule activating the erithropoiesis) and TGF-beta (Transforming growth factor; increasing cell proliferation) (Fig. 3).

Oxygen concentration also seems to be a key factor in the apparition and maintenance of the stemness state. Hypoxia would transform these cells, providing them with a higher proliferation rate, more angiogenesis capacity (Bao et al., 2006 b) and higher tumourigenesis (Heddelston et al., 2010). This step could be activated by the expression of some genes like Notch or Sox2, which have been found *in vitro* to be overexpressed in hypoxic cells (Gustafsson et al., 2005).

Hypoxia enhances CSC characteristics, increasing CSC proliferation in cultures (Pistollato et al., 2010), as well as inducing HIF-2α overexpression in CSC (Heddleston et al., 2009). Hypoxia induces the expression of HIF-2α, but it does not increase HIF-1α expression in neurospheres. Moreover hypoxic conditions *in vitro* induced an increase in Nestin and CD133 (Kolenda et al., 2010). HIF-2α expression could induce the stem cell phenotype by inducing non-stem cells to transform into stem cells and increasing stem cell proliferation (Heddleston et al., 2009). This hypothesis was later confirmed by the appearance of CD133 positive cells under

hypoxic conditions, reverting to a more differentiated condition when normoxia was applied (Griguer et al., 2008).

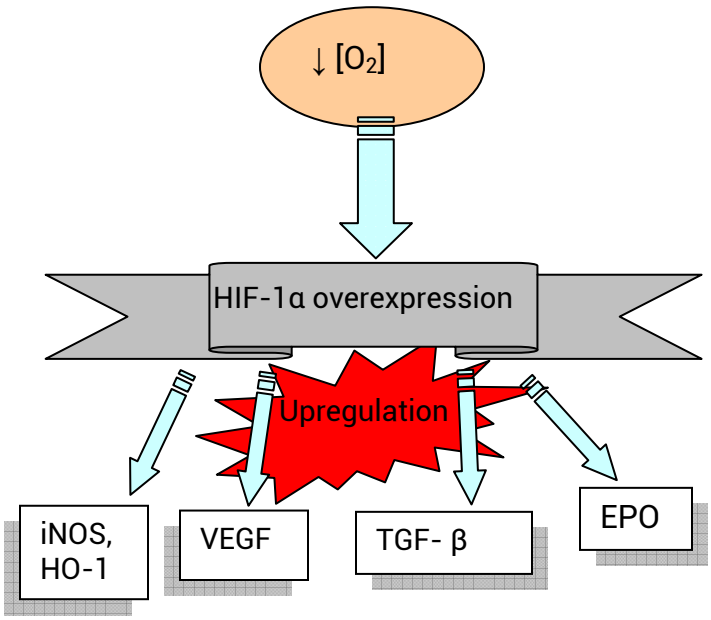

Figure 3: Angiogenesis regulation via HIF-cascade. Adapted from Loser et al., 2010.

A relationship has been described in human glioblastomas between the appearance of the tumour stem cell phenotype and intratumoural oxygen gradient (Pistollato et al., 2010). According to this research, oxygen concentration is a lead factor in cancer stem cell dedifferentiation (Fig. 4). Cancer stem cells have been identified in perinecrotic pseudopalisades, typical of glioblastoma multiforme (Jang et al., 2006; Jensen, 2006). The cells around the pseudopalisades were also found to express HIF-1α (Kaur et al., 2005), so further research into whether this hypoxic cells are cancer stem cells would be needed, to study whether the hypoxic cells adapt to the hypoxic conditions by undifferentiation.

It is believed that CSCs activate the HIF/VEGF pathway (Bao et al., 2006b), thus implying that CSCs are related to the angiogenesis process.

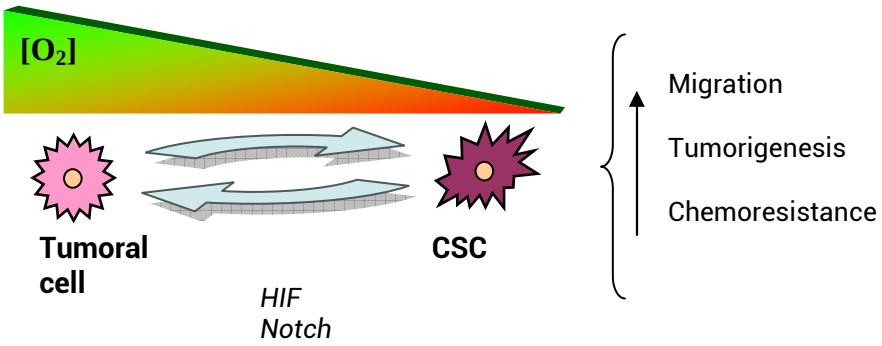

Figure 4: Scheme of the adaptations that suffer the CSCs to survive to hypoxia and the characteristics that acquire.

1.1.7-CSCs and angiogenesis

Angiogenesis is the process of building new vessels from the pre-existing ones, and is vital in many tumours, especially in gliomas. The angiogenesis process also regulates the tumoural progression and it is mainly regulated by VEGF (among other factors).

VEGF is a proangiogenic and permeability factor that has many functions in physiologic (Kamat et al., 1995) and pathologic angiogenesis (Folkman, 1995, Dvorak, 2006), regulating the tumoural neoangiogenesis (Dvorak 2007). VEGF permeabilises the vascular wall (Dvorak, 2006) by producing endothelial fenestrations, which the brain normally lacks. Alteration of the morphological substrate of the Blood-Brain Barrier produces cerebral oedema, an epiphenomenon that is the major cause of death in patients with brain tumours (Bulnes et al., 2010).

As previously stated, CSCs have beenreported *in vivo* to be located around the tumoural vasculature forming the perivascular niche. Yang and Wechsler (2007) also stated that the perivascular niche of glioma stem cells could mediate in tumoural vascular adaptation. They found plenty of CSCs around the abnormal tumour vasculature and suggested that glioma

stem cells enhance vascular niche development through secretion of proangiogenic factors, such as VEGF. Recently, VEGF has been described as inducing the tumourigenesis of cancer stem cells (Li et al., 2009), confirming the tight link between CSCs and angiogenic factors. Accordingly, it is supposed that CSCs in the perivascular niches induce angiogenesis mediated by VEGF, contributing to the regulation of hte niche microenvironment.

CD133+ cells had been previously found to express VEGF and to promote angiogenesis after being injected into nude mice (Bao et al., 2006b). In addition, CD133+ cells activate endothelial cells to increase the expression of proangiogenic factors expression (Folkins et al., 2009).

Recently, relation between CSC and the microvasculature has been studied the, suggesting that microvessels contribute to creating and maintaining a niche microenvironment where CSCs can grow (Calabrese et al., 2007). Following this hypothesis, Borovski and collaborators (2009) reported that CSCs in culture have a higher proliferation rate when cultured with microvascular endothelial cells rather than alone. This study also suggested that this effect is not only due to soluble factors such as VEGF, PDGF… implying that these niches are composed by a combination of stem cells, differentiated cells and endothelial cells. Other studies suggest the possibility of cellular transdifferentiation of CSCs into endothelial cells as part of the neoangiogenesis (Soda et al., 2011, Scully et al., 2012), but this hypothesis still needs further research.

Since the proliferation and invasion of adjacent normal parenchyma has been attributed to glioma stem cells, it is believed that these cells use the extracellular matrix of the vessel wall as a migration pathway to infiltrate normal brain parenchyma, so the CSCs also rely on the vasculature to migrate.

1.1.8-Future of CSCs in therapy

Conventional anticancer therapy includes therapies that are predominantly targeted against the whole fast-dividing tumoural cell population. Only a few therapies are targeted directly against tumoural characteristics, as is the case of antiangiogenic therapies.

Nowadays, there is an increase in the study of treatments against CSCs (Fig. 5), which mediate the invasiveness and tumourigenesis, but targeting CSCs in vivo is very difficult, because the immunomarkers to identify them are not well defined yet and the stemness status is subject to change due to the microenvironment (Hadjypanis and van Meir, 2009). However, these therapies could be doomed to failure, due to the fact that CSC status is not a permanent status (as previously believed), but a consequence of the adaptation of some cells to adverse conditions. So, after therapy against undifferentiated cells, they could simply adapt themselves to a more differentiated status in order to avoid these treatments.

Ideally, the best way to target CSCs would be to attack them when they are identifiable and to block the pathways that induce the dedifferentiation. Some approaches have been made *in vitro* and *in vivo* in order to target the CSCs. For example, Bao and collaborators in 2008 used the L1CAM (cell adhesion molecule L1), which is preferentially expressed in CD133+ gliomas, to target these cells. They showed that a shRNA-mediated knockdown of L1CAM reduces the neurosphere-forming capacities of CD133+ cells and selectively induced apoptosis of CD133+ cells, but not CD133- cells. *In vivo* L1CAM knockdown showed prolonged survival after tumour xenografts.

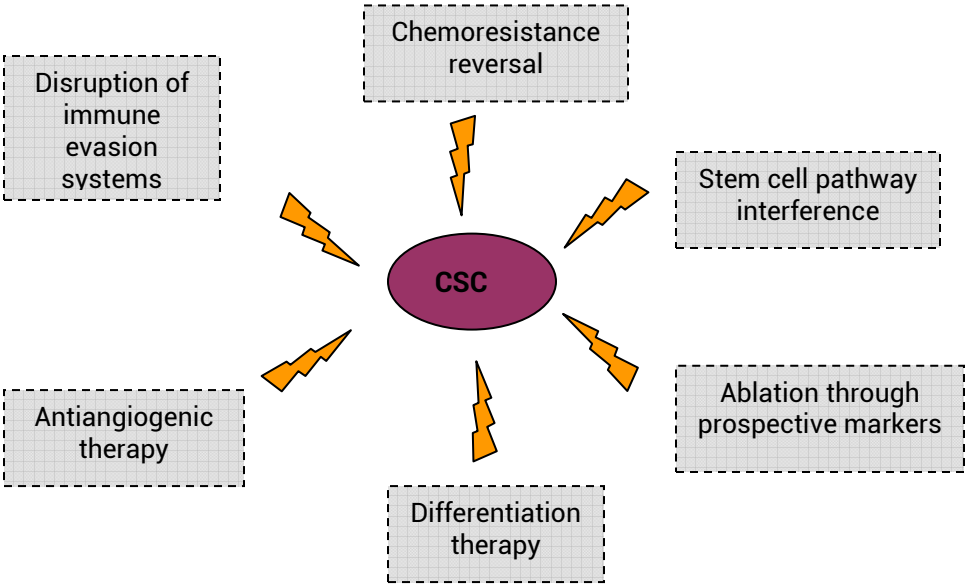

Figure 5: Possible pathways that could be targeted in future anti-CSCs therapies. Adapted from Frank et al., 2010.

1.2.-Animal models for glioma

The clinical importance of gliomas urged a search for a reliable model that could mimic all the characteristics present in human gliomas. As stated by Candolfi and collaborators in 2007 (Candolfi et al., 2007), a perfect glioma model should grow *in vivo* with predictable and reproducible growth patterns, should have close resemblance to the histopathology of human gliomas, be weakly or non-immunogenic and its progression should be highly reproducible.

The first animal models of gliomas date from the 1960s as ENU (Ethyl-Nitrosourea)-induced rat models (Druckrey et al., 1966), but lately, murine xenograft models (either intracerebral or subcutaneous) and genetically engineered mouse lines have increasingly been used (Chen et al., 2013) (Fig. 6).

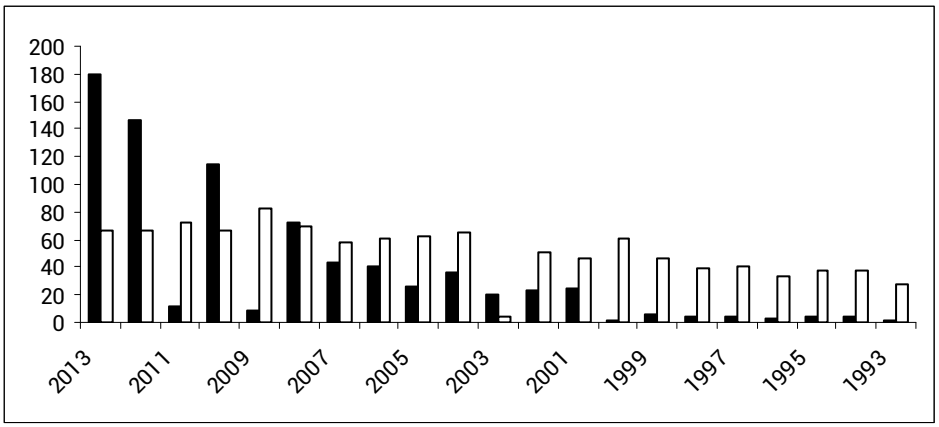

Figure 6: Graph with the published papers in the last 20 years that included "ENU" (White) or "xenograft GBM" (black). Data acquired from Pubmed.

Rat glioma models show advantages over mice models, such as larger brain and larger glioma size at death, which are easier to detect with imaging techniques (Barth and Kaur, 2009). On the other hand, rat glioma models also have disadvantages as compared to mouse models; e.g., it is more difficult to genetically engineer them (with all the implications that this has; genetic/proteic factors, pathways…) and they are more expensive.

To date, the following models are most frequently used to mimic gliomas in animals:

-**Xenograft models:** The inoculation of established cancer cell lines into mice.

These models suffer from a lack of a regular immune system, thereby not accurately representing the cellular composition of the original tumour as well as a lack of histologically-similar vasculature (Finkelstein et al., 1994). The main advantages of this model are the high reproducibility, fast

tumour development (Fomchenko and Holland, 2006) and the accurate knowledge of the location of the tumour (King et al., 2005). The injection of tumour cells can be performed subcutaneously or directly into the brain (orthotopical). Nowadays, it is the most popular method for producing CNS tumours, because the gliomas develp in a short time, it is relatively inexpensive and easy to perform, and established glioma cell lines are readily available.

-**Genetically engineered mice:** These are more representative of human cancer syndromes, rather than primary tumours, because of their origin. They are created to express oncogenes or suppress anti-oncogenes (Janbazian et al., 2014). There are numerous examples, like altering specific signalling pathways such as Ras/Akt (EGFR) or mutating genes like v-src, v-erbB or p53 (Fomchenko and Holland, 2006). The advantages of this model are the possibility of creating conditioned models of the tumour initiating lesions and immunocompetence of the mice (and so being able to control the start of the mutation). However, there are many disadvantages such as poor reproducibility, low tumour penetrance, and high latency (Fomchenko and Holland, 2006).

-**Oncogenic virus inoculation:** There are some cancer cell lines that are produced from the inoculation of oncogenic virus in mice. The most used virus is the avian sarcoma virus (Barth and Kaur, 2009).

-**Administration of chemical substances:** The exposure to chemical compounds to produce CNS tumours has been performed since the 60s (Druckrey et al., 1966). Methyl-nitrosourea and N-Ethyl-N-nitrosourea are two compounds that have proven to be tumourigenic (Bosch, 1977). They provide tumours histologically similar to human tumours (Fomchenko and Holland, 2006), but take a long time to develop (Zook and Simmens, 2005). The endogenous generation of gliomas via transplacentary injection of ENU in rats during pregnancy has been widely documented and is a well-known and reliable model to study gliomas in different stages (Zook and Simmens, 2005; Bulnes-Sesma et al., 2006). It also provides a tumour with

the hots's own cells, where the tumoural vasculature develops at the same time that the gliomas become malignant.

It is important to realize that despite all accumulated experience with the aforementioned models, no currently available animal tumour model exactly simulates human high-grade brain tumours such as glioblastoma or anaplastic astrocytomas.

1.2.1-ENU-induced glioma model

The ENU-induced glioma model provides endogenous gliomas that evolve from the smallest stages to the most malignant. It has been suggested that the long latency of the ENU-induced gliomas is due to the mechanism of generation of these tumours, in which (like spontaneous tumours) many mutations have to accumulate until the tumours develop (Schiffer et al., 2010).

ENU is a powerful mutagenic agent that alkylates DNA; more precisely it alkylates the O_6 in the guanine and the O_2 in the thiamine. ENU preferentially alters AT base pairs. GC-rich genes will not be mutated as often as those with a lower GC content. Similarly, the size of the gene will also affect the rate at which it will be mutated i.e. larger genes will provide a larger target for random mutagenesis than a smaller one (Kennedy and O`Brian, 2006).

It has been reported that ENU generates a T:A---A:T transversion and a G:C---T:A transition, and this has been largely studied (Jansen et al., 1994), but it produces mainly the transversion effect (44%), rather than the transition effect (38%). Additionally, it also produces small deletions (Slikker et al., 2004). ENU effectively induces point mutations in a genome-wide manner, which resembles most of the causes of human genetic diseases (Gondo and Fukumura, 2009). The accumulation of these successive alterations seems to be responsible for the effect of ENU in the expression of multiple genes like p53, neu/erbB-2, Osteopontin, p21 and cyclin G1, which become up-regulated (Katayama et al., 2005). The

consequences of these alterations are the development of CNS tumours. The range of these tumours is from brain tumours (which are oligodendrogliomas, astrocytomas or mixed gliomas of all degrees of malignancy) to cranial nerve tumours (mainly schwannomas from trigeminal nerves) and spinal cord tumours (Zook and Simmens, 2005). Oligodendrogliomas and mixed gliomas are the most common tumours after the ENU administration (Zook et al., 2000). It has been proposed that the majority of the brain tumours begin as oligodendroglial tumours and as they become more malignant they develop an astrocytic component, transforming the tumours into mixed gliomas (Zook and Simmens, 2005). Histopathologically, the brain tumours have all the typical characteristics of the human gliomas, like necrosis, haemorrhages, microvascular endothelial proliferation, atypical mitoses, cellular anaplasia (Zook et al., 2000; Bulnes-Sesma et al., 2006).

Prenatal exposure to ENU has also proven to produce cell cycle alterations in neural stem cells around the subventricular zone (Capilla-Gonzalez et al., 2012) and to reduce the amount of stem cells in the SVZ (Capilla-Gonzalez et al., 2010). It has been suggested that the neural precursors of the SVZ are mutated after ENU administration (Gil-Perotin et al., 2006). However, it is not known yet if these alterations have any implications in the carcinogenesis process after ENU administration.

Due to its potent mutagenic potential, ENU has been also used to induce genome-wide point mutations in mice (Gondo et al., 2010) and in rats (Huang et al., 2011), in order to phenotypically identify the causing genes by forward genetics (Gondo et al., 2010). In these projects, male mice are injected with ENU and as a result, germline mutations are induced in spermatogonia that are inherited after mating with female mice. The detected phenotypical alterations inherited by the newborn mice are all heterozygous, therefore the mutations are dominant. Nowadays, there are more than 10000 samples with over 3000 mutations each archived by

international projects like RGDMS (RIKEN-ENU based Gene-driven Mutagenesis system), KOMP, EUCOMM (Gondo et al., 2010).

1.3-Clinical diagnosis

In the same way as in humans, experimental model of gliomas do not show symptoms until the tumours are in an advanced stage of development. The main problem with animal models is that animals cannot be asked about their health, so other methods had to be developed. Rodent animal models also have the inconvenience that it is difficult to detect clinical symptoms associated with sickness, as diagnostic methods are not refined enough.

1.3.1-Animal welfare

Animals cannot tell actively if they are suffering pain, or have physical discomfort. A baseline of welfare has to be established for the animals, as well as precise methods that can discern as soon as possible when the animals become unhealthy.

In order to decrease pain and detect the lack of welfare as soon as it happens, new methods to detect early changes in the animal's behaviour should be developed.

Animal welfare is defined as an animal when it is healthy, comfortable, well nourished, safe, able to express innate behaviour, and it is not suffering from unpleasant states such as pain, fear or distress.

Aanimal welfare requires disease prevention, veterinary treatment, appropriate shelter, management, nutrition, human handling and human slaughter.

Another way to define animal welfare is the Five Freedoms (Farm animal welfare committee). These Five Freedoms include:

-Freedom from hunger or thirst by ready access to fresh water and a diet to maintain full health and vigour.

-Freedom from discomfort by providing an appropriate environment including shelter and a comfortable resting area.

-Freedom from pain, injury or disease by prevention or rapid diagnosis and treatment.

-Freedom to express (most) normal behaviour by providing sufficient space, proper facilities and company of the animal's own kind.

-Freedom from fear and distress.

Animal welfare also includes the handling of the animal by the experimenters, who must be kind and be conveniently prepared in the animal's handling.

There are three main methods to perform clinical diagnosis for any pathology; 1.-subjective tests that depend on handling and observation by the investigators, 2.-objective tests (carried out by devices) and 3.-complete monitoring of animal parameters in a controlled environment simulating their home. The advantages and disadvantages of these methods are the discussed below.

For many years, clinical diagnosis relied on non-standardised subjective protocols and tests, including human manipulation and observation. Direct handling by the experimenters has been proven to be very unreliable, due to the fact that experimenters influence the outcome of the tests, and are a source of variation in results (Chesler et al., 2002). An example of these tests is the "welfare status" performed by Morton & Griffith (1985).

On the other hand, objective tests, mimicking clinical probes, were performed in order to achieve a clinical diagnosis. Available probes are based on brief trials in standardised system like the "open-field" test, which was first developed for anxiety detection (Denenberg, 1969). These tests are carried out in a specific bounded time. It is important to note that these systems are well standardised for some uses (such as anxiety, as

previously mentioned), but it can lead to difficulties in replication of the results when applied to different situations (Mandillo et al., 2008).

In order to objectify clinical diagnosis, appropriate current methods include the automatic monitoring of the animal's food and water intake, study of its physical state, monitoring its capacity of movement…, in a controlled area. This system has been called "homecage". The first homecage systems began to be used in the 90s (Saibaba et al., 1996) in order to monitor animal behaviour with minimal human interference.

The only disadvantage of these systems is the increased time that has to be used in the tests, consuming for a couple of hours a day during several days or weeks. In the future, these methods will replace the classic diagnosis because they are cheaper and, after its standardization, they are also easier.

Behavioural changes happen almost in every disease in human and animal models, and chronic diseases are the best models to study behavioural changes in rats, because the changes happen slowly and at some point, it is presumable that behavioural changes appear before the animals externalise the discomfort or pain.

In the last decade, behavioural clinical diagnosis has been gaining weight in efforts to find an early and cheap diagnostic method, prevent animal pain and distress, learn more about the initial stages of diverse diseases and phenotypically characterise mice and rats mutant strains (Mandillo et al., 2008).

Those systems have a standardised environment and methods, offering a similar environment to the natural state, and as the data is collected by computer equipment, behavioural data is gathered objectively (Clemens et al., 2014). Unfortunately, as of now, there is little literature regarding animal behaviour in homecage systems, which makes it more difficult to use these methods for diagnosis in the animal models.

Historically, these tests have been used as a diagnostic tool in models for psychiatric diseases, but not in models that represent chronic and

mortal diseases such as cancer. Not even in humans are there many studies about gliomas and behaviour, apart from a few about gliomas and depression (Starkweather et al., 2011).

The principle of homecage systems is to maintain the animals in a familiar, stress-reduced environment. (TSE-systems. Available at http://www.tse-systems.com/products/behavior/home-cage/phenomaster/index.htm). These systems have many advantages: data can be measured for a determined time, be it from minutes to days, and collected data can be split into time-intervals if wanted (e.g.: only at night, only at day, the first/last "x" hours...). They reduce the handling and transportation of the animals (limiting stress levels and avoiding variables) and optimise the use of animals (Noldus. Available at http://www.noldus.com/content-view/home-cage-monitoring-system).

The modular design of homecage systems also allows a wide range of experimental procedures for characterising the evolution of the animal's behaviour during the experimental process (Panlab. Available at http://www.panlab.com/en/products/phecomp-system-panlab).

With homecage systems, the assessment of behaviour takes place in a fully–automated manner in the experimental animal`s own environment (Neurobsik. Available at http://www.neurobsik.nl/Homecageasses.html). Homecage systems can also provide standardised protocols that are easily reproducible, without external variables.

Natural animal behaviour is a relatively unstudied area, and even more so when it is related to physical diseases. Housing and testing animals in homecage environments helps with the animal welfare awareness and fulfilment.

With the help of these systems to identify early alterations in the behaviour and activity patterns of the rat, it is easier to detect pathologies before the animals acquire severe physical handicaps, thus improving their animal welfare.

II.-Hypothesis

Some cancer stem cells are responsible for the origin, maintenance and growth of gliomas. Despite studies about their functions, little is known about the differential distribution in various degrees of malignancy degrees, their participation in the early stages and their role in glioma development. The main hypothesis of this study is that the identification of cells expressing several stemness markers in early and advanced stages of gliomas may be useful to understand their development and progression, and eventually to design treatments against this neoplasia.

The ENU-glioma model is very useful to study morphological and molecular characteristics of cells expressing stem cell markers and, in addition, it also allows the study of clinical changes following the initial apparition of the gliomas. Clinical symptoms in rats with glioma appear quite late, when the pathology is in an advanced stage, hence the necessity of designing a method to identify these early changes. An early diagnostic suspicion based on behavioural changes such as movement, feeding, exploration, rearings (standing on rear limbs) and so on provides an easy method to unveil the initial phase of the tumour, and constitutes an indication to perform advanced imaging techniques, such as Magnetic Resonance Imaging (MRI). An adequate monitoring of vital constants and animal behaviour is a very useful and required tool to reduce pain or discomfort and to increase animal welfare in experimental research.

III.-Objectives

3.1.-Main objectives

Identify and locate Nestin-positive cells in an endogenous model of gliomas, from early to advanced stages, reporting their distribution in different tumoural areas and their co-expression with other stemness markers.

Establish a clinical protocol identifying physical and behavioural changes in order to obtain indirect evidences of tumour development before clinical symptoms are visible.

3.2.-Procedural objectives

1.-Monitor clinical and behavioural variables in rats prenatally exposed to ENU with a homecage system and the open-field test searching for clinical symptoms that suggest the apparition of a pathology.

2.-Detect the induced brain gliomas and classify them in different stages via MRI and histopathological study.

3.-Study the morphology and distribution of Nestin-positive cells inside experimental gliomas, mapping their distribution in different stages of glioma development.

4.-Analyse the co-expression of Nestin-positive cells with other stemness markers: OPN, Notch-1 and CD133 in different ENU-glioma stages.

5.-Immunophenotypical characterization and morphometrical analysis of Nestin+ cell arrangements in perivascular areas and inside gliomas at different stages of development.

IV.-Material and Methods

4.1-Tumour induction

For the present study, 94 offspring born from 10 ENU-injected Sprague-Dawley rats were used for the studies described in Table 1. From the 94 offspring rats, 36 were used for the behavioural study, 24 for the proliferation study and 13 for the MRI study. After their sacrifice, all of them, including the remaining ones, were used for the immunohistochemical study against stemness markers in the 91 gliomas that were identified.

The tumour induction was made by a single ENU (N-Ethyl-N-nitrosourea; Sigma E2129) injection in the 15th day of pregnancy. ENU was diluted at 10mg/ml in 0.9% NaCl and the solution intraperitoneally injected at 80mg/kg of body weight. For this purpose rats were slightly anaesthetised with isofluorane 2% (IsoFlo, Veterinaria Esteve, 1385 ESP).

10 pregnant rats	94 offspring rats	91 gliomas	Immunohistochemistry
	-36 behaviour		Quantification
	-24 proliferation study		
	-13 MRI		

Table 1: Scheme of the number of rats used for each study and the number of gliomas developed by all ENU-exposed rats.

Animals were bred in standard housing conditions and food and water were available *ad libitum*. All animal experiments were performed in accordance with Spanish Royal Decree 1201/2005, Directive 2003/65/EC of the European directive 2003/65/CEParliament and the EU Recommendation 2007/526/CE about experimental animal EC regarding the protection of animals used for purposes.

4.2-Tumour screening

Tumours were detected by clinical symptoms, behavioural anomalies, MRI imaging and after the autopsy by macroscopic and histopathological study.

The behavioural evaluation was performed on 36 rats (15 male and 21 female) during the ENU-glioma development from the 4th to the 8th month of age and 8 normal rats were used as controls (4 male and 4 female) of the same age. Males and females were segregated because of the big differences in the studied parameters. This evaluation consisted in 3 studies: 1.- the welfare score according to a modified version of Morton & Griffiths table (1985) (this test was performed just before they entered the Phecomp cage), 2.- a continued monitoring of the parameters listed below in a homecage system (Phecomp), (this was performed once every four weeks) 3.- application of the open-field test once every four weeks.

The parameters studied in the homecage system were: food and water intake, % of time moving, number of rearings (every time the rat stands on its rear limbs), total distance walked, and % of exploration in the first 4 hours (defined as the time the rat was exploring the central area of the cage in the first 4 hours). The parameters studied in the open-field test were % of time moving, number or rearings, total walked distance and % of exploration (defined as the time the rat was exploring the central area of the cage/the total time of the test).

4.2.1-Monitoring of the animal welfare

Animals injected with ENU were analysed every two days to establish their health status, taking into account abnormal postures, abnormal vocalisations or unusual weight loss, extreme immobility or swollen eyes.

The welfare of the rats was studied with an adaptation of the Morton & Griffith (1985) table for animal well-being (Table 2).

Parameter	Status	Score
Weight loss	No loss ≤ 10% ≥10 ≤20% ≥ 20%	0 1 2 3
Aspect	Normal Fur in bad conditions Fur in bad conditions and/or nasal or ocular secretions Abnormal posture	0 1 2 3
Spontaneous behaviour	Normal Small changes Inactivity Auto-mutilation, abnormal vocalisations, immobile or agitated animal	0 1 2 3
Induced behaviour	Normal Small changes Medium changes Comatose or aggressive animal	0 1 2 3

Table 2: Modified table score for the animal welfare. Adapted from Morton & Griffith (1985). In terms of the spontaneous behaviour, we have defined small changes as an increase in the grooming activity of their head and forepaws or not forming a bed or a specific area for self-hygiene. In the induced behaviour we have defined small changes as trying to hide more than usual and medium changes include exaggerated escape behaviour.

This test was always performed by the same person, in order to reduce the variability. To obtain the total score, one status of each parameter has to be selected (the one more suitable for the animal) and then each parameter score has to be summed up.

If two or more categories have a score of "3", all scores of "3" change to a score of "4".

Total score ranges from 0 to 16 and it is interpreted in the following way.

0-3: normal

4-7: supervision

8-12: extrasupervision and/or considering sacrifice

13-16: sacrifice; dangerous procedure

4.2.2-Homecage system

This study consists in a 48-hours stay in a controlled environment in a homecage system called a Phecomp cage (Panlab, Barcelona, Spain; Fig. 7). The device consists of a cage (Allentown Caging Equipment, ACE, 197W×306D×212H mm) provided with a grid floor. The cage is associated with one external unit for food and one for drink recording. The system records the food cosumed and the quantity of water drunk. A built-in display allows following in real-time the evolution of the total amount of food and drink consumption during the experiment. Animal horizontal activity is recorded by means of two infrared frames and rearings with two infrared frames at a height of 13 cm. We only counted the data from the two nocturnal periods (two periods of 12 hours each), when the rats are active.

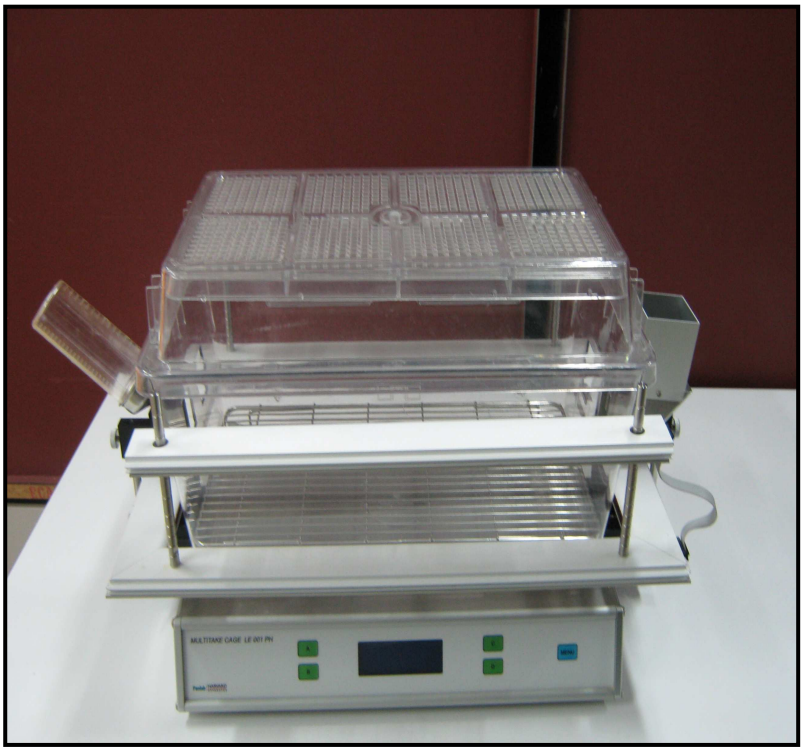

Figure 7: Phecomp cage above the registering unit. There is one unit for water and another for food and two frames (constituted by photoelectric cell and infrared beams) that detect the position of the animal and the rearings.

Once all the rats had gone through the tests, these started again; so providing continuous testing. There is a decrease in the number of rats every time, because they were sacrificed when they showed severe physical handicaps. So the 80 experimental tests and the 48 control tests correspond to the following distribution:

	ENU-group	Control group
-**4 months:**	36 rats	8 rats
-5 months:	23 rats	8 rats
-6 months:	10 rats	8 rats
-7 months:	4 rats	8 rats
-7.5 months:	4 rats	8 rats
-8 months:	3 rats	8 rats
Total:	80 test	48 tests: 128 tests

4.2.3-Open-field test

This test was performed using a photoelectric actimeter (Actitrack, Panlab, S.L., Barcelona, Spain; Fig. 8). The apparatus consisted of a transparent cage of 45 cm x 45 cm with a central area predetermined to measure 24 cm x 24 cm. The cage is connected to a photoelectric cell and locomotor activity was detected by infrared beams, with an infrafred frame at a height of 13 cm to detect rearings. All testing in the actimeter was done during 5 minutes in an isolated room between 16:00 and 17:00 hours, right after finishing the homecage test.

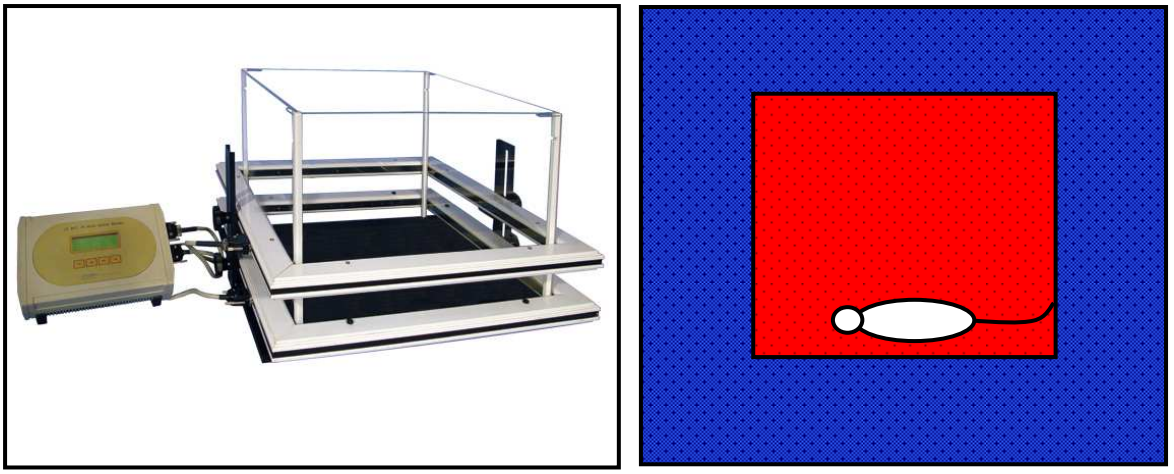

Figure 8: Image of the openfield cage, linked to the registering unit. Surrounding the cage there can be seen the two infrared frames that determine the position and activity of the rat during the test. On the right there is a representation of the rat and the two areas predetermined by the experimenter as the external and internal areas.

All the behavioural data was automatically collected and interpreted with *Compulse 1.1* (Panlab, Barcelona, Spain) and *Actitrack 2.7.13* software (Panlab, Barcelona, Spain) (Fig. 9).

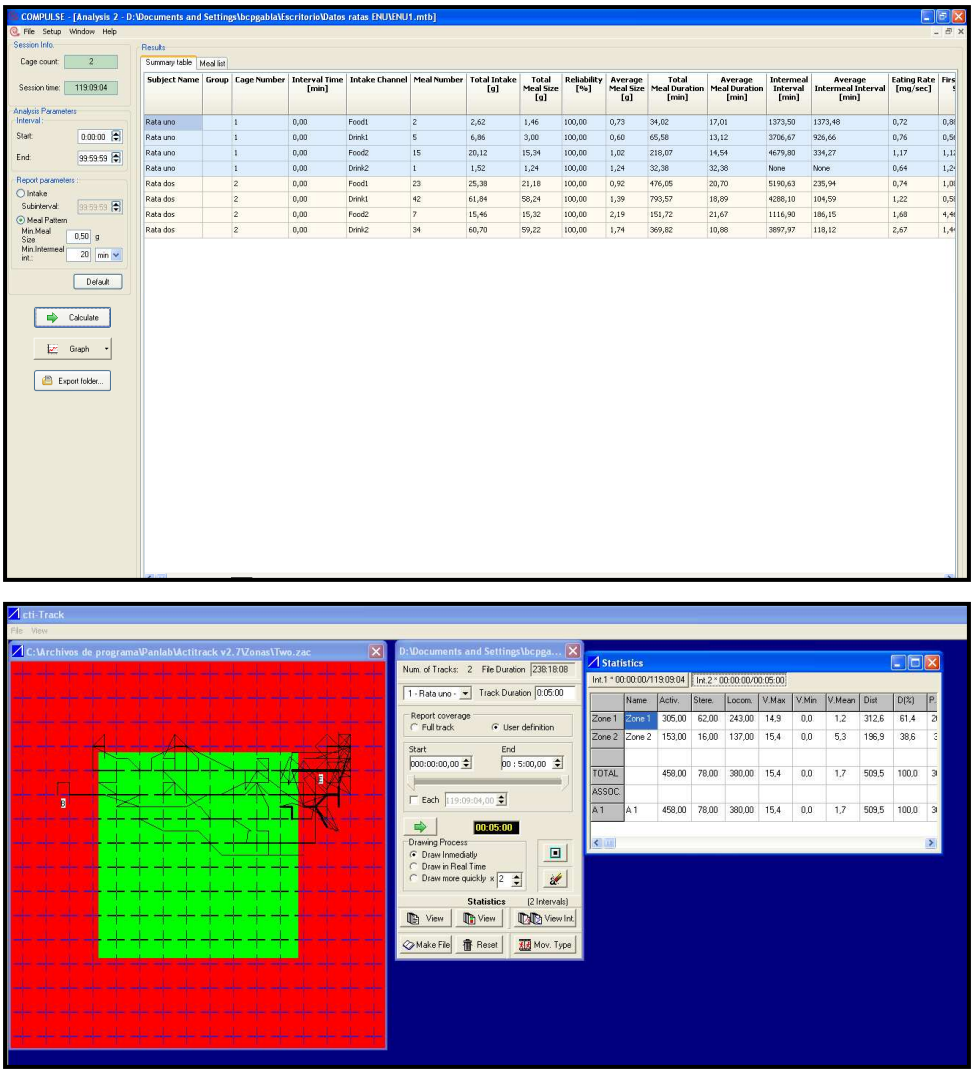

Figure 9: **Screen captures of Compulse (up) and Actitrack (down) software** to analyse the data collected with the Phecomp cage and Open-field test.

4.3-Magnetic resonance imaging study

13 rats were selected for MRI study when they reached the 5th month (7 rats) and 6th month (6 rats) of life (MRI, Biospec BMT 47/40, Bruker, Ettlingen, Germany, operating at 4.7 Tesla in the CAI (Research Support Centre) of the Complutense University of Madrid, Fig. 10). In order to scan the brain, animals were anaesthetised with isofluorane and

intraperitoneally injected with 1.5 ml/kg.body weight of gadolinium (Gd-DTPA, Magnevist, Schering AG, Berlin, Germany). Coronal and sagital images on T2-w fast spin-echo (TR/ effective TE= 3000/60 ms) and on T1-w spin-echo sequence (TR/TE = 700/15 ms) were obtained immediately after contrast administration.

MRI is based on the movement of the hydrogen protons of the tissue, motivated by the variations in the magnetic field induced by radio frequency pulses. T1 and T2 are different relaxing times of the protons, T1 being the longitudinal relaxing time, and T2 the time the protons take to disorganise.

Figure 10: Image of the MRI device used for the tumour detection. Device located in the CAI of Universidad Complutense de Madrid.

4.4-Proliferation assay

BromodeoxyUridine (BrdU) was used to study the cell proliferation. For this purpose 80mg/kg body weight of BrdU (Sigma-Aldrich; B5002), diluted in NaCl 0.9%, was injected intraperitoneally to 24 rats three times at intervals of three hoys. One hour after the last injection, animals were sacrificed by perfusing them with PFA 2% and the tissue was processed for histological examination.

4.5-Tissue processing

The rats were sacrificed when they showed deficits that could threaten their life or when they reached a score of 11 or more in our adapted Morton & Griffiths table (meaning they had a critical health status and had lost their welfare) or when a tumoural mass was observed in the MRI images. 94 rats were anaesthetised by intraperitoneal injection of chloral hydrate at 10% and transcardially perfused with a 0.9% NaCl solution, following with 4% paraformaldehyde (Panreac; ref: 141541.1211) in PBS 0,1M (pH=7.4).

Afterwards, the brains were removed and postfixed by placing them in a 4% PFA solution at 4ºC overnight. Medulla was extracted when visible symptoms of mobility incapacity were appreciated. The next day, the brains were washed with PBS 0.1M and cut into coronal sections. The coronal sections were used in two different protocols:

a) Some sections were embedded in paraffin like following:

- Brain section are placed in unicasettes and placed overnight in alcohol 50º.
- The brains are placed in two baths of ethanol 50º for two hours.
- Two baths of alcohol 70º of two hours.
- Overnight immersion in ethanol 96º (ENMA; ref: 190).
- Two baths of ethanol 100º (ENMA; ref: 180) for two hours.
- Three baths of 90 minutes in chloroform (JT Bajer; ref: RS69387).
- One bath of 30 minutes in a mixture of xylene/paraffin 50%.
- The brains are kept overnight in paraffin (Histosec; Merck; ref.:11609) at
  56º C.
- One bath of paraffin at 56º C.
- Create the blocks using moulds and a paraffin dispenser (MYR EC350-1; EC351.0349).

- Finally the sections embedded in paraffin were cut with a microtome (Microm: ref: HM-440-E) at 4 µm.

b) Other sections were stored one day in a 30% sucrose (Panreac Química ref: 131621) solution in PBS 0.1M at 4ºC. The sucrose solution is used to prevent the formation of crystals in the tissue while the freezing. Then the sections were cut with a cryotome at -25ºC and 50 µm thickness. The slices were kept in a 0,5% azide (Sigma-Aldrich, ref:S-2002) solution in PBS 0.1M.

4.6-Histopathological study

We used some 4 µm thick sections obtained by microtomy (Anglia, Type 200) for the Hematoxylin/Eosin staining to detect and classify the tumours according to histopathological features such as haemorrhages, cysts, cellular anaplasia, nuclear atypias, high mitosis and vascular proliferations.

Hematoxylin/Eosin staining was performed as follows:

- Deparaffination by two baths of 10 minutes in xylene (Panreac; ref:211679.174).
- Hydration of the sections by immersion in decreasing gradient alcohols every 5 minutes in 100º, 96º, 80º, 70º, 50º and distilled water.
- Immersion in Harris Hematoxylin for 2 minutes.
- Wash with distilled water.
- Differentiation in 0.5% HCl (Panreac Química ref:131020.1611) in 100º ethanol for two seconds.
- Wash in tap water for a couple of seconds.
- Immersion in Eosin for 20 seconds.
- Dehydration by immersion in increasing gradient ethanol every 5 minutes in 70º, 80º, 96º, 100º, 100º.
- Two immersions in xylene for 5 minutes.

- Protection with cover-slides using DPX resin (Sigma-Aldrich, ref.: 44581).

4.7-Lectin histochemistry

Lectins are vegetal glycoproteins with the capacity to bind selectively to foreign glycoconjugates. Many lectins have demonstrated their utility as markers of the vascular wall. For this study we have used the tomato Lectin (*Lycopersycum esculentum agglutinin,* LEA).

This histochemistry was performed on 50 µm thick free-floating sections with FITC-conjugated *Lectin lycopersycum* (1:100; Sigma-Aldrich; ref: L0401). The entire histochemistry is carried out in dark conditions, because the LEA primary antibody is attached to a green fluorescent molecule.

- Firstly the sections were washed twice with PBS 0.1M.
- The sections were placed in a blocking solution of PBS 0.1M+BSA 5% (Sigma-Aldrich; ref: A7906) + Triton X-100 (Sigma-Aldrich ref: T-6878) 0.5% for 2 hours.
- Add primary antibodies diluted in the blocking solution like previously stated and incubate overnight at 4º C.
- Wash three times with PBS 0.1M.
- Incubate 5 minutes with Hoechst 33258 (Sigma-Aldrich) 5µg/ml in PBS 0.1M.
- Wash three times with PBS 0.1M.
- Mount the sections in gelatinised slides and cover with Vectashield (Vector laboratories ref: x-0517) and cover-slides.

Some representative cases were double stained with CD133.

All fluorescence images were acquired with an Olympus Fluoview FV500 confocal microscope using sequential acquisition to avoid overlapping of fluorescent emission spectra. The images have been treated with *FV 10-ASW 1.6 Viewer* and *Adobe Creative Suite 4*.

4.8.-Immunohistochemistry

Immunohistochemistry assay was carried out on paraffin sections against stem cell markers: Nestin (monoclonal anti-Nestin 1:200, Santa Cruz sc-33677), Osteopontin (monoclonal anti-Osteopontin 1:200, Santa Cruz sc-21742) and Ki-67 (monoclonal anti Ki-67 1:100; Monoclonal, DakoCytomation, M7248).

- Deparaffinate the sections by two baths of 10 minutes in xylene.
- Hydration by immersion in decreasing gradient alcohols every 5 minutes in 100º, 96º, 80º, 70º, 50º and distilled water.
- Immersion in methanol + H_2O_2 (Foret; ref: 7722-82-1) 4% during 20 min.
- Boil 5 minutes in citrate buffer (pH=6.0) and let it cool.
- Block with PBS 0,1M + BSA 1% (Sigma-Aldrich; ref: A7906) for 2 hours.
- Add the primary antibody diluted in the blocking buffer and incubate overnight at 4ºC in a moist chamber.
- Wash twice with PBS 0.1M.
- Add biotinylated secondary antibody as prescribed in the Anti-mouse Vectastain ABC kit (Vector Laboratories, ref: PK-6102) and incubate for 1 hour in a moist chamber.
- Add avidin-biotin-peroxidase complex as prescribed in the Anti-mouse Vectastain ABC kit and incubate for 30 minutes in a moist chamber.
- Wash twice with PBS 0.1M.
- Develop the reaction with 3.3-diamino-benzidine (DAB) (Ref.: 8001, Sigma-Aldrich, 0.25 mg/ml) and H_2O_2 solution (0.01%).
- Counterstain with Harris Hematoxylin for 45 seconds.
- Dehydration by immersion in increasing gradient alcohols every 5 minutes in 50º, 70º, 80º, 96º, twice 100ºC and twice xylene (Panreac; ref: 211679.174)

- Protect with cover-slides using DPX resin (Fluka Chemie, Ref.: 44581).

Negative controls omitting primary antibodies were performed on each run. Visualisation was made with an optical microscope (Olympus SA ref: BH-2).

4.8.1-BrdU immunofluorescence

The tissue was stored in a 30% sucrose (Panreac Química ref: 131621) solution in PBS 0.1M until cut into thick sections of 50 um with a cryotome. The immunohistochemistry was carried as follows:

- Wash the sections twice with PBS 0.1 M.
- The sections were placed in a blocking solution of PBS 0.1M+BSA 5% (Sigma-Aldrich; ref: A7906) + Triton X-100 (Sigma-Aldrich ref: T-6878) 0.5% for 2 hours.
- Incubate in HCl 2N at 37ºC for DNA denaturalisation for 30 minutes.
- Wash with Tetraborate sodium decahydrate (Sigma-Aldrich; ref: B9876) 0,1M at pH 8.5 for 10 minutes.
- Incubate overnight at 4ºC with primary antibody against BrdU 1:100 (Santa-Cruz; ref: sc-51514) in blocking solution.
- Wash three times with PBS 0.1M.
- Add the secondary fluorescent antibody FITC-conjugated anti-mouse IgG (Ref.: F-9137, Sigma-Aldrich, 1:400) diluted in the blocking solution and incubate for 1h at room temperature.
- Wash three times with PBS 0.1M.
- Incubate for 5 minutes with Hoechst 33258 (Sigma-Aldrich) 5µg/ml in PBS 0.1M.
- Wash three times with PBS 0.1M.
- Mount the sections in gelatinised slides and protect with Vectashield (Vector laboratories ref: x-0517) and cover-slides.

The visualisation was made with a fluorescent microscope (Olympus Optical SA: ref BX-41).

4.8.2-Double immunofluorescence

Brain sections 50 µm thick were used to locate stem cell markers (Nestin 1:400 ref: sc-21247 Santa Cruz, CD133 1:100 ref: ab-16518 Abcam, OPN 1:300 ref: sc-21742 Santa Cruz, Notch-1 1:200 ref: bs-1335R Bioss) and to identify the relation of stem cells with tumoural vasculature (LEA 1:100; Sigma-Aldrich; ref: L0401, Von-Willebrand factor 1:100 ref: ab-7356 Millipore), BBB (GluT-1 1:200 ref: 07-1401 Millipore, EBA 1:200 ref: SMI 71 Sternberger) and other structures (GFAP 1:400 ref: sc-6170 Santa Cruz, MAP-2 1:200 ref: M4403 Sigma , VEGF 1:200 ref: sc-152Santa Cruz). The immunofluorescence technique was carried out in 24 well plates with the following mix of the primary antibodies as stated in Table 3.

Policlonal Ab / Monoclonal	GFAP	VEGF	Glut-1	Notch-1	CD133	Von-Willebrand

Ab						
Nestin	Done	Done	Done	Done	Done	-
EBA	-	-	Done	-	-	-
MAP-2	Done	Done	-	-	-	Done
LEA	-	-	-	-	Done	-
Osteopontin	Done	Done	-	Done	-	-

Table 3: Double immunofluorescences performed in the 50 µm thick criotome sections.

The secondary antibodies cocktail was formed of FITC-conjugated anti-mouse IgG (Ref.: F-9137, 1:400, Sigma-Aldrich) and TRITC-conjugated anti-rabbit IgG (Ref.: T-6778, 1:400, Sigma- Aldrich) (Fig. 11).

From step 5 onwards, the experiment is carried out in dark conditions, because the secondary antibodies are attached to fluorochromes.

- Firstly the sections were washed twice with PBS 0,1M.
- The sections were placed in a blocking solution of PBS 0.1M+BSA 5% (Sigma-Aldrich; ref: A7906) + Triton X-100 0.5% (Sigma-Aldrich; ref:T-6878) for 2 hours.

- Add the primary antibodies diluted in the blocking solution as previously described and incubate overnight at 4º C.
- Wash three times with PBS 0.1M.
- Add the secondary fluorescent antibodies diluted in the blocking solution and incubate for 1h at room temperature.
- Wash three times with PBS 0.1M.
- Incubate 5 minutes with Hoechst 33258 (Sigma-Aldrich) 5µg/ml in PBS 0.1M.
- Wash three times with PBS 0.1M.
- Mount the sections in gelatinised slides and cover with Vectashield (Vector laboratories ref:x-0517) and cover-slides.

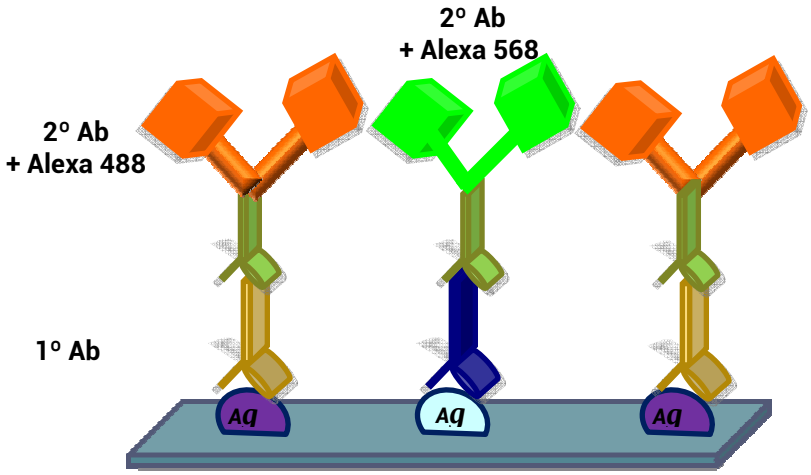

Figure 11: **Schematic representation of a double immunofluorescence** with different primary antibodies attached to their specific antigens. Then specific secondary antibodies with fluorescent binding are added. The result can be viewed with a fluorescent microscope.

4.9-Quantitative studies

4.9.1-Positivity index for Nestin, Osteopontin, Ki-67 and BrdU

We calculated the positivity index for Ki-67, Nestin and Osteopontin in 85 gliomas classified in three different degrees of malignancy according to previous work carried out in our laboratory (Bulnes et al., 2009), 31 of grade I, 24 of grade II and 30 cases of grade III.

To calculate the positivity index of Nestin and Osteopontin , 400 tumour cells were counted at high magnification (×400) with a reticule of 62500 μm^2, from the most representative area of the tumour, and the percentage of cells expressing the antigen was reported. We only counted the positive cells that were not in contact with the vessels and only when the cells were located individually, and not when they appeared as dense aggregations of cells. KI-67 index was quantified the same way, but counting the positive nuclei.

Only the cells inside the quantification grid and the cells in contact with two external sides were counted (as shown in Fig. 12).

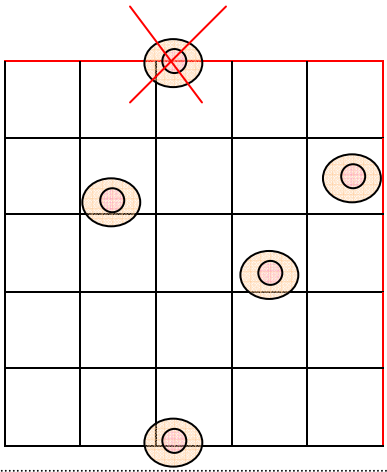

Figure 12: Scheme of the quantification grid and the cells that are counted.

4.9.2-Nestin expression vs. cell proliferation

We calculated the number of BrdU and Nestin-positive cells/mm^2 in 21 cases: 6 of grade I, 6 of grade II and 9 of grade III. To calculate this data we counted the number of BrdU positive cells in five different and representative areas of the tumour. Brain sections were visualised using a fluorescent microscope (Olympus BX41). Controls without primary antibody showed no staining. Then the means of BrdU and Nestin positive cells per mm^2 were calculated.

In order to avoid the inter-observer variability factor, the quantitative evaluation was performed by the same researcher.

4.9.3-Quantification of Nestin spheroid aggregates

We also counted the number and density of Nestin+ intratumoural aggregates in the same cases as the positivity index for Nestin, counting as an aggregate a group of six or more Nestin-positive cells. Finally, the area of the clusters, segregated into 8 from stage I; 67 from stage II and 134 from stage III tumours, was calculated using *Image J* software, measuring the area with the freehand selection tool (Fig. 13).

Quantifications were performed by the same researcher in order to avoid inter-observer variability.

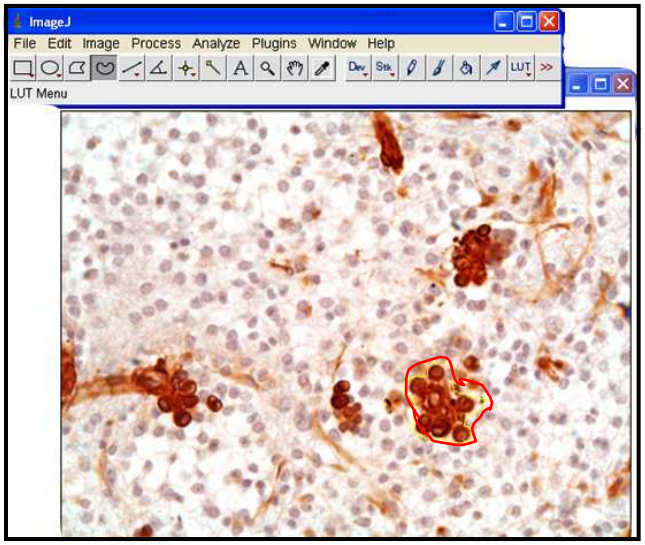

Figure 13: Representation of Nestin+ aggregates quantification with Image J software.

4.10-Statistical analysis

All the statistical analysis was performed using *GraphPad Prism 5.00*.

For the behavioural analysis, ANOVA tests were performed when 3 groups were available, and a t-test when there were only 2 groups to compare.

For differences in the mean age of tumour apparition, a t-test was performed.

An unpaired *t-test* was used to analyse differences among the averages of Nestin, its niches and Osteopontin positivity index. To compare Nestin and proliferation indexes, a *r* of Pearson was performed.

Data is described as mean ± SEM. A p value less than 0.05 was considered statistically significant.

V.-Results

5.1-Clinical diagnosis

This part of the study was performed in order to establish an early and non-invasive way to diagnose, or at least to suspect, CNS tumours, before the rats develop severe clinical symptoms (cachexia, abnormal posture or respiratory difficulties).

5.1.1 Evaluation of general welfare status

For this analysis we have separated the ENU-exposed rats into two groups according to the score obtained in the adapted tests from Morton & Griffith: rats with a welfare score=0 (without physical symptoms of disease) and rats with a welfare score >0 (with physical symptoms of disease). No parameter was altered in a way that drew attention.

From the homecage system (Phecomp cage) and open-field tests we have obtained the data shown in Table 4. The weight was measured before the homecage stay and then food and water intake, % of time moving, number or rearings, total distance walked, and % of exploration were recorded. In this table, we have separated male and female rats and the mean and standard deviation for each parameter is shown. The data is shown for each time when the tests were carried out, in order to observe the temporal variation of the studied parameters.

The results of the Table 4 show that female rats from the 7^{th} month onwards, and the male rats from 6^{th} months onwards, only displayed a welfare score=0, because the animals with physical symptoms were sacrificed as has bee previously described. The data shows that there is a huge variability in the studied parameters among all the rats, and many times there is no pattern in the parameters along time.

The majority of the behavioural differences were observed in the homecage stay test, rather that in the open-field test. We can observe that many parameters tend to decrease from the control group to the “score=0 group" and even more to the “score>0 group", but this does not always happens. On the other hand, in many of the cases there is more variability

in the numerical values of any parameter of the “score=0 group" and the “score>0 group" than in the control group. This can be explained because in these groups there are rats in different states of health, expanding the variability.

A surprising fact is that in some cases, the rats in the “score=0 group" and the “score>0 group" weigh less than control rats, despite of having a bigger food intake and having made a greater amount of movement.

MALE

	Homecage							Open-field			
Age and condition	**Weight (g)**	**Food (g)**	**Drink (ml)**	**Distance (m)**	**Rearing (n)**	**% interior**	**% movement**	**Distance (cm) open**	**Rearing (n) open**	**% interior open**	**% movement open**
4 months control	413.8± 9.465	27.08± 3.13	18.15± 2.3	62.31± 11.05	1299± 218.3	18.41± 2.42	16.53±0.65	-	-	-	
4 months score=0	352.0± 28.6 **	19.35± 2.03	18.45± 1.95	68.87± 2.43	1212± 186	18.39± 2.84	16.6±0.52	-	-	-	-
4 months score>0	295.0± 40.41 ***, #	16.63± 5.65	14.62± 4.90	51.37± 10.81 *, #	527± 99.4	14.1± 4.67	13.7±2.49	-	-	-	-
5 months control	433.8± 4.8	13.10± 7.865	27.18± 5.979	75.79± 5.63	1732± 700.9	30.70± 11.38	17.99± 1.05	-	-	-	-
5 months score=0	351.7± 21.4***	19.67± 8.54	22.63± 6.985	79.83± 20.57	1181± 682.7	21.97± 7.014	18.16± 3.46	2439± 398.8	53.83± 13.88	3.62± 1.66	51.38± 8.28
5 months score>0	286.7± 40.4 ***, ##	8.92± 15.45	11.18± 18.76	56.36± 10.96	863.7± 378.0	10.63± 7.92 *	15.90± 3.35	1858± 526.8	40.33± 4.91	1.57± 0.47	68.27± 2.97

	Weight (g)	Food (g)	Drink (ml)	Distance (m)	Rearing (n)	% interior	% movement	Distance (cm) open	Rearing (n) open	% interior open	% movement open
6 months control (n=4)	453.8± 2.4	24.38± 3.96	27.95± 3.88	81.93± 44.41	2470± 1804	27.48± 7.814	18.48±2.16 1	-	-	-	-
6 months score=0	365.0± 21.1 *	30.4± 3.72	22.53± 2.26	82.3± 17.52	2013± 2030	17.54± 11.74	18.28±7.26 7	2052± 1418	35.40± 22.35	6.360± 5.849	61.46±13. 68
7 months control	445.0± 21.8	21.36± 1.03	26.55± 2.23	114.8± 37.5	2034± 538.3	8.6± 3.39	24.68±1.7	1321± 72.1	41.5± 15.5	2.17± 1.01	61.28±2.8
7 months score=0	335.0± 25.0 *	-	23.96± 6.72	74.12± 43.5 **	2881± 625.5	17.65± 3.05	15.1±0.7 **	457± 258 *	10.09± 2.6 *	0.35± 0.35	30.35±10. 6 *
7.5 months control	508.8± 8.8	18.58± 4.19	28.01± 5.27	67.67± 5.92	2415± 559	21.7± 3.96	16.03±1.39	639± 268	6.5± 3.88	10.75± 0.6	39.05±11. 1
7.5 months score=0	382.5± 17.5 **	17.22± 7.36	13.18± 7.62	78.46± 8.25	1373± 536	18.7± 5.8	17.05±2.15	810± 356	0.5± 0.5	16.9± 16.6	42.4±13.1

FEMALE

	Weight (g)	Food (g)	Drink (ml)	Distance (m)	Rearing (n)	% interior	% movement	Distance (cm) open	Rearing (n) open	% interior open	% movement open
4 months control	268.8± 22.13	18.64± 3.94	20.76± 1.81	84.87± 8.6	1020± 88	20.18± 0.92	28.97± 3.28	-	-	-	
4 months score=0	209.1± 22.44 ***	16.69± 1.32	19.21± 1.64	90.65± 3.95	1054± 67	21.12± 2.58	25.99± 6.55 ***	-	-	-	-
4 months score>0	164.5± 22.57 ***, ###	3.29± 1.7 ***, ###	4.28± 2.54 ***, ###	45.34± 2.68 ***, ###	418± 163 ***, ###	18.25± 5.81	12.16± 0.68 ***, ###	-	-	-	-
5 months control	300.0± 35.82	16.55± 4.83	22.51± 10.47	89.06± 16.27	1090± 541.8	29.43± 25.37	21.19± 2.58	4110± 1050	42.00± 9.764	11.63± 4.884	73.93± 31.96
5 months score=0	249.4± 24.04 *	23.44± 5.23	30.24± 14.82	104.9± 34.06	947.2± 353.7	21.80± 11.79	21.20± 5.02	3215± 1092	41.44± 14.38	6.54± 4.03	71.30± 12.23
5 months score>0	193.3± 36.70 ***, ##	19.05± 10,60	15.04± 8.99	76.60± 29.26	709.3± 540.0	21.52± 16.60	20.83± 7.03	3002± 751.7	49.33± 19.06	6.85± 4.99	56.43± 18.08

	Weight (g)	Food (g)	Drink (ml)	Distance (m)	Rearing (n)	% interior	% movement	Distance (cm) open	Rearing (n) open	% interior open	% movement open
6 months control	328.8± 25.94	20.80± 10.73	31.33± 9.034	94.45± 14.32	1026± 363.2	18.18± 4.882	19.84±1.73	-	-	-	-
6 months score=0	263.3± 25.17	14.53± 2.102	16.49± 16.03	87.18± 42.29	749.3± 444.5	16.80± 14.88	16.35±6.27	3366± 1661	40.00± 13.11	7.93± 4.15	79.07±13.4
6 months score>0	213.8± 48.61 **	10.31± 10.30	8.405± 10.34 *	67.02± 34.64	430.0± 444.1	18.33± 14.70	16.50±7.69	1797± 1080	22.13± 21.48	5.66± 4.79	49.06±6.8 #
7 months control	317.5± 18.87	14.37± 5.52	22.24± 6.05	109.3± 1.2	761.3± 79.67	15.05± 3.47	24.68±1.8	4106± 230	22.50± 1.31	9.87± 1.56	66.25±9.13
7 months score=0	275.0± 15	17.69± 0.01	34.31± 15.26	70.54±5.2 **	798.5± 177.5	26.5± 18	15.1±0.7 **	2293± 155 **	22.35± 9.50	3.15± 2.05	45.45±26.05
7.5 months control	333.8± 12.8	16.82± 5.89	19.74± 5.29	1224± 11.7	1837± 398	30.5± 3.6	23±2.1	4486± 349	30.01± 5.20	13.15± 3.33	79.93±2.9
7.5 months score=0	270.0± 20 *	14.29± 2.81	25.93± 0.31	597.8± 57.1 **	950.5± 293	10.35± 2.64 *	13.46± 0.8 **	2339± 633 *	10.03± 2.10	2.45± 0.35	46.1±12.1 *

	Weight (g)	Food (g)	Drink (ml)	Distance (m)	Rearing (n)	% interior	% movement	Distance (cm)	Rearing (n)	% interior	% movement
8 months control (n=4)	342.5± 10.31	20.19± 9.19	31.6± 5.38	67.21± 3.27	673.5± 91.5	12.3± 4.47	15.8±1.17	-	-	-	
8 months score=0	307.5± 57.5	18.05± 2.01	20.94± 4.9	153.0± 77.4	843.8± 101.23	63.25± 10.85 **	27.33±10.33	-	-	-	-

Table 4: **Mean of the measured parameters after the homecage stay and open-field test**. Standard deviation is represented. Grey boxes represent significant statistical differences; * means significant statistical difference rewarding control group, and # means significant statistical difference rewarding score=0 group.

As we can see in Table 4, it is not possible to determine the status of the animals only with the welfare score of the modified Morton & Griffith table (because there are behavioural alterations in both the "welfare score=0" and the "welfare score>0" groups). Nevertheless, the Morton & Griffith test helped us to further define the groups to study behavioural alterations.

The variable that most changed in any group with respect to controls was the weight. Nevertheless, this alone does not provide enough information about the health status, and therefore we analysed the behavioural parameters individually.

5.1.2 Individual behavioural analysis

For this study, the same parameters as the ones used before were compared to the mean value of the control group for their age (shown in Table 5). Individual values of each test were considered abnormal when they were outside the 95% Confidence Interval (CI) of the mean, which implies there is a statistically significant difference compared with the control group.

We have not taken into account the weight of the rats, since we have seen that there is a decrease of the mean weight in the rats at all ages in comparison to control rats (70% of the time it was a significantlly statistical difference ($p<0.05$). Only in one of the 74 performed tests did the open-field test provide more information than the homecage stay. In all other cases, the open-field test did not provide extra information over the homecage.

Only one rat did not develop any tumour, so the total number of tests passed by ENU-exposed rats that developed at least one tumour was 74. From these 74 tests, Table 5 shows the relationship between the welfare score and the alterations in the behavioural parameters of the total tests performed.

Behavioural parameters	Morton & Griffith welfare score: Score=0 (n=53)	Score>0 (n=21)	
No alterations *vs* control mean (n=31)	0.392 (n=29) **A**	0.027 (n=2)	0.419
Increase in any value *vs* control mean (n=19)	0.257(n=19) **B**	0.0 (n=0)	0.257
Decrease in any value *vs* control mean (n=24)	0.054 (n=5)	0.270 (n=19) **C**	0.316
	0.724	0.276	1

Table 5: Contingency table representing the different groups of rats and their welfare score. N means the total tests performed in each category. Group A (green) are rats in good health status, Group B (orange) are rats without physical symptoms but an increase in any of the measured parameters and Group C (red) show physical symptoms observable with the Morton&Griffith test and a decrease in at least one parameter.

The results in Table 5 show that from 21 animals that started the test with a score >0, only two cases showed an increase in any of the variables studied (6.5% of the time). In all other cases (93.5%) the rats displayed a decrease in at least one of the variables. Not having variations in any variable correlated positively (in 93.55% of the cases) with a healthy state of the rat (indicated by a score=0). An increase in the behavioural parameters correlated at 100% with a welfare score=0.

This table also shows 3 big groups of rats with a specific welfare score and behavioural tests correlation. Rats in Group A show a welfare score of 0 with no alterations in the homecage or open-field tests (these would be

healthy rats); Rats in Group B , that are rats in a state of alarm, prior to showing physical problems in the welfare test; and finally, there is Group C, that are rats with physical symptoms of the tumours. The mean time that rats took to go from Group A to B is of 34.8 days, and from Group B to Group C of 29.8 days. We also calculated the mean elapsed time for the rats that went directly from Group A to Group C finding that this was 29.6 days (very similar to the time for going from Group B to Group C).

From 24 rats that started with a score=0 and had any alteration in the behavioural variables with respect to controls, 19 of them showed an increase in one or more of the variables, compared with control rats (82.6%). Only in the remaining 4 cases did we observe a decrease in variables, after a score=0 in the welfare table. Two of these cases were from the same rat that developed an extra-CNS tumour (breast tumour). In the other two instances, the rats developed a glioma.

Observing the chronology of behavioural evaluation (followed by the rat's death) in Table 6, it can be observed that of all the rats that were sacrificed after the first evaluation (4^{th} month of age), 61.5% of cases belong to Group C, which means that 8 rats made their debut in the most severe group. The rest of the animals at this timepoint belonged to Group A. These lasts were sacrificed without having behavioural alterations. In total, 42% of rats from Group C only passed the first behavioural test. Remaining cases sacrificed after the 2^{nd} and 3^{rd} evaluations, came from asymptomatic groups (5 cases from Group A and 6 from Group B).

After the second evaluation, only half of the sacrificed rats belonged to Group C (5 rats came from Group A and one from Group B). Nevertheless, there were also a 25% of rats that were sacrificed belonging to Group A and the other 25% belonging to the group with no behavioural parameter altered and “welfare score>0” or decrease in behavioural parameters and “welfare score=0”

In the third evaluation, it is possible to observe the expected tendency in these rats; they started belonging to Group A in the first evaluation, evolved to

Group B in the second one and lastly ended into Group C just before being sacrificed.

Rats that survived more than 7 months do not show any pattern in their behavioural parameters over time.

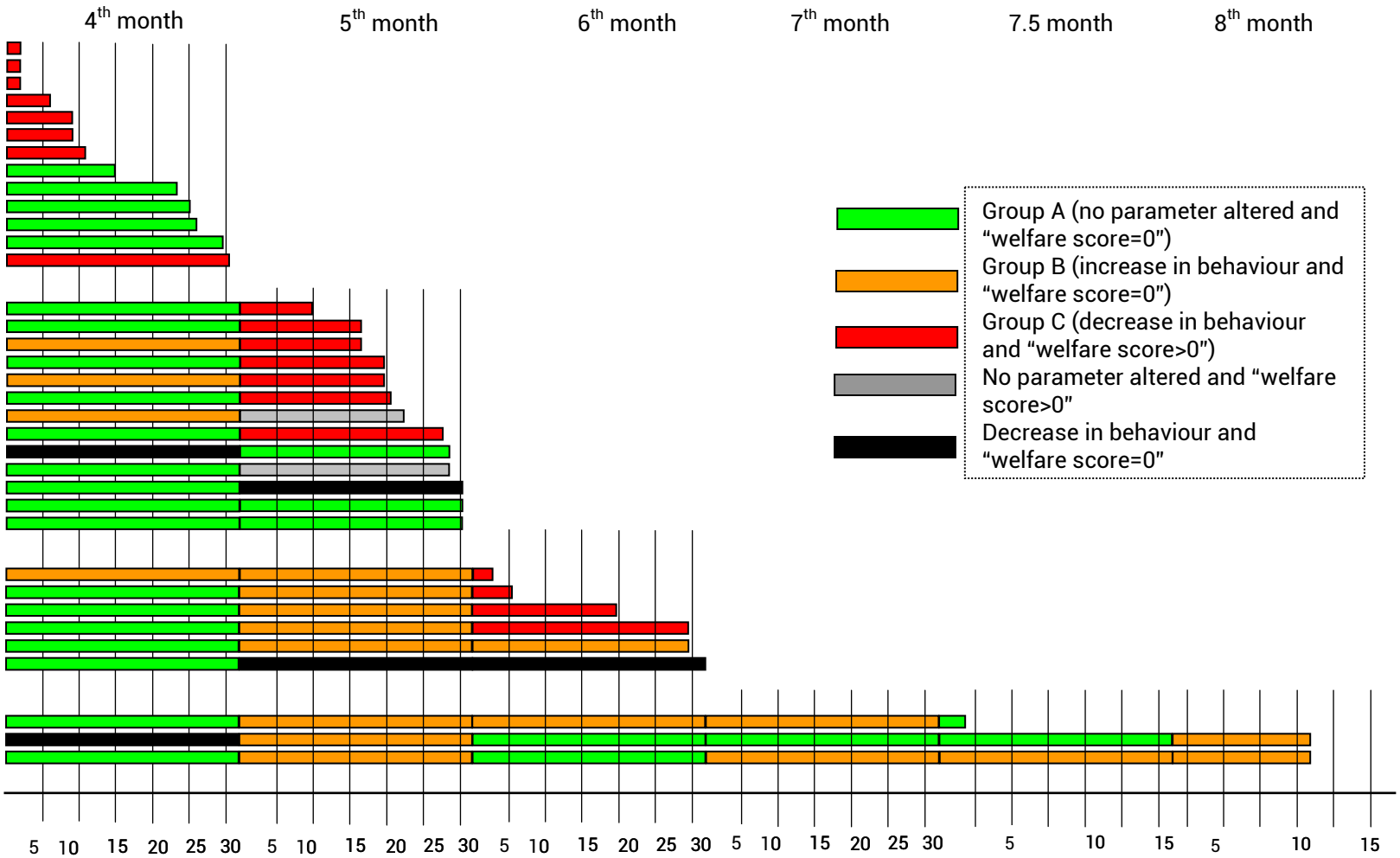

Table 6: **Chronology of the behavioural evaluations and the end point of the studied animals.**

Finally, we observed that the most repeatedly altered parameter *vs.* control rats in Groups B and C was the distance run as seen in the Table 7. Rats in Group B mainly had differences in parameters related with the mobility (distance and rearings), while rats in Group C had differences *vs.* control group regarding intake parameters (water and food intake).

	4 months	5 months	6 months	7 months	7,5 months	8 months
Group B	Rearing (n=4)	Distance (n=4)	Distance (n=2) % moving (n=2)	Distance (n=4)	Distance (n=3) % interior (n=3)	Distance % moving % interior
Group C	↓ Food (n=7) ↓ Drink (n=7)	↓ Distance (n=7)	↓ Distance (n=4) ↓ Drink (n=4)			

Table 7: The most repeated parameters that were altered in ENU-exposed rats *vs* control rats. Parameters in Group B were increased vs control and in Group C are decreased.

5.1.3-Survival time depending on behavioural status

The survival time after the last behavioural tests shows that rats that belong to Group A, and were sacrificed in this status (n=9) lived a further of 23.8±3.1 days (median= 26; range=3-31) after the tests. Rats from Group B rats that were sacrificed in this status (n=3) have a slightly shorter survival time, with 16.03±7.0 days (median=9; range=9-30) and Group C rats (n=19) that were sacrificed in this status have only 14.11±2.15 days (median=11; range=3-31) of mean survival time. There is a statisticallly significant difference between the Groups A and C (*$p \leq 0.05$). The mean survival time is slightly higher in the rats in Group A, than in those in Group B, but there is no statistically significant difference (Fig. 14).

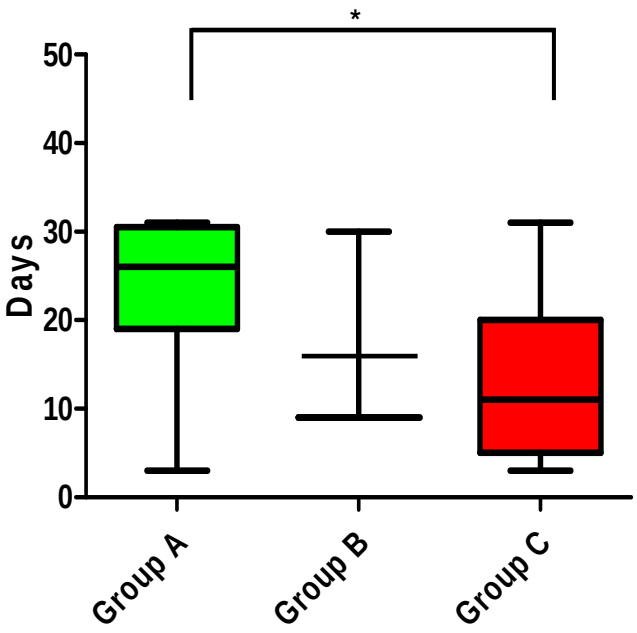

Figure 14: Mean survival time of the rats after the behavioural tests. The rats with a score higher than 0 in the welfare test and a decrease in any variable in the test were the rats with lower survival time. There is a statistically significant difference between Group A and Group C.

5.2-Tumour analysis

For this part of the study we used several techniques in order to correctly classify the tumours induced after the ENU-prenatal administration. These tumours were classified into: intracranial intraaxial tumours, intracranial extraaxial tumours, spinal cord tumours and extra-CNS tumours.

5.2.1-ENU-induced tumour incidence

From the 94 sacrificed rats, at least one tumour was identified in 88 of them, so the incidence of tumour development was 93.61%. Our results show 30 extraaxial tumours that in some cases grew together with the intraaxial tumours. The total number of tumours developed is shown in Table 8. Besides 62 rats with at least one intracranial tumour (some rats displayed more than one at the same time), there were also 4 spinal tumours (composed of liquid protuberances) in the last third of the medulla, associated with the nerves of the sacro-lumbar zone. Finally, two breast masses were detected and only 6 rats had not developed any tumour at sacrifice time.

CNS tumours	% Incidence (n=94)
Total tumours	93.62
Intracranial intraaxial	65.96
Intracranial extraaxial	31.91
Spinal cord tumours	4.25

Table 8: Incidence (number of rats that show at least one tumour) of the different tumours induced after the prenatal exposure to ENU.

5.2.2-Intracranial tumour diagnosis

The intracranial tumours are divided into intraaxial tumours (which are gliomas of different malignancy; including multifocal gliomas) and extraaxial tumours. Extraaxial tumours after prenatal exposure to ENU have been previously reported to be schwannomas and meningiomas (Zook and

Simmens, 2000), but are not the primary object of this study. In total, gliomas including a multifocal location were found in 35% of the rats, who developed 91 gliomas overall.

5.2.2.1-Intraaxial tumours

The MRI study of 13 rats at the 5th and 6th month of age showed that rats did show intracranial tumours as soon as this age. In total we could observe 20 tumours; 12 of them were intraaxial tumours and 8 were extraaxial. In the MRI, T1 and T2 images showed hyperintense signals for mid and advanced intraaxial tumours (later identified as gliomas), whereas small sized, less malignant tumours only showed hyperintense signals in T2 (Fig. 12), without gadolinium capture in T1. Advanced-stage tumours show heterogeneous T1 signalling and a more homogeneous hyperintense signalling of T2. The intraaxial tumours showed histopathological features similar to human gliomas e.g.: diffuse infiltrating border, necrotic areas, haemorrhages, cysts, cellular anaplasia, nuclear atypias, high mitosis and vascular proliferations among others. There is a predominance of oligodendroglial-like tumours.

According to these characteristics and the previous work carried out in our laboratory (Bulnes-Sesma et al., 2006), we have classified the intracranial intraaxial gliomas in three different stages:

Stage I gliomas correspond to cell proliferations with small to middle size cells proliferations forming well-delimited tumours, mainly associated with subcortical white matter (Fig. 15 j). They are made up of isomorphic round cells, with well-defined regular nuclei (Fig. 15 m), a clear halo around them and fine microvessels constituting a network mimicking normal brain microvasculature.

Stage II gliomas are mainly constituted by anaplastic tumours of small, round cells typical of oligodendrogliomas. Macroscopically, these tumours appear as a soft mass of tissue with small foci of haemorrhages (Fig. 15 k).

These tumours show sporadic cellular aberrations such as nuclear polymorphism (Fig. 15 n).

The advanced and most malignant **stage III** is equivalent to anaplastic oligodendroglioma or glioblastoma multiforme. Macroscopically, they usually have a lot of red zones of haemorrhages and they also usually have big cysts and brown/yellow necrotic areas (Fig. 15 l). These tumours are characterised by having many cellular aberrations such as nuclear and cellular polymorphism, atypical mitosis, and other features like necrosis and haemorrhages (Fig. 15 o). In this stage we can also find many vascular abnormalities like glomeruloid vessels and vascular proliferations.

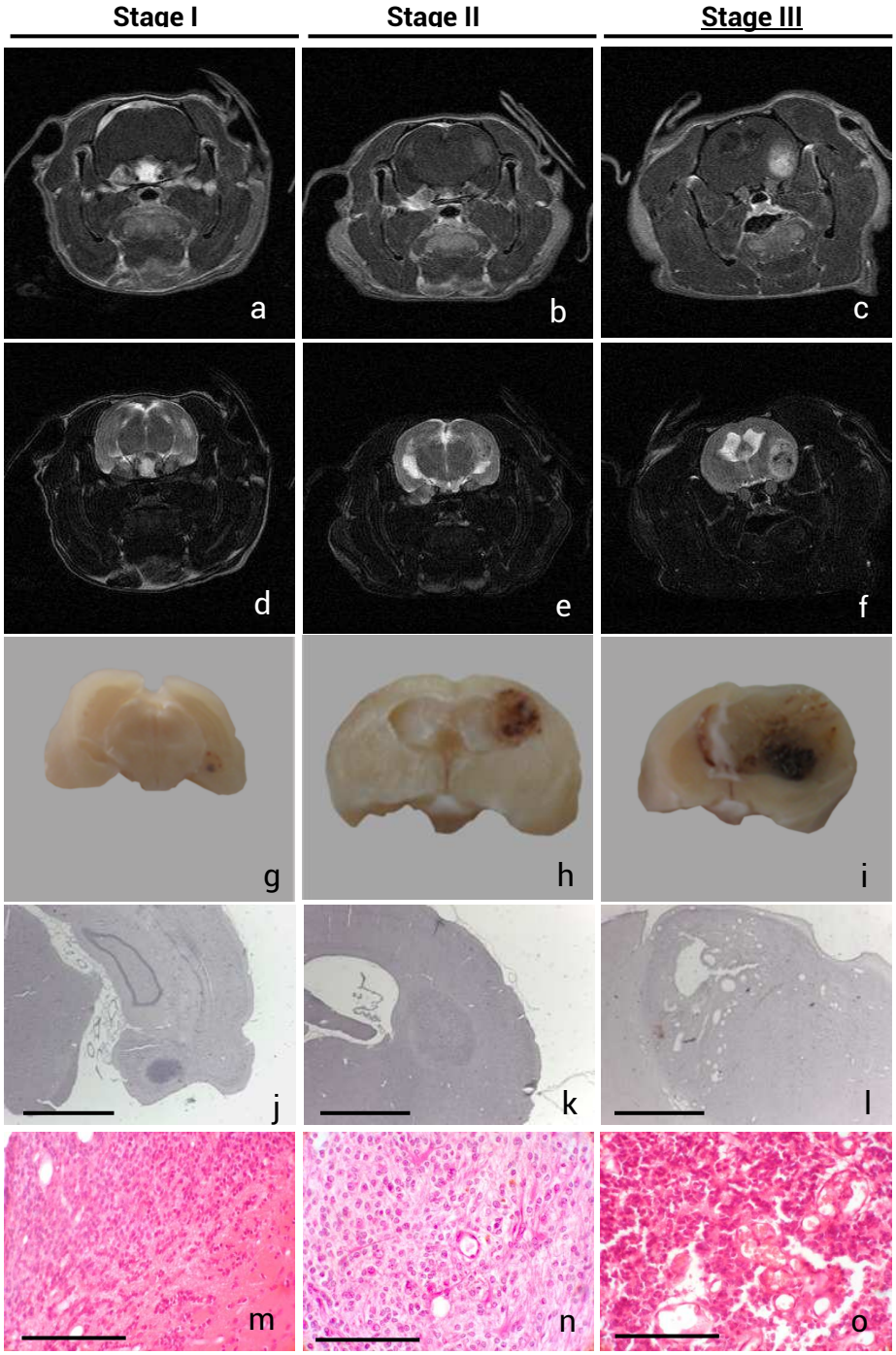

Figure 15: ENU-gliomas identification via MRI and H/E staining. T1 images of gliomas with hyperintese signal in stage II and III gliomas (**a-c**), T2 images of the same gliomas with hyperintense signal in all stages gliomas (**d-f**), macroscopic view of gliomas after the rats perfusion (**g-i**), H/E staining of gliomas of different stage at lower magnification (**j-l**), H/E staining of the tumours at higher magnification (**m-o**). Scale bar (j-l)= 2.5 mm, scale bar (m-o)= 25 µm.

In total, 91 gliomas had developed by the age of sacrifice in the rats prenatally exposed to ENU. The classification according to their malignant characteristics showed 31 stage I gliomas, 33 stage II gliomas and 27 stage III gliomas, as shown in Table 9.

ENU-glioma stage	% (N=91)
Stage I	34.07
Stage II	36.26
Stage III	29.67

Table 9: Percentage of gliomas developed in each stage of development. N means the total number of gliomas

5.2.2.2-Extraaxial tumours

We could also observe in the MRI images, and macroscopically after the sacrifice of the rats, other intracranial ENU-induced tumours, which we have denominated extraaxial tumours (Fig. 16). These tumours were usually situated under the brain and were associated with the 5th cranial nerve. Sometimes the tumours also spread over the brain, as though they were wrapping it. When extraaxial tumours keep growing, they press against the brain, causing it to deform. Macroscopically, they are white and do not infiltrate the brain. In the MRI images, extraaxial tumours are more easily observed as a heterogeneous hyperintense signal in the T1 images with gadolinium capture (Fig. 16 a-c).

Histopathologically, we have described the extraaxial tumours as high cellular-density tumours (Fig. 16 g, h), with haemorrhagic process and hemosiderin deposits, as we can see in Figure 16 i. Extraaxial tumours did not usually show necrotic areas; only the most malignant ones have necrosis. According to previous research and to work carried out in our laboratory, they are malignant peripheral nerve stealth tumours (MPNST) (Bulnes-Sesma et al., 2006) positive for S-100 and negative for GFAP and NF, and meningiomas (Zook et al., 2000).

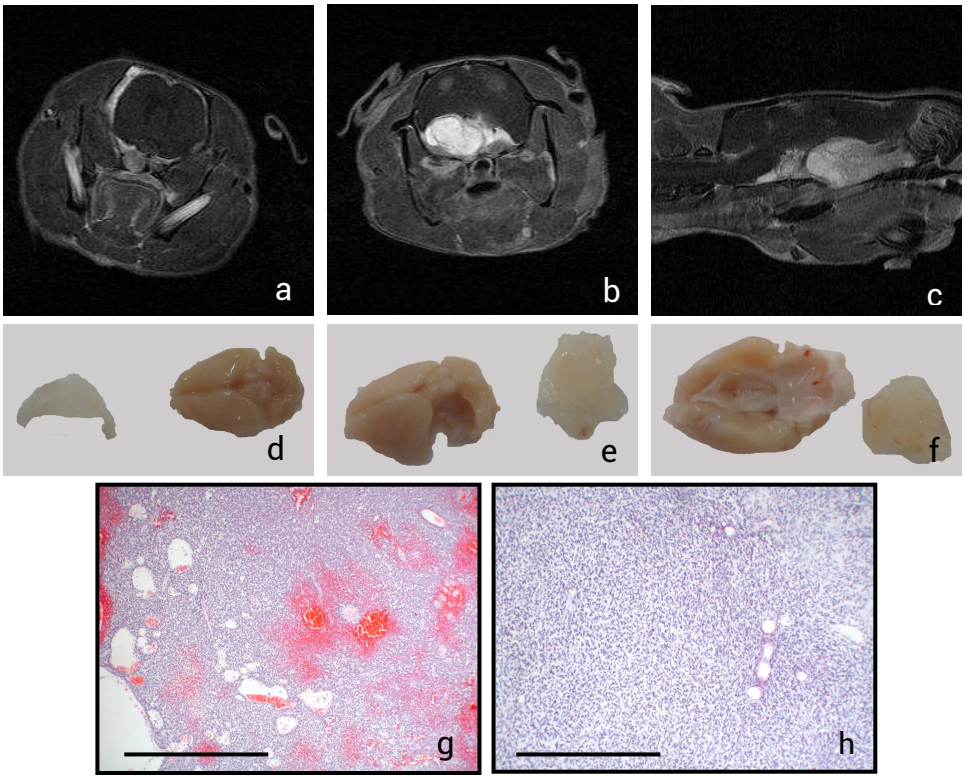

Figure 16: Extraaxial tumours identification via MRI and HE/staining. a-c: T1 MRI images of extraaxial tumours. **d-f**: microscopical view of the extraaxial tumours. **g, h**: H/E staining of the extraaxial tumours showing their characteristical hemorrages and cellular density. Scale bar= 2.5 mm.

5.2.3-Mean rat survival time and tumour classification

According to the age of death of the rats and the consequent tumoural identification, we calculated the mean survival time of the different intracranial tumours. When one or more tumours appeared, we took into consideration the tumour with the highest degree of malignancy, grading them from highest to lowest degree of malignancy: stage III glioma, extraaxial tumours, stage II glioma and stage I glioma. The age of sacrifice of all the rats ranged from 113 to 276 days of age (Fig. 17).

Looking at the data, extraaxial tumours and stage I gliomas are the CNS tumours with the shortest survival times, with a mean age of 178 days of age,

while stage III gliomas are the ones with the longest survival times, with a mean age of 215 days.

Tumour	Mean survival time (days)
Stage I gliomas	178.5±20.43
Stage II gliomas	195.6±7.81
Stage III gliomas	215.3±5.91
Extraaxials	178.6±9.41

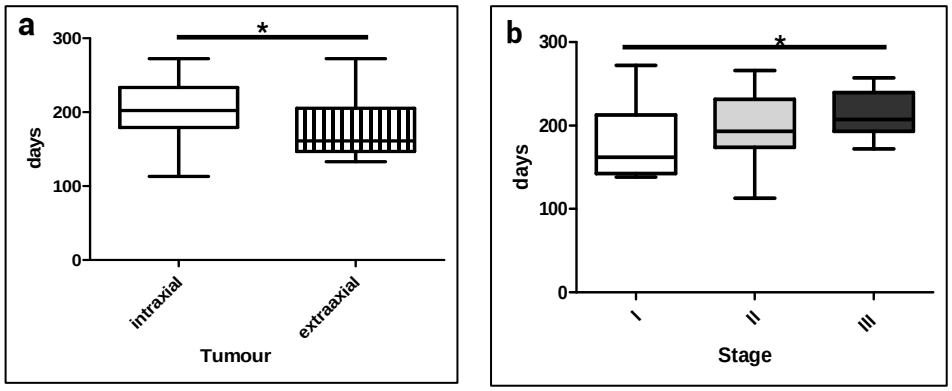

Figure 17: Mean survival time of apparition of the CNS tumours induced by ENU prenatal exposure.
There is a significant difference in the mean age of intraaxial *vs* extraaxial tumours, *p≤0.05 (**a**). Mean age of all the intraaxial tumours (divided in stage, I, II, III tumours), and it can be observed a statistical significant increase in the mean time of apparition between stage I and III, *p≤0.05 (**b**).

5.2.4-Correlation of clinical diagnosis with the classification of ENU tumours

After the histopathological classification of the ENU-tumours, we tried to see if there is a clear correlation between the altered parameters and the diagnosed tumours. As we can see in Table 10, only in the case of rats with gliomas there is a parameter (distance) that was altered when the rats did not showed clinical symptoms (and they had a welfare score=0). As previously mentioned, we did not take the weight into account, because it is altered at almost all ages after exposure to ENU.

	Most altered variable
Glioma	↑ Distance (60%)
Extraaxial	None
Spinal cord	None
Extra CNS	↓ Distance and ↓ in all open-field variables

Table 10: Most times altered variables in rats with the different classified tumours developed in the rats with welfare score=0, excluding the weight. 60% of the rats that were identified with a glioma, had previously an increase in the distance run during the homecage stay prior to symptoms.

5.3-Stemness markers expression and distribution

Nestin is the leading stem cell immunomarker used in this study. This antibody is expressed in all stages of ENU-glioma, and its expression increases significantly as tumoural malignancy increases. In the gliomas, Nestin expression can be found in cells that show different morphologies and tumour distribution in the different stages.

5.3.1-Nestin expression in the different stages

After the quantification of psotovity index of Nestin (mean number of Nestin+ cells) in the three stages of the gliomas, we have clearly observed an increase in Nestin expression within the glioma progression. In the initial stage the positivity index for Nestin is 5.26 ± 0.60 (n=30), in the intermediate stage is 10.25 ± 0.91 (n=25) and 15.94 ± 1.27 in the most advanced stage (n=31) (Fig. 18).

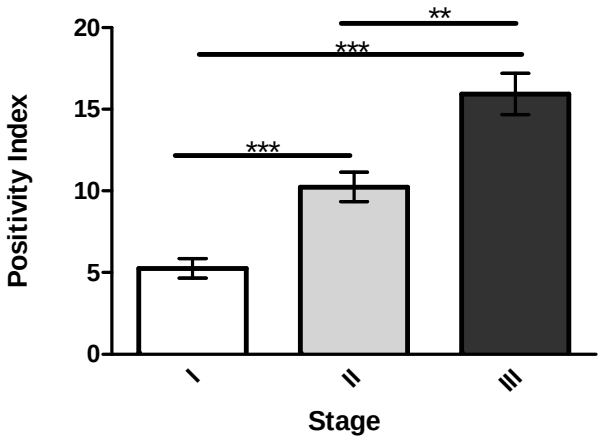

Figure 18: Index of Nestin positivity in all stages. There are significant statistical differences between stage I *vs* stage II (***p≤0.001), between stage I *vs* stage III (***p≤0.001) and between stage II *vs* stage III (**p≤0.01).

BrdU and Ki-67 indexes were both quantified to assess the degree of malignancy of ENU-gliomas. After quantifying the index of BrdU expression (Fig. 19 a), we found that its expression is increased during tumour development with astatistically significant difference between stage I (81.6±3.6 n=6) and stage II (147.1±12.1 n=6) with p≤0.0001 (***) and stage I and stage III (171.6±14.66 n=9) with p≤0.0001 (***). Nestin quantification in the same cases (Fig. 19 b) showed a statistically significant difference between all stages. Stage I (80.82 ± 5.216 n=6) and stage II (118.7 ± 5.261; n=6); p≤0.001 (***), stage I and stage III (144.7 ± 3.342; n=9); p≤0.001 (***) and stage II and stage III; p≤0.01 (**).

Ki-67 expression has been previously evaluated in 26 cases, which were also quantified for Nestin in Fig. 18. The expression of this antibody also increases with the tumoural development and is significantly different between all groups (Fig. 19 c).

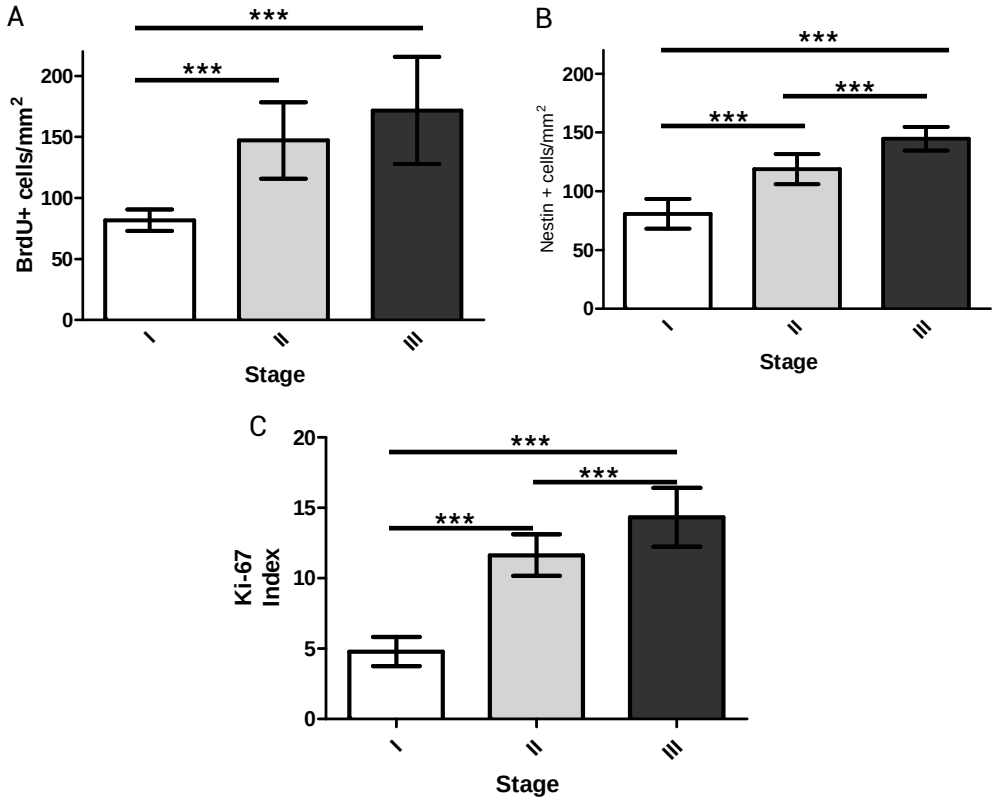

Figure 19: Proliferation markers quantification. **a**) BrdU positive cells/mm^2 BrdU expression increases significantly as the gliomas grow, **b**) Nestin positive cells/mm^2 in the same tumours also get increased. **c**) Ki-67 positivity index. Increases as well significantly.(**p≤0.01, ***p≤0.001)

After performing a correlation test, the results show a statistical significance using the "r of Pearson" coefficient in Nestin *vs.* BrdU (*** p≤0.001) and Nestin *vs.* Ki-67 (*** p≤0.001). These data suggest a positive correlation between the expression of BrdU, Ki-67 and Nestin markers. Unfortunately, double staining of Nestin and BrdU could not be performed.

5.3.2-Distribution of stemness markers in the different stages

Nestin-positive cells can be found from stage I of ENU-gliomas as cells with a big cytoplasm and large prolongations, and are found scattered throughout the tumoural mass (Fig. 20 c) and in a few cases we have observed Nestin+ cells forming groups of small round cells with scarce cytoplasm and hyperchromatic nuclei that we have called "spheroid aggregates" (Fig. 20 f). At the second stage of glioma development, Nestin is

expressed in two different patterns; around slightly tortuous vessels as perivascular expression or as "spheroid aggregates". The expression of Nestin in the most malignant stage depends on its location; in the interior of the tumour there are many of these aggregates of very different sizes (with a tendency to be increasingly big as the number of these arrangements increases). Adjacent to the aberrant vessels, such as the dilated and glomeruloid-like vessels appear numerous isolated Nestin-positive cells forming the perivascular expression, and in addition there is a border expression with large elongated cells showing positivity for Nestin distributed heterogeneously. It is also very frequent the find Nestin-positive cells inside the pseudopalisades surrounding the necrotic areas of advanced stage gliomas (Fig. 20 i).

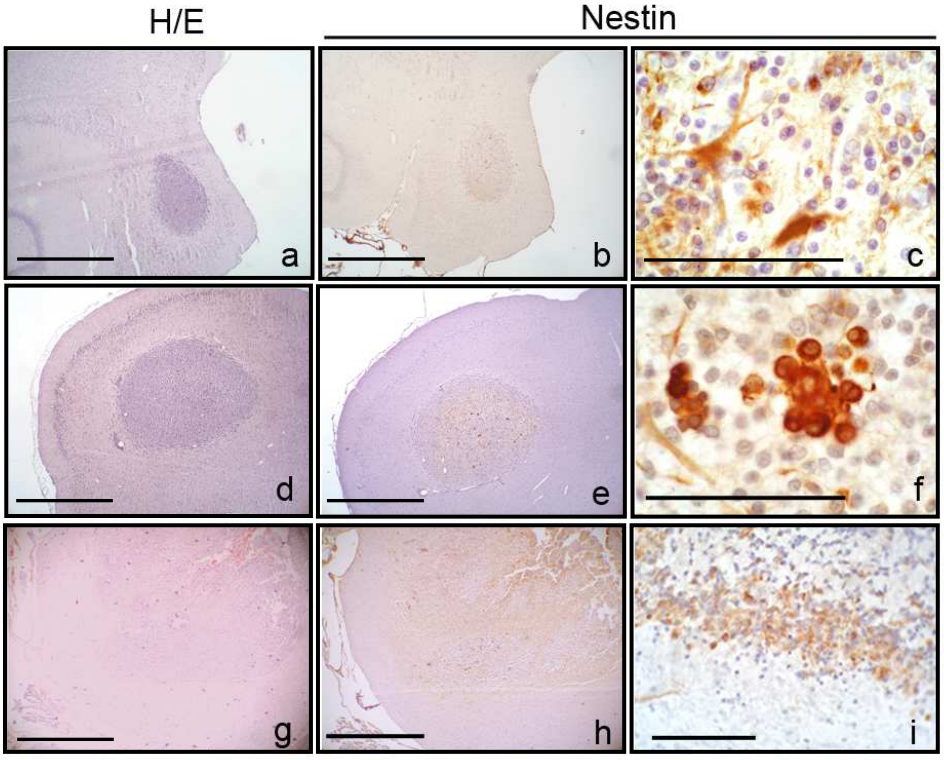

Figure 20: H/E staining and Nestin immunohistochemistry during glioma development. **a, b:** In the first stage of ENU-gliomas there are few Nestin-positive cells, distributed randomly inside the tumour (**c**). In the intermediate stage (**d, e**) some expression in spheroid aggregates begins to appear (**f**). In the most advanced stage (**g, h**) there is Nestin expression around the necrosis forming pseudo palisades. (**i**).Scale bar (**a, b, d, e, g, h**) =2.5 mm; scale bar (**c, f, i**) =10 µm.

Nestin expression is located directly adjacent to the vessels, around the wall of the aberrant vessels. Nestin-positive cells are found around all types of vessel and display large cellular prolongations. Nestin perivascular expression can be observed around the tortuous vessels (Fig. 21 a, b), as well as around dilated vessels (Fig. 21 c), frequently in patches, and is greates around the glomeruloid-like vessels (Fig. 21 d).

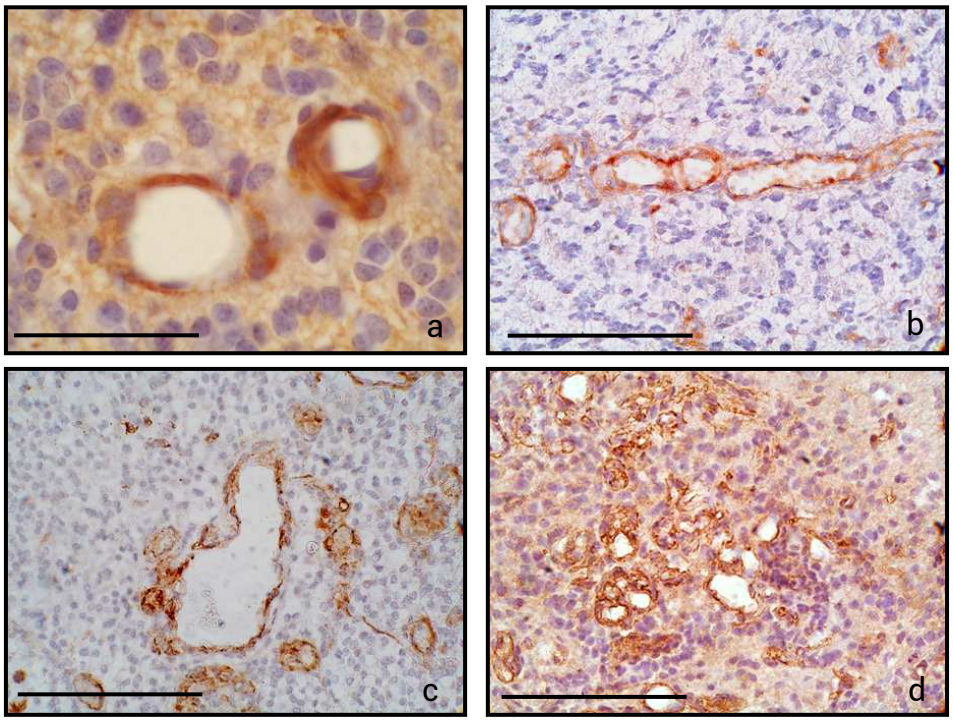

Figure 21: Nestin immunohistochemistry around tumoural vasculature. Nestin is expressed close to the endothelium in the slightly aberrant vessels (**a, b**), around huge dilated vessels (**c**), and around the most aberrant vessels; glomeruloids (**d**).Scale bar (**a**) =10 µm; scale bar (**b, c, d**) =25 µm.

Spheroid aggregates are characterised as being groups of at least six cells positive for Nestin. Cells in these aggregates have a characteristic morphology, with a small, round small cytoplasm and few or no cytoplasmatic prolongations. The aggregates appear in all the stages of glioma development and tend to form a circular shape (Fig. 22), differing greatly in their size; some of them consist of just six cells (Fig. 22 a, c) while others are clearly bigger, with a great number of cells (Fig. 22 b, d). The huge aggregates tend to

maintain the shape and mostly, the cells inside maintain their morphology. However, sometimes we observed cells with cellular prolongations and some vessels (mostly, but not exclusively) in the border or inside the aggregates.

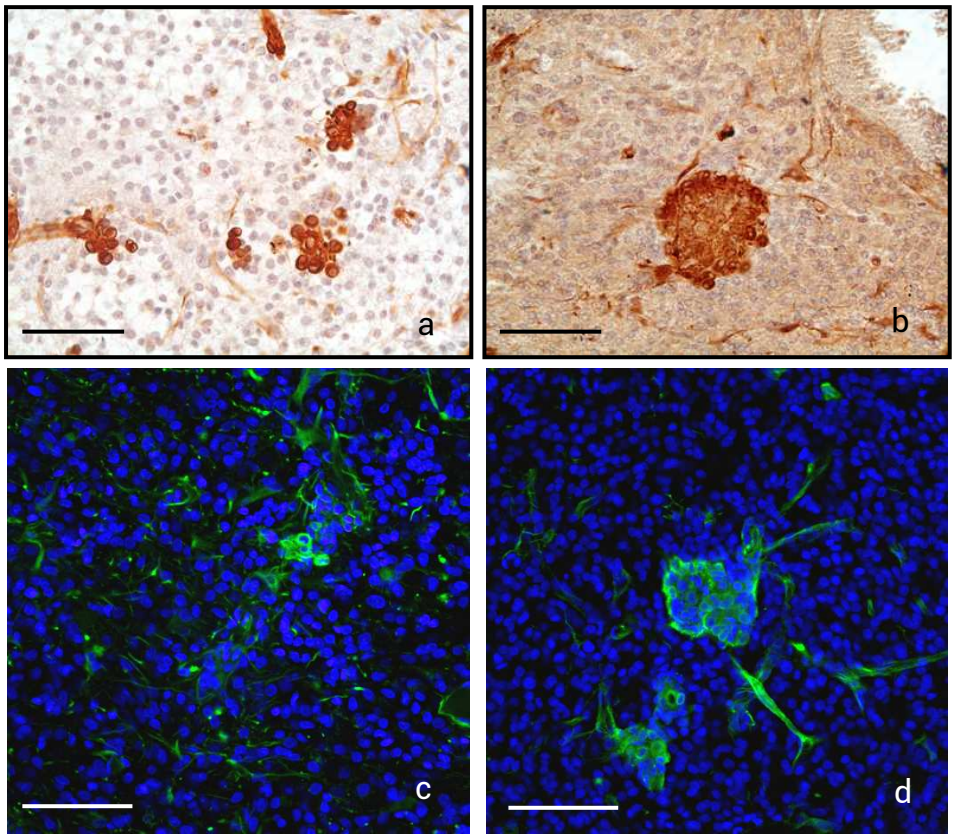

Figure 22: Different "spheroid aggregates" that we observed with Nestin. Immunohistochemistry (a, b) and immunofluorescence (c, d). **a**) and **c**) show Nestin aggregates composed of few cells. **b**) and **d**) show bigger spheroid aggregates, with occasional fibbers of Nestin, besides the small round cells. Scale bar =75 µm.

In addition to Nestin expression, some ENU-glioma cells express other stem cells markers like CD133, Osteopontin and Notch-1.

CD133 expression in the tumour can only be observed in stages II and III around aberrant tumoural vessels as perivascular expression (Fig. 23) or

forming part of "spheroid aggregates" (Fig. 23 c), similar to Nestin expression.

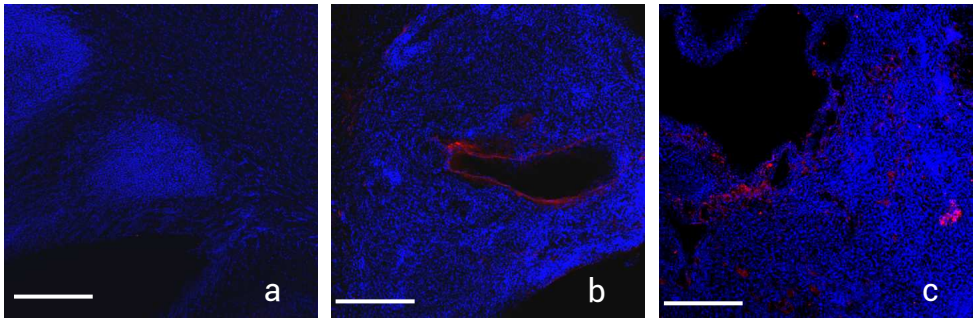

Figure 23: Immnunofluorescence against CD133 in the different stages of glioma development. Stage I gliomas (**a**) do not show CD133 positivity, CD133+ cells can only be seen in stages II (**b**) and III (**c**) of glioma development (**b, c**). CD133+ cells are located around the abnormal vasculature or forming spheroid aggregates inside the tumoural mass (**c**). Scale bar=1 mm.

Osteopontin expression begins in the first stage (Fig. 24 a) as isolated cells inside the tumoural mass, but is in stages II (Fig. 24 b) and III (Fig. 24 c) that the OPN-positive cells appear distributed mostly around the tumoural border.

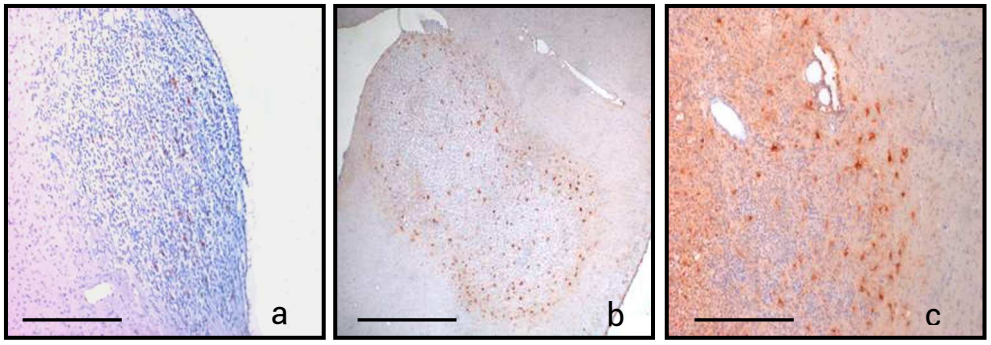

Figure 24: Immunohistochemistry against OPN in the different stages of glioma development. OPN cells can be seen since the early glioma stages., but it is only during the most malignant stages (**b, c**) that its expression gets organized in the tumoural border. Scale bar =1 mm.

OPN quantification showed an increase in its expression as tumoural malignancy increases. In the initial stage, positivity index for OPN is 4.11 ± 1.52 (n=6), in the intermediate stage is 8.60 ± 1.14 (n=14) and 11.43 ± 1.03 in the most advanced stage (n=8). We have appreciated a statistical increase in OPN expression between stage I and stage II $p \leq 0.05$ and stage I *vs.* stage III $p \leq 0.01$ (Fig. 25).

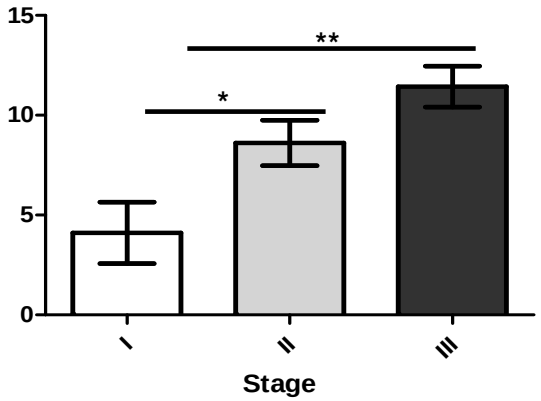

Figure 25: OPN quantification in the different glioma stages showing an increase in its expression. There are statistical significant differences between stage I *vs* stage II (*$p \leq 0.05$) and stage I *vs* stage III (**$p \leq 0.01$).

Notch-1 expression could only be observed as fibrilar cells in the border and peritumoural area in stages II and III (Fig. 26 b), and sometimes in the interior in lesser amounst and without any pattern (Fig. 26 c). There is an increase in the area covered by Notch-1 expression as the gliomas become malignant, but we have not quantified it.

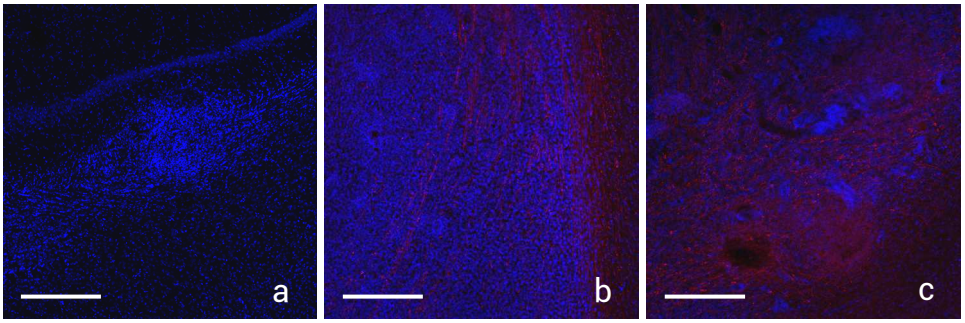

Figure 26: Immunofluorescence against Notch-1 in the different stages of glioma development. In stage I gliomas (**a**) there is no Notch-1 positivity, but in the border of the malignant stages (**b**) it is expressed, as well as in some areas of the tumour interior (**c**). Scale bar =1 mm.

Following the results of the location of Nestin and other stem cell markers, it was found that the expression of Nestin and other markers depends on the degree of malignancy of the glioma and their location inside the tumour as follows:

As regards the hypoxic interior area of mild to advanced gliomas, Nestin- and CD133-positive cells appear mainly as intratumoural aggregates of cells taking spheroidal shapes. There is also expression of Nestin and CD133 around tortuous and hyper-dilated vessels. In the tumoural border, the majority of the Nestin+ cells appear around the glomeruloid vessels. There is positivity for CD133 around these types of vessels. In the border isolated cells positive for Nestin are also shown. There are also isolated OPN-positive cells and Notch-1 expression in this zone. Both OPN and Notch-1 are very slightly expressed in the interior of the tumour.

5.3.3-Perivascular expression of markers related to stem cells

The ENU-induced tumours show a high vascular density with many vascular aberrations. These aberrations are all the typical vascular features that are also present in human gliomas; like tortuous vessels, vascular wall proliferations and vascular glomeruloids.

In the ENU-gliomas we have observed three categories of vascular aberrations; those are, in order of malignancy: tortuous vessels, present since the first stage of glioma development (Fig. 27 b); huge dilated vessels present since stage II of glioma development (Fig. 27 c) and glomeruloid-like vessels (Fig. 27 d), present only in the most malignant stage.

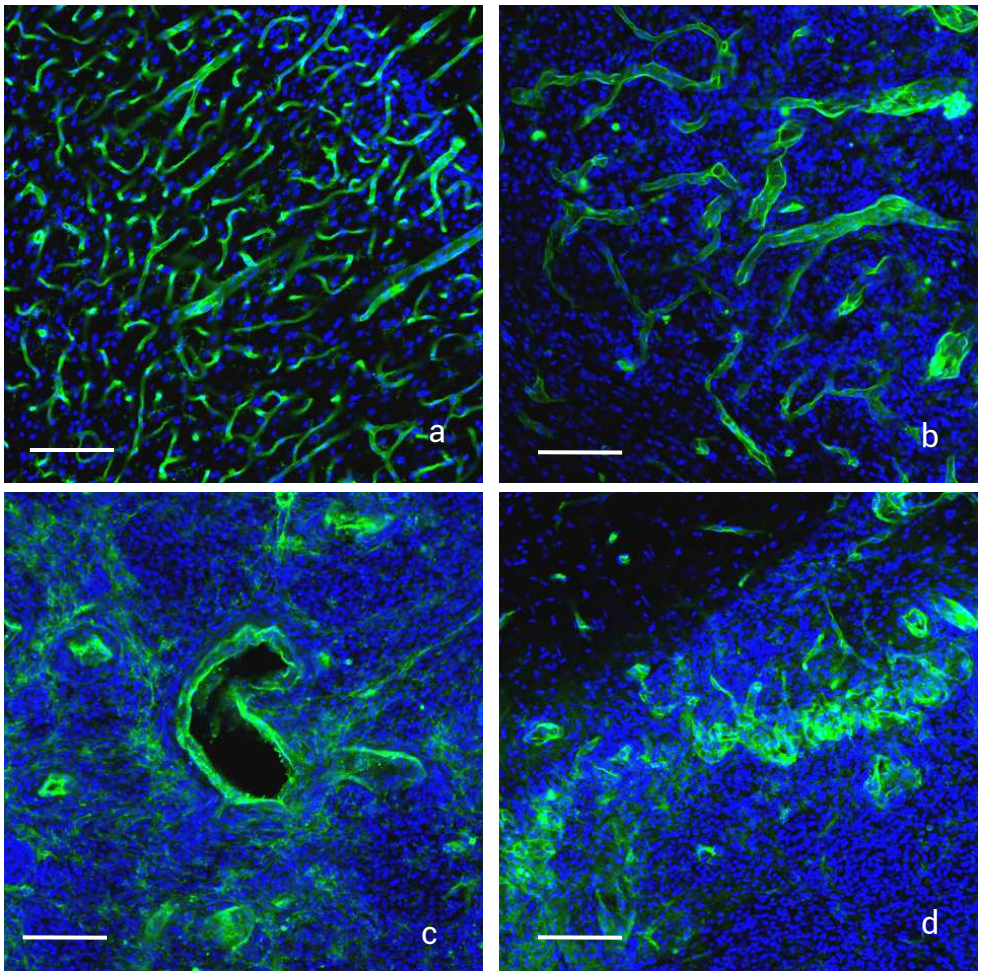

Figure 27: Morphology of the vessels marked with LEA during glioma development. a) There can be observed normal vessels, **b**) tortuous vessels that appear when the tumour is not very malignant. In the most malignant gliomas there can be seen **c)** hyper-dilated vessels as well as glomeruloids **d**), these lasts mainly in the border of the tumours.
Scale bar =50 μm.

The analysis of the BBB markers showed that both EBA (a protein expressed specifically by endothelial cells of rat brain barrier vessels) and GluT-1 are expressed on all types of aberrant vessels, but differently on each one. In the tortuous vessels, both markers are expressed in the endothelial cells and co-localizing (Fig. 28 a, d). Both markers also appear both co-localizing on hyperdilated vessels, but sometimes in patches. In glomeruloid-like vessels, GluT-1 expression remains, but EBA is sometimes totally unexpressed (Fig. 28 b, e). VEGF is expressed around all types of tumoural vessels, but slightly more intensely around dilated and glomeruloid vessels, and always more externally than the BBB marker EBA (Fig. 28 c, f).

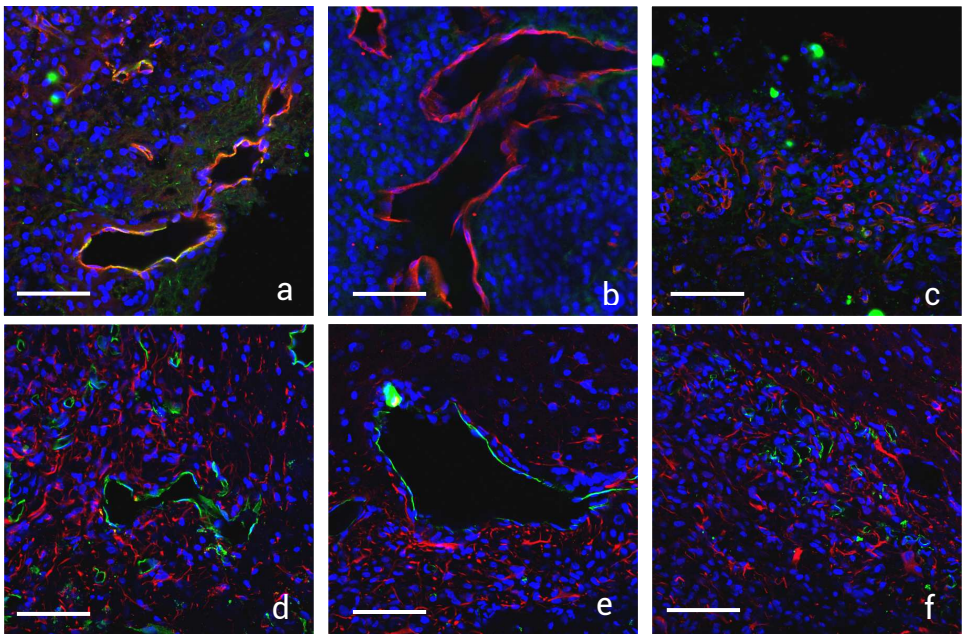

Figure 28: Immunofluorescence of BBB markers and GFAP in tumoural vasculature (**a-c**) EBA (green) and Glut-1 (red) and (**d-f**) EBA (green) with VEGF (red) in different types of vessels. Glut-1 can be seen around all types of vessels (**a-c**), while EBA expression gets lost in dilated (**b**) and glomeruoild-like vessels (**c**). VEGF is overexpressed around all types of vessels (**d-f**) Scale bar =75 µm.

Cells positive for Nestin are to be found around several abnormal types of vessels, such as the glomeruloid ones located directly adjacent to the vessel wall co-expressing slightly CD133. Cells positive for CD133 are located slightly externally from the Nestin+ ones around huge dilated vessels. CD133 is only slightly expressed around tortuous vessels (Fig.29 a, f, k).

CD133 is expressed externally in small and round cells outside and very close to the vascular endothelium marked with LEA in the hyperdilated vessels (Fig. 29 b, g, l) and both markers co-locate just slightly around the most aberrant glomeruloid vessels (Fig. 29 o).

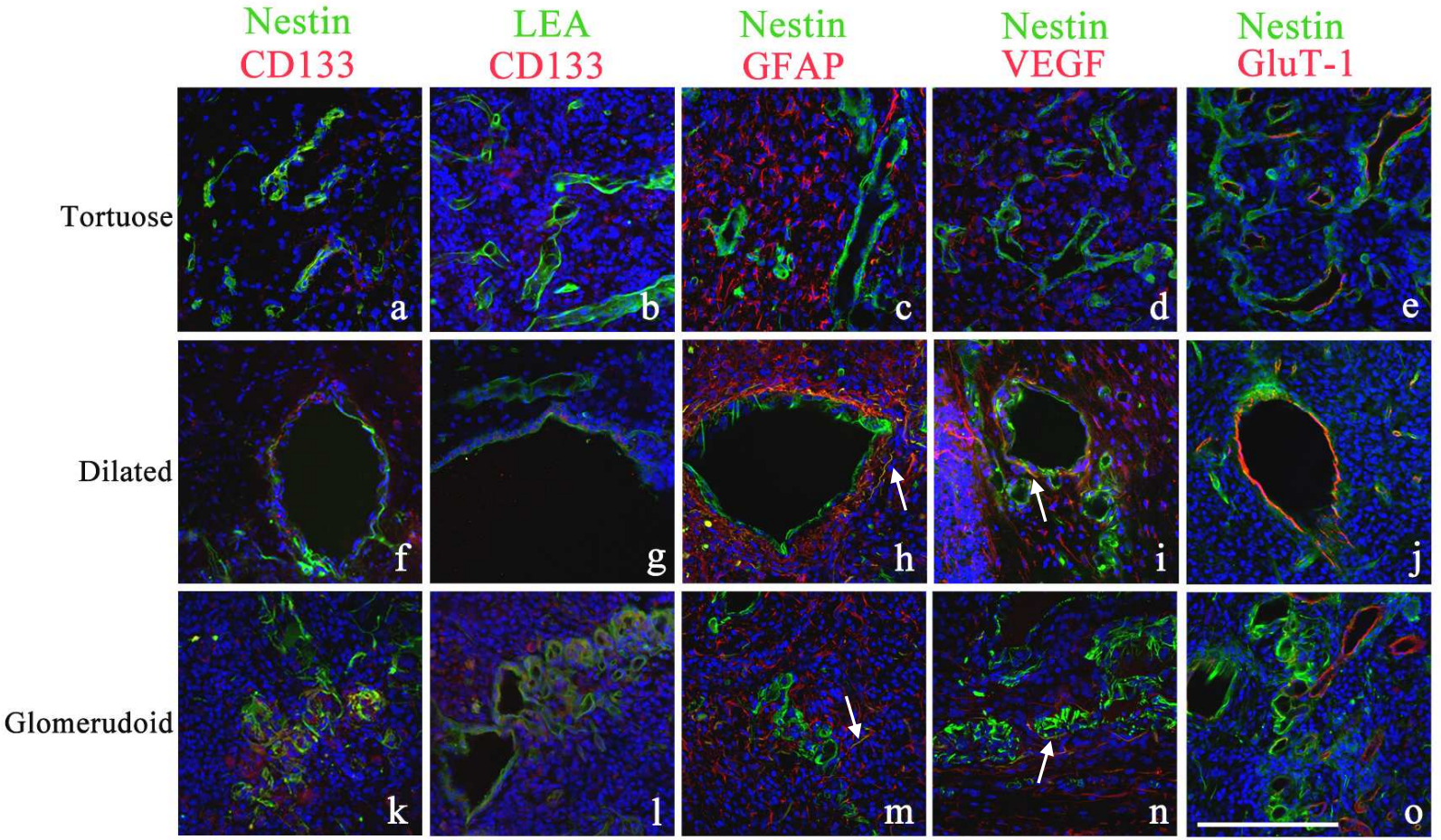

Figure 29: Colocation (yellow) of stem cell markers (Nestin and CD133) and other specific markers (VEGF, LEA, GFAP and Glut-1) in the perivascular subpopulation. All tumours are counterstained with Hoechst (blue). **a-c**) Perivascular aggregates of Nestin+ cells are displayed adjacent to the gluT-1 positive cells. All of these vessels maintain the glucose transport of the BBB, patched sometimes around glomeruloid vessels. There is co-expression of Nestin-CD133 only around the glomeruloid vessels (**i**). CD133 is expressed externally from LEA (**c, h, m**), with both markers co-expressing only slightly around glomeruloid vessels. There are more Nestin+ cells than GFAP+ (**d, i, n**) and VEGF+ (**e, j, o**) cells in the perivascular aggregate. Some of the Nestin+ cells co-express VEGF and GFAP (**i, j**). Scale bar =50 µm.

Perivascular Nestin+ cells have a slight co-expression with GFAP (Fig. 29 c, h, m) and VEGF (Fig. 29 d, i, n), around dilated and glomeruloid vessels. The few cells that co-express Nestin-GFAP and Nestin-VEGF (Fig. 29 h, I, m, n arrows) are not located directly at the vessels wall, because VEGF and GFAP are expressed more externally with respect to the vascular wall than Nestin, especially around the hyperdilated vessels. Nestin expression is located directly close to the BBB marker Glut-1 around the tortuous and glomeruloid vessels (Fig. 29 e, j), but when vessels become dilated (Fig. 29 o) Nestin expression moves away from the endothelial wall

Taking a closer look at the glomeruloid like vessels, we could clearly observe how Nestin is expressed (Fig. 30 a) internally compared to Glut-1. Nestin+ cells co-express with VEGF (Fig. 30 b) at some points of the glomeruloid vessels. CD133 expression co-localises with LEA expression (Fig. 30 c), even though there are more CD133+ cells surrounding these vessels than directly close to the endothelial wall.

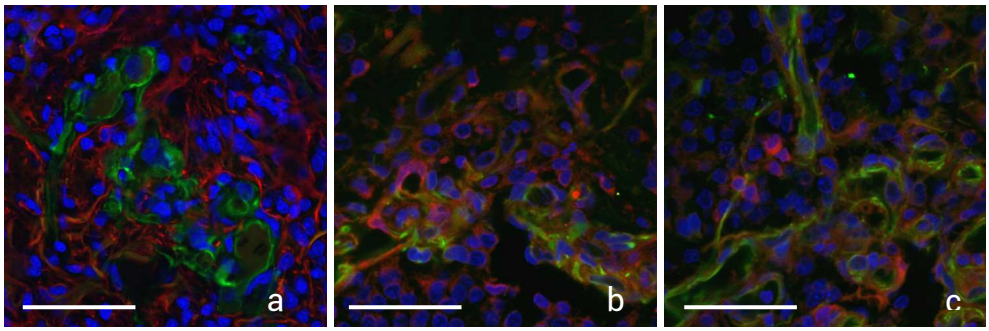

Figure 30: Double immunofluorescence of the glomeruloid vessels. **a)** Expression of Nestin (green) and Glut-1 (red) around glomeruloid-like vessels, with Nestin in an internal layer. **b)** Nestin (green) and VEGF (red) expression with colocation (yellow) around these vessels. **c)** LEA (green) and CD133 (red) with light colocation (yellow) at some points of the vessels. Scale bar= 25 µm.

We also observed MAP-2 staining around some tumoural vessels. MAP-2 is not expressed elsewhere inside the tumour, neither in the small proliferations (Fig. 31 a), nor in the most malignant gliomas (Fig. 31 b), but around some tumoural vessels in the most advanced stages, there is sometimes a small layer of cells positive for MAP-2 (Fig. 31 c). These MAP-2 cells are located externally with respect to the endothelial cells (Fig. 31 d), and do not co-express GFAP (Fig. 31 e).

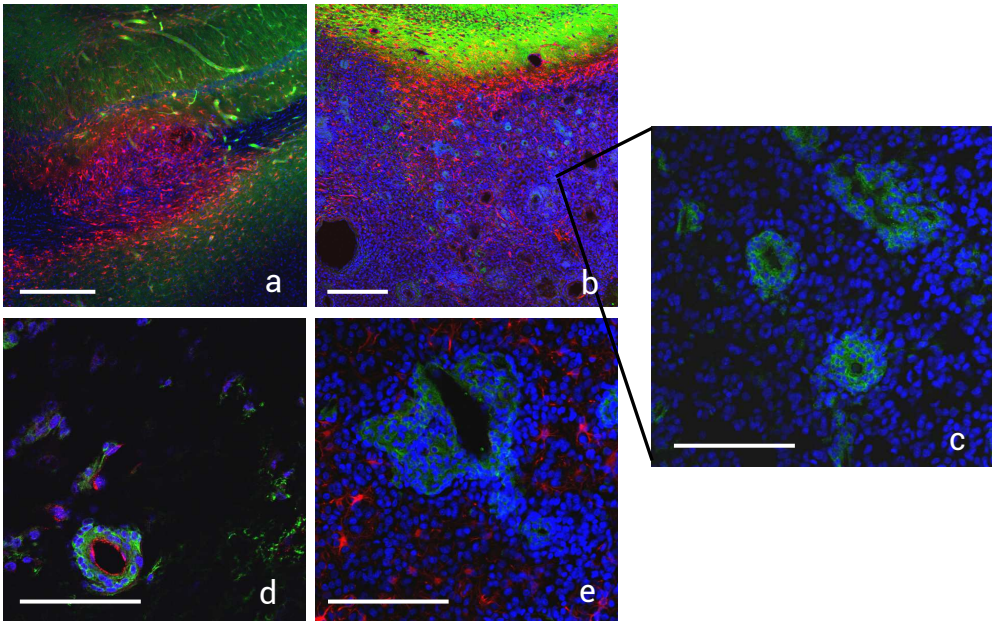

Figure 31: MAP-2 (green) expression in the ENU-gliomas a) There is no MAP expression inside the low grade gliomas with GFAP (red) positivity, **b**) in the high grade gliomas MAP is expressed strongly outside the tumour, with high VEGF (red) expression and sometimes around mildly aberrant vessels like show in **c**) and **d**) with MAP expressed around vessels positive for von Willebrand Factor (red). **e**) This Map-2 expression does not co-locate with GFAP cells around the vasculature (red). Scale bar (**a**) =1mm, scale bar (**b-e**) =50 µm.

5.3.4-Border expression of markers related to stem cells

The border of stage II and III gliomas is another area where we have observed stemness marker expression in the ENU-gliomas. There are cells in the border that are positive for the Nestin, Osteopontin and Notch-1 markers.

The Nestin-positive cells (Fig. 32 a) have an elongated morphology with many cellular prolongations. Osteopontin expression (Fig. 32 b) is to be seen as granules in the cytoplasm of some cells around the border. In the case of Notch-1 (Fig. 32 c), cells positive for this marker have a fibre-like (stringy) morphology and are abundant in the peritumoural area.

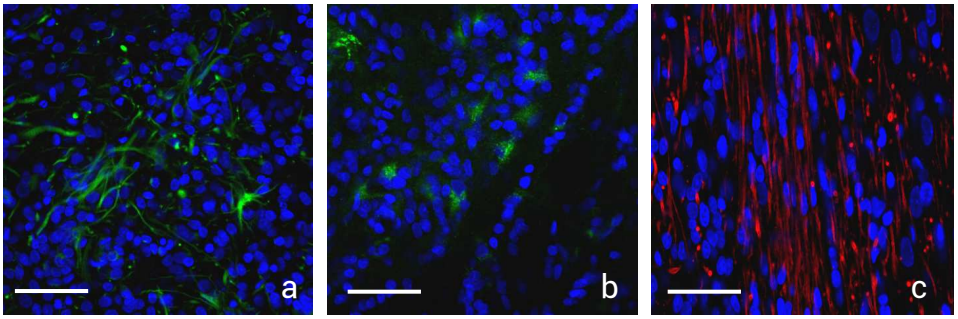

Figure 32: Immunofluorescence of Nestin (a), Osteopontin (b) and Notch (c) in the border area of the tumours. Nestin (a) is expressed in astrocyte-like cells with big cellular prolongations. OPN (b) is marked in the cytoplasm of many cells in the border and Notch-1 (c) expression is fibre-like surrounding the tumour
Scale bar =50 µm.

There are many cells positive for Nestin that appear isolated at the tumoural border in stages II and III (Fig. 33 a, b). These cells have a similar morphology to the scattered one found throughout the tumoural mass in the early stage (Fig. 33 c). These cells have astrocyte-like morphology, are positive for GFAP (Fig. 33 a) and sometimes for VEGF as well (Fig 33 b). Osteopontin is also expressed in the border for a subset of cells. Distribution of positivity is as lumps inside the cytoplasm and many of the Osteopontin-positive cells co-locate with GFAP (Fig. 33 c) and VEGF (Fig. 33 d) displaying their astrocytic morphology as well.

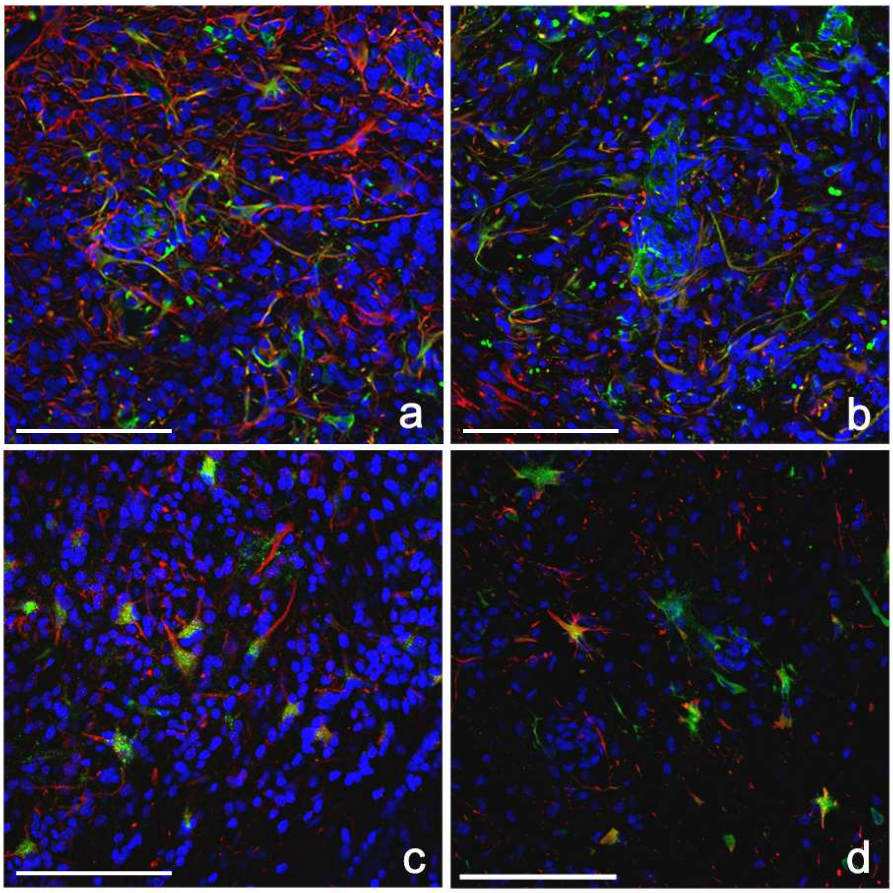

Figure 33: Double immunofluorescence of Nestin (green) with VEGF (a, red) and GFAP (b, red) and Osteopontin (green) with VEGF (c, red) and GFAP (d, red) in the tumoural border. There is some co-location (yellow) of Nestin and VEGF around the tumour and a bit less of Nestin and GFAP. OPN positive cells co-locate intensely in the border both with GFAP and VEGF. Scale bar =50 µm.

As previously mentioned, Notch-1 is expressed in the borders of the gliomas as a fibrilary expression (Fig. 34 a). It has no relationship with Nestin expression (Fig. 34b), or with the vasculature of the border (Fig. 34 c). Notch-1 and OPN expressions are complementary in the cytoplasm of some cells (Fig. 34 d).

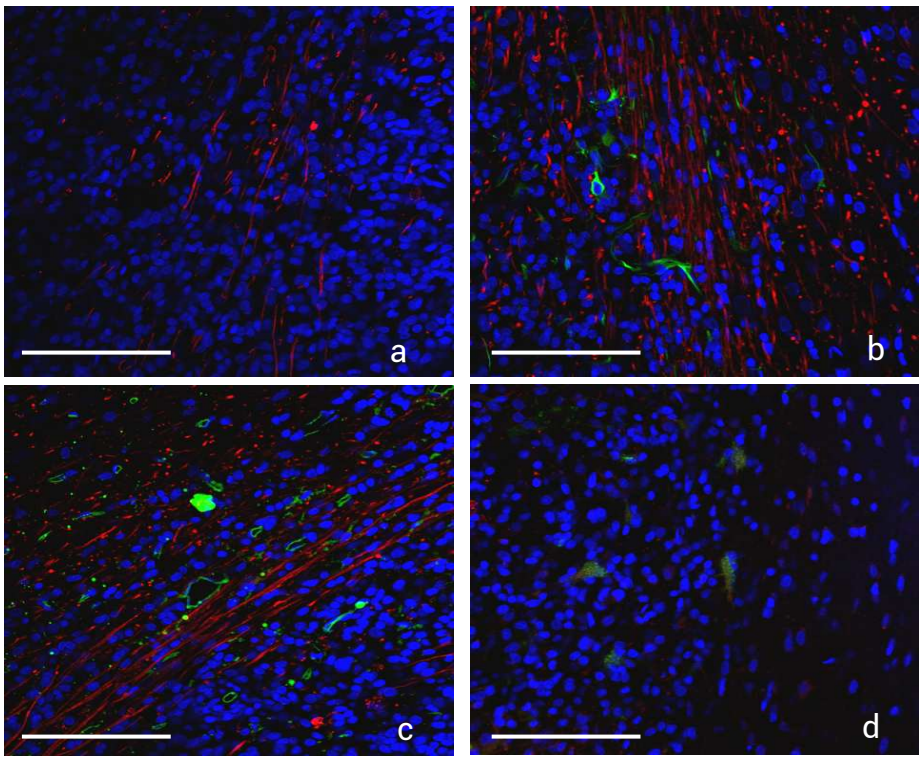

Figure 34: Double immunofluorescence of Notch (red) and other markers in the tumoural border. **a**) Notch expression around the border **b**) Nestin (green) does not co-express with Notch, **c**) Vessels marked with LEA(green) does not co-locate with Notch expression, **d**) Only in OPN (green)/Notch can be seen some co-expression of both markers.
Scale bar =50 µm.

5.3.5-"Spheroid aggregates"

Following double immunostaining assays against Nestin and antigens like: GFAP, CD133, GluT-1, and VEGF, it has been found that inside the spheroid aggregates there are Nestin+ cells, CD133+ cells and Nestin/CD133+ cells. The co-expression of Nestin and CD133 can be observed in some cells with small size (Fig. 35 c, arrow). Those cells have a round morphology with scarce cytoplasm and dense nuclear chromatin.

GFAP-positive cells are to be seen surrounding the aggregates, as though "encapsulating" these cellular aggregates (Fig. 35 b). At the periphery

of these aggregates, and to some extent inside them, there are VEGF+ cells and also cells that slightly co-express VEGF and Nestin (Fig. 35 a, arrows). Both GFAP and VEGF immunomarkers stain astrocyte-like cells.

Most of the small aggregates do not have vessels inside them. Occasionally, some capillaries immunopositive for GluT-1 were found near these shapes (Fig. 35 d, arrow).

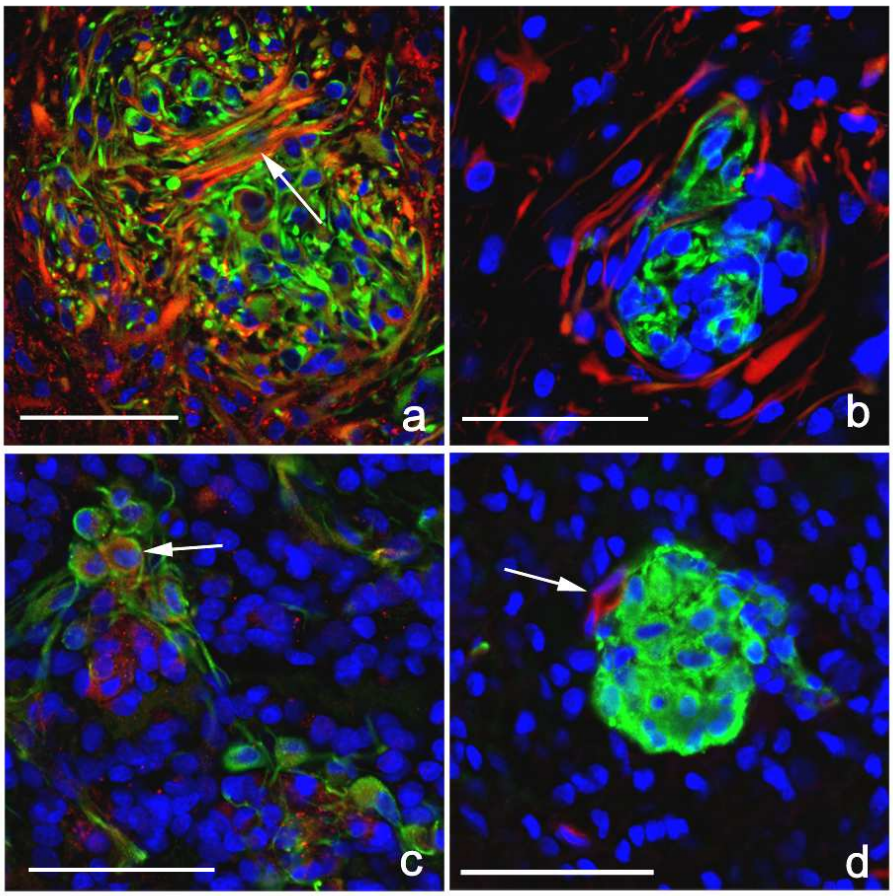

Figure 35: Double immunofluorescence study of stem cell markers expression in the spheroid aggregates; Nestin-VEGF (**a**), Nestin-GFAP (**b**), Nestin-CD133 (**c**) and Nestin-GluT-1 (**d**). VEGF (**a**) only co-locate with Nestin in some cellular prolongations, mainly around the Nestin-positive cells. GFAP (**b**) is located externally from the Nestin-positive cells. There are some cells co-expressing Nestin and CD133 (**c**), and it appears that Nestin is located a bit farther from the nuclei than CD133. There is no co-expression of Nestin and GluT-1 in the aggregates (**d**). Scale bar =25 µm.

Some of the huge aggregates were structures similar to the small ones, but bigger in size by having a greater number of cells inside. These aggregates also have bigger Nestin-positive cells with prolongations (Fig. 36 a). In the interior and the periphery of these huge aggregates there are occasionally aberrant vessels positive for the BBB marker GluT-1 (Fig. 36 b) and also some large Nestin+ cells co-expressing VEGF (Fig. 36 c).

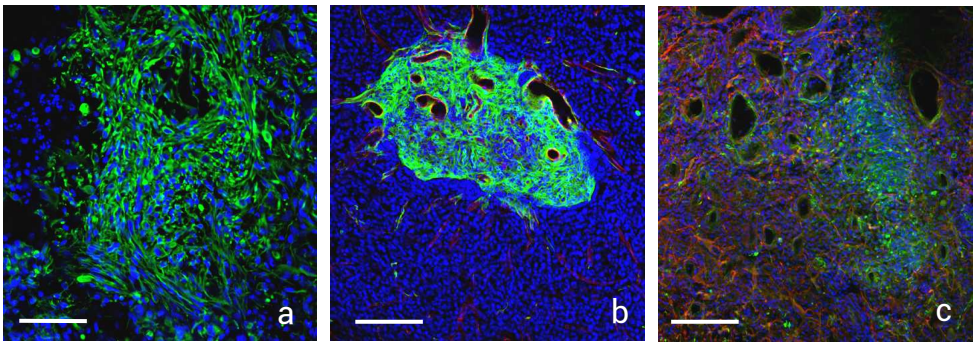

Figure 36: Immunofluorescence staining of the huge cellular aggregates marked with Nestin (a), Nestin/Glut-1 (b) and Nestin/VEGF (**c**). In all images can be seen great aggregates of Nestin cells with different shape. Some of these aggregates have vessels positive for Glut-1 (**b**). VEGF is expressed greatly outside these huge aggregates (**c**).
Scale bar =50 μm.

5.3.5.1-Quantitative study

The quantification of the number of spheroid aggregates (Fig. 37) marked with Nestin showed that even though they can appear in the first stage (27% of stage I tumours have at least one aggregate), the vast majority of them are shown in stage II (when they are found 81% of tumours) and III gliomas (in 78% of tumours in this stage). There is an increase in the number of spheroid aggregates in the intermediate and advanced stages, compared to stage I gliomas. There is a significant difference in the number of them between stage I (0.55±0.14; n=28) and stage II (4.455±0.8445; n=22) ($p \leq 0.0001$) and stage III (4.750±1.018 N=28) ($p \leq 0.001$) (Fig. 37). We also measured the density of the spheroids inside these gliomas and observed that the highest density appears in stage II (1.102±0.224; n=23). In stage I

there is almost the same density (0.9993±0.3351; n=28), but in stage III there is a great reduction in the density of the aggregates (0.5410±0.1203; n=31). There is only statistical significance between stage II and stage III ($p \leq 0.05$). Finally, the mean areas of the aggregates showed an increase during tumour development, without statistically significant differences. In the first stage, the area of the aggregates is 17.39 ± 4.73 μm^2, n=8, in the intermediate stage, 29.08 ± 6.99μm^2, n=67 while it si 29.94 ± 7.59 μm^2, n=134 in the advanced stage.

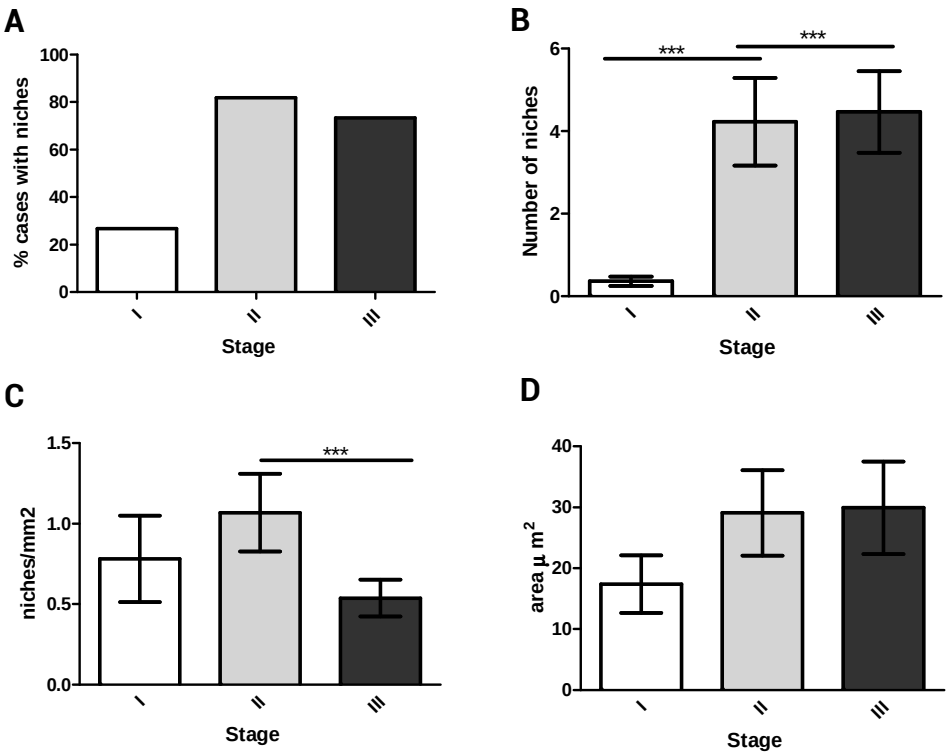

Figure 37: Nestin positive cell aggregates quantification A) % of cases in each stage show spheroid aggregates. **B**) Mean number of spheroid aggregates in the different stages of glioma growth. They are almost absent in the first stage, but the number increases greatly in the second and third stage. **C**) The density of aggregate per mm^2 of tumour is highest in stage II of glioma development. **D**) Mean size of the spheroid aggregates, there are no significant differences. ***$p \leq 0.001$.

VI.-Discussion

This study has provided useful information about the distribution of cells expressing stem cell markers in endogenous gliomas during tumour development.

This study has also helped greatly in order to advance in the knowledge of behaviour in animal models of gliomas. The data gathered in the homecage systems will help to establish the early diagnosis of gliomas in order to prevent animal pain or discomfort as well as to optimise experimental designs.

6.1-Behaviour for early diagnosis

The ENU-model for glioma generation is a chronic model that can be very stressful and painful for the rats, therefore we pretend to mitigate rat discomfort by preventing the pain and making the early diagnosis of tumours easier. This model for glioma induction has the disadvantage of the latency time for tumours to arise, but it also has another handicap (inherent to most glioma models), which is the identification of the tumours, including the low-grade tumours. The results show that weighing the animals does not provide enough information about their health status; therefore other methods are needed in order to correctly identify the early asymptomatic stages of the tumour. For this purpose, we performed a continued behavioural monitoring of the rats. This way, we were able to observe changes that correlated to tumour growth. We have carried out these tests (homecage system and open-field test) from the 4^{th} month onwards because previous work carried out in our laboratory showed gliomas could appear as early as the 6^{th} month of age (Bulnes and Lafuente, 2007). For the behavioural analysis, we have used the data obtained in two nights, corresponding to rats' active period when they are awake and more active (Yasenkov and Deboer, 2012).

The study of the behaviour (analysing parameters like food and water intake, distance, % of time moving, exploratory index or rearings) has provided us with extensive and valuable data for healthy and glioma-

developing rats during tumour growth. Comparing the two methods usedin this study, automatic monitoring of behaviour with a homecage has proven to be a reliable test to detect behavioural anomalies (increase or decrease in the measured parameters vs control rats) in the rats prior to physical symptoms, while the open-field test (carried out according to our performed protocol) did not add additional information over the homecage test**;** in all cases where open-field testing detected an altered parameter, it could also be detected the with homecage system. A possible solution to this problem could be to increase the frequency of the open-field tests in order to increase their sensitivity and to try to identify earlier behavioural anomalies. Increasing the number of the open-field tests is also easier than the homecage stay, because it is a shorter test and no more cages are needed.

Both tests used in this study are automated tests that allow data to be collected from the animal without human manipulation, thus minimizing errors and bias.

6.1.1-Behavioural changes of prenatally-exposed rats to ENU

The General Adaptation Syndrome (GAS) (Fig. 38) (Selye, 1946) seems to fit with the response observed in the rats in the ENU model. In this model, there are three phases: the alarm reaction, the resistance stage and the exhaustion stage. Figure 38 shows the body's reaction in an individual affected by a stressor (it can be either physical or psychological). The line represents the level of resistance. In the alarm reaction, there is an increase in the adrenaline and glucose levels, and also in the metabolic activity and muscle tone. The resistance stage is characterised by having an increase in the adrenaline and corticoid levels. This phase can have a plateau or not, depending on the strength of the stressor. Finally, in the exhaustion stage there is a decrease in metabolic activity and immune dysregulation (due to a decrease in neuroendocrine hormones), as described by Stojanovich, 2010.

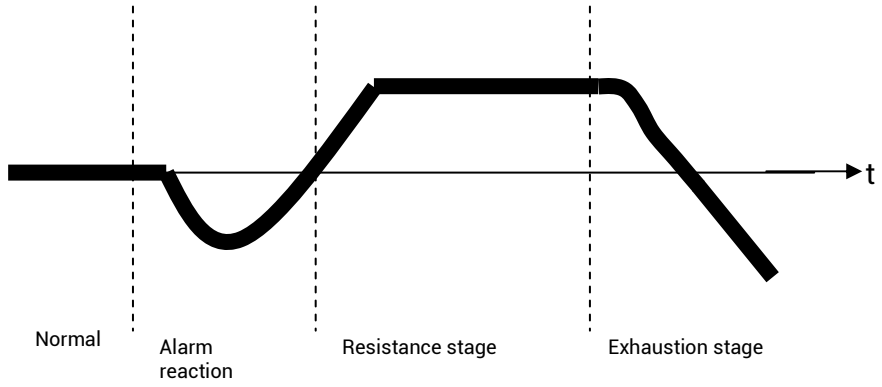

Figure 38: General adaptation Syndrome as described by Selye in 1946. The black line represents the general animal status. When something alters the welfare of an animal, there is a decrease in the animal health that is rapidly counteracted by the animal defence system, generating the resistance stage. But the body can not hold in this status forever, and if the alteration does not disappear, the animal enters in an exhaustion stage, decreasing the animal defences and general welfare.

The behavioural data collected in the tests we performed follows a similar pattern to the general adaptation syndrome. The resistance stage would be equivalent to the functional reserve and in this study would vary in its duration depending on the malignancy of the tumour, the location etc. The exhaustion stage would represent the time frame when the animals express their physical discomfort and would correspond to our group C rats, which show at least one of the items of the Morton and Griffiths welfare scale (1985) and a decrease in the measured parameters.

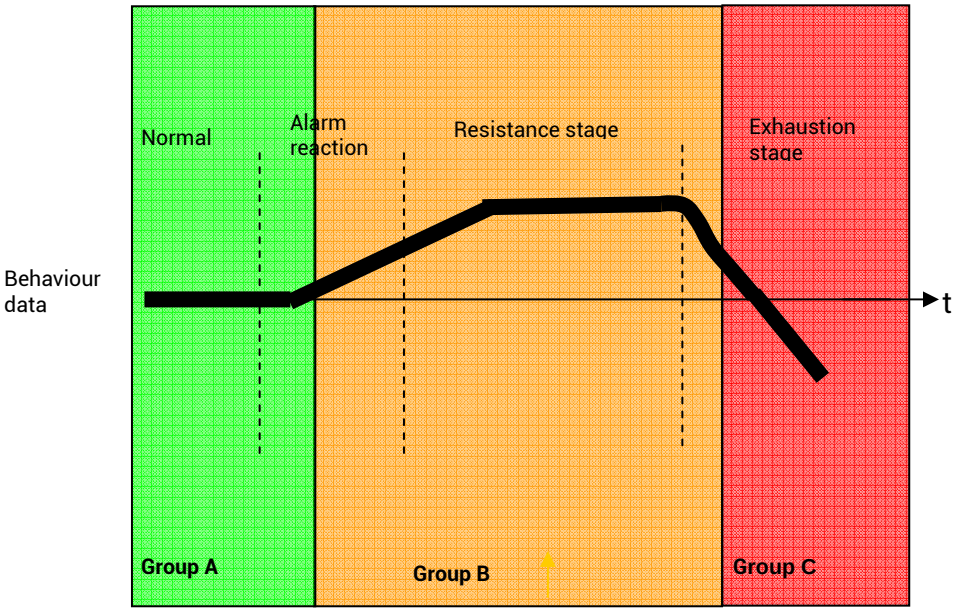

Figure 39: Rat behavioural groups during tumour growth represented by a temporal sequence. The black line represents the mean of the control group and the variations *vs.* ENU-exposed rats. In the Group A (green) there is no alteration in their welfare score (measured with the Morton & Griffith table) or activity. Group B shows an increase in any of the measured behavioural data, but no alteration in the welfare score. Finally in Group C the rats have an increase in their welfare score and a decrease in the behavioural data.

The three groups of ENU-exposed rats that have been identified in the results (Groups A, B and C) seem to follow a temporal sequence, as observed in figure 39. As previously stated, Group A are rats without physical or behavioural symptoms, Group B are rats without physical symptoms and an increase in at least one of the measured behavioural parameters and Group C are rats that display physical symptoms observed with the Morton and Griffith test and a decrease in at least one of the measured variables. Many rats started in group A, then they moved to Group B and finally they got into Group C, meaning that the Group B would be the intermediate point where the rats have behavioural alterations, before they show physical handicaps. The changes over time for the defined groups are be represented in Fig. 39.

Group B mean time of appearance (almost 6 months) coincides with the timing of tumoural development previously reported for this method (Zook and Simmens, 2005) and determines that it would be appropriate at this time to establish, via MRI, the type and location of the tumours, because rats in this group do not display any physical handicap yet. Also, 3 rats went from group B to C in the 5th month, 6 in the 6th month, and one in the 7th and 8th month. So between the 5th and 6th month of age would be the critical age for an early diagnosis of the gliomas in this model. The fact that group C has a lower time of appearance than Group B can be explained because 42% of the rats in group C appeared during the 4th month. Of these rats, 37.5% presented an extracranial. Extracranial CNS tumours induced by prenatal exposure to ENU have been previously identified as meningiomas and malignant schwannomas (Zook and Simmens, 2005). These schwannomas are very malignant, fast progressing and appear earlier than the gliomas. More repetitions of the tests (at shorter intervals) and an earlier start of the behavioural tests would help to establish with higher accuracy the time of appearance of each tumour.

Group C rats present alterations in parameters linked to mobility, but also in metabolic related parameters, like food and water intake. That means that when this Group appears, the vital parameters are already altered and the general rat's health status is compromised.

Animals with “welfare score >0” have a higher variability in the range of the parameters than rats with “welfare score=0”. This can be explained because in the group “welfare score>0”, there are rats in different states of health (including rats with clear physical symptoms), increasing the variability of the measured data. The variables that allowed us to observe behavioural changes before physical symptoms appeared were mainly those related to the activity of the animals, like distance walked or rearings. It has been previously reported that measuring the behaviour or the locomotive pattern in rodents (Martin and Bateson, 1986; Jansen et al.,

1995) could help to identify the general adaptation syndrome and/or prevent animal discomfort. Our results point in that direction.

6.2-ENU-induced glioma incidence and classification

ENU prenatal injection has become a well-known method to obtain gliomas since it was first reported in the 60s (Druckrey et al., 1966).

The data obtained in this study corroborates previous studies that show the induction of several types of CNS tumours, such as different grade gliomas, meningiomas and schwannomas (Mennel et al., 2004, Zook and Simmens, 2005).

The incidence (almost 100% of the rats develop a CNS tumour) is similar to that previously reported in the literature (Bulnes-Sesma et al., 2006) and the tumoural development occurs as the rats grow, in the same way as human gliomas. This fact allows a closer look into tumoural development that other models, such as tumour xenografts, cannot offer.

The fact that we have observed that intracranial extraaxial tumours have the shortest life expectancy coincides with their related malignancy (Zook and Simmens, 2005). It also means that the malignancy of ENU-induced tumours is related to the rat's age, with the most malignant tumours developing as the rats get older. On the other hand, rats with post-mortem identified stage III gliomas were rats with the greatest age, despite having the most malignant tumours. This can be explained by the long time that gliomas take todevelop after ENU exposure and that in this model, gliomas become malignant over time.

The classification of CNS tumours after the ENU exposure, and particularly of the gliomas, corresponds with previous studies with this model (Zook et al., 2000). Gliomas usually start as small proliferations resembling oligodendrogliomas that acquire malignant characteristics like necrosis, haemorrhages or diffuse borders as they develop (Fig. 13). The tumoural malignancy increases slowly with time and provides tumoural vasculature that evolves at the same time as the gliomas. That is a great

advantage over fast growing glioma models, which lack of histologically-acute vasculature (Fomchenko et al., 2006). Our classification for the ENU-induced gliomas relies on histopathological features of the tumours, but it also bears in mind the size of the neoplasias. Stage I tumours are small proliferations of cells that never become large enough to displace neighbouring structures. On the other hand, stage III gliomas are usually big tumours that often occupy a whole hemisphere.

MRI can detect the CNS tumours, but there are procedural difficulties (money and time lost transporting the animals to another city where the MRI device is) that hinder the temporal resolution, so we came up with the idea of monitoring possible behavioural changes of the rats as a non-invasive method to identify the ENU-induced tumours. With the present data, it is difficult to evaluate the relationship between behavioural data and glioma development and future work should be targeted in this direction in order to correctly identify the glioma stage before the animal is sacrificed.

6.3-Stemmness markers in ENU-induced gliomas

The presence of CSCs has been previously described in human glioblastomas and also in animal models (Dahlstrand et al., 1992; Singh et al., 2003). Nowadays there are many studies about the role of stem cells in GBM, for example they have the capacity to initiate tumours (Hadjipanyis and Van Meir, 2009), and may be responsible for a high *in vitro* migration capacity and high *in vivo* infiltration capacity (Yu et al., 2011, Calabrese et al., 2007; Sadahiro et al., 2013) as well as higher levels of hypoxia resistance (Seidel et al., 2010). But little is known about the distribution of cell aggregates that we have called "spheroid aggregates" (Fig. 22) inside the tumour or their participation in the early forms of gliomas.

There are few published studies of the presence and distribution of stem cells in low-grade gliomas. For this purpose, animal models are an important tool for studying these tumours, because they allow performing

studies throughout the developmental process. The endogenous generation of CNS tumours via transplacentary administration of ENU in rats during pregnancy has been widely documented and is a well-known and reliable model to study gliomas in different stages (Zook and Simmens, 2005; Bulnes-Sesma et al., 2006). The early tumours are small masses of cells resembling classic oligodendroglioma. The most malignant forms show areas of necrosis and pseudopalisades, like anaplastic oligodendrogliomas or glioblastoma multiforme. In fact, this model has been previously used to research many cellular, biological and genetic aspects of gliomas, (Jang et al., 2004; Jang et al., 2006; Bulnes et al., 2011). However, it has not been used to study the presence and distribution of immunopositive cells for stemness markers during tumour growth.

Despite numerous studies about the tumoural stem cells presence in gliomas, there is still controversy about the identification potential of these markers. Nestin remains questioned as a CSC marker, because it is a neural lineage undifferentiation marker expressed in the brain at the hippocampus and the SVZ in rats (Nogueira et al., 2014). Nestin is also overexpressed in areas of active neurogenesis after brain injury (Holmin et al., 1997; Michalczyk and Ziman, 2005) and it has been used to label immature brain endothelium (Matsuda et al., 2013). In the ENU-glioma model, the perivascular Nestin-positive cells (Fig. 29, 30), the closest ones to the endothelium, resemble pericytes. There are few studies about Nestin expression in pericytes (Birbrair et al 2014); though there are some examples of these cells playing a relevant role in tumoural vasculature (Cheng et al., 2013) and being present in the perivascular stem cell niche (Brooks et al., 2013). Although Najbauer and collaborators observed both Nestin+ cells and pericytes around tumoural vasculature in a xenograft model of glioma, they stated that there is no co-location of Nestin and pericyte-associated markers (Najbauer et al., 2012). The main challenge in order to definitely identify these Nestin-positive cells as pericytes is the

lack of specific markers for pericytes (Armulik et al., 2011); yet Birbrair and collaborators claim that there is a subpopulation of pericytes positive for Nestin and NG2 and that this subtype of pericytes plays an important role in tumoural angiogenesis. However, it is controversial to assure that fact since NG2 has been previously used as a marker for immature oligodendrocytes (Kang et al., 2010) and an NG2 subpopulation of oligodendroglial precursor cells has also been described to be responsible for the tumourigenesis in ENU-gliomas (Briançon-Marjollet et al., 2010). In order to clearly evaluate whether the perivascular Nestin+ cells are pericytes or not, further studies with electron microscopy would be necessary to closely examine the location and morphology of these cells.

The use of CD133, despite being the most used marker for the identification of tumour stem cells, is also controversial. Recent research points to CD133 as a marker related to a bad survival rate in GBM, rather than to stemness (Olausson et al., 2014). Some studies claim that CD133 is only expressed in gliomas with small round cell morphology with hyperchromatic nuclei (Schittenhelm et al., 2011) or under stress conditions (Griguer et al., 2008). Other studies propose that CD133- cells (apparently non-CSCss), can give rise to tumours (Ogden et al., 2008) and to CD133+ cells in specific conditions (Wang et al., 2008), so CD133 expression would also depend on the microenvironment or culture conditions. This debate around the suitability of CD133 marker expression as a cancer stem cell (CSC) marker could be partially explained by the plasticity model. According to this model, the stemness status in the tumours is not a definitive status and is driven by the environment around the cells. Thus, CD133-negative cells could adapt to hostile environments and transform themselves into CD133-positive cells, capable of generating a tumour.

Presence and prevalence of stem cell markers in tumours have been previously used as a prognostic factor, mainly through quantification of the

expression of Nestin, CD133 and Osteopontin in humans and animal models (Jang et al., 2006; Zhang et al., 2008; Zeppernick et al., 2008). Accordingly, an increasing expression of any of these markers is described as a bad prognostic factor. Specifically, Nestin expression increases with glioma malignancy (Ehrmann et al., 2005, Shin et al., 2013).

Our data demonstrates that the number and the size of the spheroid aggregates increases in the malignant stages of the ENU-gliomas, supporting the hypothesis of of Nestin+ aggregates as a bad prognostic factor.

This study also shows how the cellular Nestin expression gets increased in relationship with markers of proliferation, like BrdU and Ki-67 and it suggests a relation between those markers. Both BrdU and KI-67 expression have been related to the degree of malignancy and are linked to a bad prognosis. Further studies about the link between stemness markers (Nestin among others) and proliferation should be performed, in order to research their relationship (Johanessen and Torp, 2006).

6.3.1-Perivascular expression of stem cell markers

Previous work from our group has described the adaptations of the vascular network during glioma development and how the vessels acquire aberrant morphologies that provoke an irregular blood flow (Bulnes et al., 2009). In the ENU-induced glioma model, we have also observed how VEGF has different patterns of expression during glioma malignancy (Bulnes et al., 2007): in the low-grade gliomas there is a low level of VEGF expression, increasing hugely in the intermediate stage, the so-called “angiogenesis switch". This stage is defined as an alteration in the balance between pro- and anti-angiogenic factors (Baeriswyl et al., 2009). Our results show that Nestin- and CD133-positive cells are found inside the ENU-induced gliomas in different perivascular locations. In the neoangiogenic tumoural border Nestin and CD133+ cells are found to co-locate with GFAP and VEGF around the glomeruloid vessels forming “perivascular niches". The

glomeruloid vessels have been reported as a characteristic mark of GBM (Kleihues et al., 2002) and they have been found to express VEGF (Brat and van Meir, 2001). Furthermore, the glomeruloid tufts are thought to be created after a response to VEGF secreted by hypoxic conditions (Brat and van Meir, 2001) while, in the hypoxic interior of the tumour, Nestin and CD133+ cell aggregates appear located close to tortuous and dilated vessels (forming also the perivascular cluster) (Fig. 29).

The perivascular distribution of CSCs has been previously reported (He et al., 2012) and it is composed of Nestin positive cells (Calabrese et al., 2007) along the vessels, with clusters of CD133+ cells close to the vessels (Christensen et al 2008), among other markers such as Notch-1 and iNOS (Filatova et al., 2012). Neural stem cells have been confirmed to appear in vivo in vascular niches, as the endothelial cells provide a favourable environment for them (Shen et al., 2008; Gomez-Gaviro et al., 2012), and do CSCs also appear in vivo (Calabresse et al., 2007; Borovski et al., 2009). The endothelial cells have been proposed to increase the protection of tumour stem cells against radiotherapy in the perivascular microenvironment (Garcia-Barros et al., 2003) by absorbing most of the radiation damage, so they are also important in the regulation of the niche.

Our results corroborate the existence of a perivascular cluster of cells positive for Nestin and CD133 (and sometimes co-expression of both markers), but in our results we have not seen spheroid-like structures of these markers around the tumour vasculature. The role of CSCs in tumoural angiogenesis has been previously reported (Bao et al., 2006; Folkins et al., 2009), and the presence of Nestin/VEGF co-expressing cells in the intermediate and advanced stages would support this model. Thus, our results support a model where Nestin and/or CD133 positive cells would trigger angiogenic stimuli when the tumour needs to increase its nutritional demand (Bulnes et al., 2009).

This hypothesis of the perivascular cells being highly responsible for the process of tumoural angiogenesis is supported by the expression of

angiogenic factors like VEGF, among others. It has been stated that CSCs in a hypoxic environment produce HIF-2 alpha that induces the production of VEGF (Heddleston et al., 2009; Heddleston et al., 2010). Angiogenesis would be driven in the tumoural interior mainly by Nestin/CD133 positive cells placed around the aberrant vessels. Some of these cells may express one or both stemness markers.

Mildly abnormal vessels express BBB markers like GluT-1 or EBA. Glucose transporter 1 is developed very early as a basic system for the nutrition of cells and it can also be seen around very aberrant vessels. In opposition, EBA belongs to a more evolved system specific of the brain endothelium that disappears in glomeruloid vessels.

The only place where we have observed light co-location of CD133 and LEA in any tumoural stage is around the glomeruloid vessels, supporting the hypothesis of cellular transdifferentiation in tumours (Zhao et al., 2010; Soda el al., 2011; Scully et al., 2012). These studies hypothesise that cancer cells (and CSCs) can give rise to endothelial cells *in vivo* or mimic vasculature *in vitro*. Specifically in gliomas, it has been proposed that CD133+ cells can give rise to tumour endothelium (Wang et al., 2010).

On the other hand, CD133 is also known for being positive for endothelial precursor cells (EPCs). EPCs are a very small portion of circulating blood cells with the ability of differentiating to endothelial cells. EPCs have been characterised by being positive for CD34/CD133/VEGFR-2 (Xiao-Qin et al., 2014). It has been reported that EPCs are recruited into certain tumours and take part in the neoangiogenesis process (Xiao-Qin et al., 2014). Although there is currently no data showing EPC involvement in angiogenesis in gliomas, an increase in EPCs has been described (detected with the previous mentioned antigens) in peripheral blood (Rafat et al., 2010).

So it is difficult to say if the CD133 positive cells in our ENU-gliomas are tumour cells or EPCs, as more investigation should be carried out in order to explain their origin.

MAP-2 is a major component of the cytoskeleton and is expressed in neural differentiated cells (Liu et al., 2003). Nevertheless, its expression has also been observed in many neoplasms such as small cell carcinoma, medulloblastoma and some breast tumours. Following our MAP-2 expression results, the perivascular cell MAP-2 expression observed in ENU-gliomas has been previously reported in human astrocytomas (Wharton et al., 2002), oligodendrogliomas (Blümcke et al., 2001) and in some glioma cell lines (Shiras et al., 2003). In human studies, cytoplasmatic MAP-2 expression has been described, both in isolated cells or forming a perivascular pattern (Wharton et al., 2002), in the same way as we have also observed in the ENU-induced gliomas. Messam and collaborators reported that a small fraction of Nestin+ cells during CNS development that are also positive for MAP-2 (Messam et al., 2000), but further studies are needed in order to decipher the potential role of MAP-2 in gliomas and cancer stem cells.

Even though MAP-2 is not a stemness marker, its expression has been observed in Nestin+ cells (Messam et al., 2000) and MAP-2 cDNA expression has been reported in some neurospheres (Suslov et al., 2002), in part due to the heterogeneity of stem cells.

6.3.2-Stemness marker expression in the tumoural border

Osteopontin expression in glioma models (Jang et al., 2006), has been described as a bad prognostic factor, even though some authors claim that a high OPN expression correlates with higher survival in animal models, as OPN is related with a decrease in cellular migration (Selkirk et al., 2008). OPN expression is related to Nestin and VEGF expression in the tumour border (Takano et al., 2000); therefore this is found sometimes around vessels but mainly in the tumoural border. We have found an increase in

OPN+ cells in the tumoural border in the advanced gliomas. Previously it has been reported that OPN overexpression induces angiogenesis (Wang et al., 2011) and cellular migration in glioma cells *in vitro* (Lu et al., 2012), so the border OPN expression in the present study could be related to angiogenesis and tumoural migration.

Cells expressing Nestin at the border have the morphology of well-differentiated astrocytes that co-express GFAP and VEGF (Fig. 33), so most probably these Nestin-positive cells would be astrocytes involved in tumoural border angiogenesis. VEGF expression at the border has been previously reported both in isolated cells and in perivascular cells around the vascular glomeruloids, typical of the most malignant gliomas (Brat and Van Meir, 2001).

Notch-1 is a factor needed for stem cells renewal (Matsuda el al., 2013) and its expression in glioblastomas has been previously described as a factor that enhances stem-like properties (Charles et al., 2010) and radio resistance (Wang et al., 2010 b). As previously observed in Fig. 33 d, OPN and GFAP co-locate in the cytoplasm of astrocyte-like cells in the tumoural border and we have also observed that OPN and Notch-1 are co-expressed complementarily in some cells of the tumoural border. Notch-1 has been strongly related to the astrocytic differentiation process (Tanigaki et al., 2001), so it could explain the Notch-1 expression in this study.

We have observed an increase in Notch expression around the border zone mostly in the malignant gliomas. Similarly, we have observed Nestin/CD133 expression (mainly around the aberrant glomeruloid vasculature) in the tumoural border. Notch signalling has been linked with angiogenesis (Li and Harris, 2009) and it becomes up-regulated in glioma vasculature (Li et al., 2007). It has been reported that Notch signalling can directly up-regulate Nestin in human gliomas (Zhang et al., 2008), thus the Notch expression in the tumoural border zone. Notch-1 expression in our study does not co-express with Nestin positivity, so it is more probable that Notch-1 expression could be related to the angiogenic border. Notch-

1 has also been related to hypoxic conditions (Gustafsson et al., 2005) and to the stem-like phenotype, promoting the self-renewal of glioma-derived CSCs and inhibiting their differentiation (HU et al., 2011).

6.3.3-Spheroid aggregates of Nestin positive cells

These spheroid clusters are defined as limited areas in the tumour with cells positive for Nestin and CD133 and similar morphology to *in vitro* stem cell morphology growth.

The spheroid aggregates in the ENU-induced gliomas appear in the first stage (Fig. 37) of glioma development (classic oligodendrogliomas), but it is not until the intermediate stage that these aggregates appear in greater numbers. Further studies should be undertaken to determine wheter they have a relation with the "angiogenesis switch", which happens around the same stage and is the moment when an overexpression of pro-angiogenic factors begin to appear (Bergers and Benjamin, 2003). We have observed that "spheroid aggregates" show many parallelisms to tumour neurospheres, such as cell morphology, (small and round with dense nuclei and without cellular prolongations), immunomarker expression (Nestin, CD133, GFAP), etc (Bez et al., 2003; Pavon et al., 2014). Neurospheres have also been isolated from human and animal model gliomas and show Nestin/CD133 positivity (Singh et al., 2003; Bexell et al., 2009), as well as Sox-2 (Brazel et al., 2005) and even GFAP (Jensen and Parmar, 2006), but this GFAP expression appears mainly in the most differentiated cells of the exterior of the neurospheres. Tumourspheres (from CNS tissue) and neurospheres (from the SVZ) are also similar to each other (Vik-mo et al., 2011) and only differ in nuclear morphology, the tumourspheres having more nuclear atypias and expression of some markers like β-III-tubulin. So, the spheres from cancer and neural stem cells are comparable.

As previously stated by Pastrana and collaborators (Pastrana et al., 2011), the gold standard assay to identify stem cells is the *in vitro* sphere growth. Protocols vary substantially between different assays, but in all of them, a restrictive medium and preventing the cells to adhere to the plate are necessary conditions to induce the stem cells to form spheres. So the CSCs could form spheres *in vitro* in order to protect themselves against adverse conditions such as absence of nutrients. In the same way, we hypothesise that Nestin and CD133 positive cells *in vivo,* in the ENU-induced tumour model, could form the spheroid aggregates to protect themselves against hypoxia, lack of nutrients or maybe also chemotherapeutics (Bao et al., 2006; Rich, 2007; Denysenko et al., 2010). In addition, these arrangements could represent a cell aggregate proceeding from a single cell clone (Pastrana et al., 2011), formed before the cells begin to spread. The cells in the spheroid aggregates could stimulate cells around them to produce angiogenic factors in order to escape from the adverse conditions. Similarly, we have frequently observed VEGF-positive cells around the spheroid arrangements. The encapsulation of these structures by VEGF and GFAP positive cells would also serve to isolate the cells inside and provide them with a favourable microenvironment.

The spheroid clusters in this model form the necessary microenvironment for the stem cells' maintenance and development. It has been previously proposed that niches of stem cells could act as a reservoir (Christensen et al., 2011) and could be responsible for the high rate of relapse of malignant gliomas, and this could be done by the spheroid aggregates. In the ENU-gliomas, we observed that the mean size of spheroid aggregates increased with malignancy. It has been reported that even though the *in vitro* size of tumourspheres varies greatly, between 40-150μm (Pastrana et al., 2011), it is possible to culture huge neurospheres with 300 or even 400μm of diameter under certain conditions (Mori et al., 2006); in the same way we could observe some huge spheroid aggregates

in the most malignant gliomas (Fig. 36). Therefore, our data supports a model where aggregates of Nestin/CD133+ cells would act as a reservoir of immature cells, protected by a layer of more differentiated astrocyte-like cells.

6.4-Future perspectives

Research into glioma stem cells in recent years has provided a lot of information about the mechanism of stemness in gliomas and all the consequences they have in tumour growth, angiogenesis and treatment. As a result of these efforts, some methods have already been proposed to selectively attack CSCs *in* vitro and *in* vivo (Bao et al., 2008, Gil-Ranedo et al., 2011).

Nevertheless, early diagnosis of the tumours is also critical, both in humans and in animal models). Research into behavioural characterization is becoming increasingly important, so as to prevent animal pain and discomfort and to provide cheaper and non-invasive diagnostic methods.

6.4.1-CSCs in the future of GBMs

Further research is needed to elucidate the exact role of these spheroid aggregates and to better understand their parallelism to the neurospheres. However, future perspectives of the advantages of identifying the spheroid niches as an *in vivo* approximation of the neurospheres would include the non-invasive identification of the "spheroid aggregates" to unveil their distribution and the possibility of targeting them in order to attack the most malignant cells in the tumour.

If the spheroid aggregates in the ENU-model were really neurospheres analogues, this would open up new ways to research the neurospheres' behaviour *in vivo* and *in vitro,* and the relation with other structures like tumoural vasculature.

Therefore, the ENU-induced tumour model could provide helpful information to aid understanding the nature of tumoural stem cells and

study their properties. An *in vivo* characterization would be the first step for a proper identification, giving raise to guided therapies against these cells, as they are the ones that lead the tumourigenesis and angiogenesis processes.

6.4.2-Behaviour as a future diagnostic tool

Behaviour and metabolic alterations measured through continued monitoring can be used for an early diagnosis tool before the animals display any physical handicaps. This method provides a non-invasive way to identify gliomas (and potentially other pathologies) and at the same time, prevents and reduces animal pain. In order to correctly achieve that aim in the future for gliomas and other pathologies, it is necessary to know the normal behaviour of the animal studied and the alterations that the animals suffer during glioma development, as we have accomplished in this study.

VII.-Conclusions

1.-The ENU-induced glioma model provides endogenous tumours that allow the study of neoplastic growth and their microenvironment from the early stages.

2.-Diagnosis through clinical signs and changes in behaviour is a non-invasive method that provides useful information about tumoural development, but no consistent correlation with the severity of tumours was found. However, the information allows a significant improvement in the animal welfare. During the continued monitoring, distance run was the most significant parameter to detect alterations before the apparition of symptoms.

3.-Repeated monitoring of rats in a homecage system is a useful way to detect changes in the clinical state suggesting the presence of a CNS tumour before devastating physical consequences appear. Open-field testing does not provide extra information about the rat's welfare, but confirms the suitability and reliability of data obtained by the homecage system.

4.-Nestin expression is present from the earliest stages of glioma and its expression increases during development. Nestin+ cells show different morphologies and a small fraction of them are small round cells with scarce cytoplasm, like the stem cell morphology. On the other hand, CD133 is only immunodetected in the most malignant stages.

5.-Cells expressing various stemness markers are distributed throughout the heterogeneous tumour mass identifying three different tissue areas: the tumoural border, the perivascular region and the interior of the glioma.

6.-In the tumoural border, there are many cells expressing Nestin and Osteopontin that are big and morphologically well differentiated and co-express GFAP and VEGF, suggesting their involvement in border angiogenesis.

7.-Numerous perivascular cells are positive for Nestin and CD133. This expression appears around aberrant vessels, being highest around glomeruloids, where slight co-location with VEGF is frequent.

8.-This model shows arrangements of cells positive for Nestin and CD133, which we have named "spheroid aggregates". The most undifferentiated cells are present inside these formations with a small and round morphology without prolongations. Spheroid aggregates are surrounded by VEGF/GFAP+ cells and as a whole resemble the *in vitro* cell arrangements named neurospheres.

VIII.-Bibliography

- **Ahmed R, Oborski MJ, Hwang M, Lieberman FS, Mountz JM.** Malignant gliomas: current perspectives in diagnosis, treatment, and early response assessment using advanced quantitative imaging methods. Cancer Manag Res. 2014 24;6:149-170.

- **Al-Hajj M, Wicha MS, Benito-Hernandez A, Morrison SJ, Clarke MF.** Prospective identification of tumorigenic breast cancer cells. Proc Natl Acad Sci U S A. 2003 ;100(7):3983-8.

- **Altman J, Das GD. Autoradiographic and histological studies of postnatal neurogenesis. I.** A longitudinal investigation of the kinetics, migration and transformation of cells incorporating tritiated thymidine in neonate rats, with special reference to postnatal neurogenesis in some brain regions. J Comp Neurol. 1966; 126(3):337-89.

- **Alvarez-Buylla A, Garcia-Verdugo JM.** Neurogenesis in adult subventricular zone. J Neurosci. 2002; 22(3):629-34.

- **Armulik A, Genové G, Betsholtz C.** Pericytes: developmental, physiological, and pathological perspectives, problems, and promises. Dev Cell. 2011 ;21(2):193-215.

- **Artavanis-Tsakonas S, Rand MD, Lake RJ.** Notch signaling: cell fate control and signal integration in development. Science. 1999; 284(5415):770-6.

- **Baeriswyl, Vanessa, and Gerhard Christofori**. Seminars in Cancer Biology. Nature Clinical Practice Oncology 2009. 19: 329–337.

- **Bao S, Wu Q, McLendon RE, Hao Y, Shi Q, Hjelmeland AB, Dewhirst MW, Bigner DD, Rich JN.** Glioma stem cells promote radioresistance by preferential activation of the DNA damage response. Nature. 2006; 444(7120):756-60.

- **Bao S, Wu Q, Sathornsumetee S, Hao Y, Li Z, Hjelmeland AB, Shi Q, McLendon RE, Bigner DD, Rich JN**. Stem cell-like glioma cells promote

tumor angiogenesis through vascular endothelial growth factor. Cancer Res 2006; 66:7843-7848.

- **Bao S, Wu Q, Li Z, Sathornsumetee S, Wang H, McLendon RE, Hjelmeland AB, Rich JN.** Targeting cancer stem cells through L1CAM suppresses glioma growth. Cancer Res. 2008; 68(15):6043-8.

- **Barth RF, Kaur B.** Rat brain tumor models in experimental neuro-oncology: the C6, 9L, T9, RG2, F98, BT4C, RT-2 and CNS-1 gliomas. J Neurooncol. 2009; 94(3):299-312.

- **Bergers G, Benjamin LE.** Tumorigenesis and the angiogenic switch. Nat Rev Cancer.2003; 3(6):401-10.

- **Bexell D, Gunnarsson S, Siesjö P, Bengzon J, Darabi A.** CD133+ and nestin+ tumor-initiating cells dominate in N29 and N32 experimental gliomas. Int J Cancer. 2009; 125(1):15-22.

- **Bez A, Corsini E, Curti D, Biggiogera M, Colombo A, Nicosia RF, Pagano SF, Parati EA.** Neurosphere and neurosphere-forming cells: morphological and ultrastructural characterization. Brain Res. 2003; 993(1-2):18-29.

- **Birbrair A, Zhang T, Wang ZM, Messi ML, Olson JD, Mintz A, Delbono O. Type-2 Pericytes Participate in Normal and Tumoral Angiogenesis. Am J Physiol Cell Physiol. 2014 .**

- **Blümcke I, Becker AJ, Normann S, Hans V, Riederer BM, Krajewski S, Wiestler OD, Reifenberger G.** Distinct expression pattern of microtubule-associated protein-2 in human oligodendrogliomas and glial precursor cells. J Neuropathol Exp Neurol. 2001 ;60(10):984-93.

- **Bonnet D, Dick JE**. Human acute myeloid leukemia is organized as a hierarchy that originates from a primitive hematopoietic cell. Nat Med.1997 Jul;3(7):730-7.

- **Borovski T, Verhoeff JJ, ten Cate R, Cameron K, de Vries NA, van Tellingen O, Richel DJ, van Furth WR, Medema JP, Sprick MR.** Tumor microvasculature supports proliferation and expansion of glioma-propagating cells. Int J Cancer. 2009; 125(5):1222-30.

- **Bosch DA**. Short and long term effects of methyl- and ethylnitrosourea (MNU & ENU) on the developing nervous system of the rat. I. Long term effects: the induction of (multiple) gliomas. Acta Neurol Scand. 197; 55(2):85-105.

- **Brat DJ, Van Meir EG.** Glomeruloid microvascular proliferation orchestrated by VPF/VEGF: a new world of angiogenesis research. Am J Pathol. 200; 158(3):789-96.

- **Brazel CY, Limke TL, Osborne JK, Miura T, Cai J, Pevny L, Rao MS.** Sox2 expression defines a heterogeneous population of neurosphere-forming cells in the adult murine brain. Aging Cell. 2005 ;4(4):197-207.

- **Briançon-Marjollet A, Balenci L, Fernandez M, Estève F, Honnorat J, Farion R, Beaumont M, Barbier E, Rémy C, Baudier J**. NG2-expressing glial precursor cells are a new potential oligodendroglioma cell initiating population in N-ethyl-N-nitrosourea-induced gliomagenesis. Carcinogenesis. 2010 ;31(10):1718-25.

- **Brooks MD, Sengupta R, Snyder SC, Rubin JB**. Hitting Them Where They Live: Targeting the Glioblastoma Perivascular Stem Cell Niche. Curr Pathobiol Rep. 2013 ;1(2):101-110.

- **Bulnes-Sesma S, Ullibarri-Ortiz de Zarate N, Lafuente-Sanchez JV.** Tumour induction by ethylnitrosourea in the central nervous system. Rev Neurol. 2006; 43: 733-738.

- **Bulnes S, Lafuente JV**. VEGF immunopositivity related to malignancy degree, proliferative activity and angiogenesis in ENU-induced gliomas. J Mol Neurosci 2007; 33:163-172.

- **Bulnes S, Bilbao J, Lafuente JV.** Microvascular adaptive changes in experimental endogenous brain gliomas. Histol Histopathol 2009; 24:693-706.

- **Bulnes S, García-Blanco Á, Bengoetxea H, Ortuzar N, Argandoña EG, Lafuente JV.** Glial stem cells and their relationship with tumour angiogenesis process. Rev Neurol. 2011; 52(12):743-50.

- **Calabrese C, Poppleton H, Kocak M Hogg TL, Fuller C, Hamner B, Oh EY, Gaber MW, Finklestein D, Allen M, Frank A, Bayazitov IT, Zakharenko SS, Gajjar A,Davidoff A, Gilbertson RJ.** A perivascular niche for brain tumor stem cells. Cancer Cell 2007; 11:69-82.

- **Candolfi M, Curtin JF, Nichols WS, Muhammad AG, King GD, Pluhar GE, McNiel EA, Ohlfest JR, Freese AB, Moore PF, Lerner J, Lowenstein PR, Castro MG.** Intracranial glioblastoma models in preclinical neuro-oncology: neuropathological characterization and tumor progression. J Neurooncol. 2007; 85(2):133-48.

- **Capilla-Gonzalez V, Gil-Perotin S, Garcia-Verdugo JM.** Postnatal exposure to N-ethyl-N-nitrosurea disrupts the subventricular zone in adult rodents. Eur J Neurosci. 2010; 32(11):1789-99.

- **Capilla-Gonzalez V, Gil-Perotin S, Ferragud A, Bonet-Ponce L, Canales JJ, Garcia-Verdugo JM.** Exposure to N-ethyl-N-nitrosourea in adult mice alters structural and functional integrity of neurogenic sites. PLoS One. 2012;7(1):e29891

- **Charles N, Ozawa T, Squatrito M, Bleau AM, Brennan CW, Hambardzumyan D, Holland EC.** Perivascular nitric oxide activates notch signaling and promotes stem-like character in PDGF-induced glioma cells. Cell Stem Cell. 2010; 6(2):141-52.

- **Chen L, Zhang Y, Yang J, Hagan JP, Li M.** Vertebrate animal models of glioma: understanding the mechanisms and developing new therapies. Biochim Biophys Acta. 2013; 1836(1):158-65.

- **Cheng L, Huang Z, Zhou W, Wu Q, Donnola S, Liu JK, Fang X, Sloan AE, Mao Y, Lathia JD, Min W, McLendon RE, Rich JN, Bao S.** Glioblastoma stem cells generate vascular pericytes to support vessel function and tumor growth. Cell. 2013 ;153(1):139-52.

- **Chesler EJ, Wilson SG, Lariviere WR, Rodriguez-Zas SL, Mogil JS.** Influences of laboratory environment on behavior. Nat Neurosci. 2002; 5(11):1101-2.

- **Christensen K, Schroder HD, Kristensen BW.** CD133 identifies perivascular niches in grade II-IV astrocytomas. J Neurooncol 2008; 90:157-170.

- **Clemens LE, Jansson EK, Portal E, Riess O, Nguyen HP.** A behavioral comparison of the common laboratory rat strains Lister Hooded, Lewis, Fischer 344 and Wistar in an automated homecage system. Genes Brain Behav. 2014; 13(3):305-21.

- **Dahlstrand J, Collins VP, Lendahl U.** Expression of the class VI intermediate filament nestin in human central nervous system tumors. Cancer Res. 1992; 52(19):5334-41.

- **Das S, Srikanth M, Kessler JA**. Cancer stem cells and glioma. Nat Clin Pract Neurol. 2008; 4(8):427-35.

- **Denenberg VH.** Open-field behavior in the rat: what does it mean? Ann N Y Acad Sci. 1969;159(3):852-9.

- **Denysenko T, Gennero L, Roos MA, Melcarne A, Juenemann C, Faccani G, Morra I, Cavallo G, Reguzzi S, Pescarmona G, Ponzetto A.** Glioblastoma cancer stem cells: heterogeneity, microenvironment and related therapeutic strategies. Cell Biochem Funct. 2010; 28(5):343-51.

- **Doetsch F, García-Verdugo JM, Alvarez-Buylla A.** Regeneration of a germinal layer in the adult mammalian brain. Proc Natl Acad Sci U S A. 1999; 96(20):11619-24.

- **Donnenberg VS, Donnenberg AD.** Multiple drug resistance in cancer revisited: the cancer stem cell hypothesis. J Clin Pharmacol. 2005; 45(8):872-7.

- **Druckrey H, Ivanković S, Preussmann R**. Teratogenic and carcinogenic effects in the offspring after single injection of ethylnitrosourea to pregnant rats. Nature. 1966 25; 210(5043):1378-9

- **Ehrmann J, Kolár Z, Mokry J.** Nestin as a diagnostic and prognostic marker: immunohistochemical analysis of its expression in different tumours. J Clin Pathol. 2005; 58(2):222-3.

- **Eriksson PS, Perfilieva E, Björk-Eriksson T, Alborn AM, Nordborg C, Peterson DA, Gage FH.** Neurogenesis in the adult human hippocampus. Nat Med. 1998 Nov;4(11):1313-7.

- **Fan, Xiaolong, Leif G Salford, Bengt Widegren.** Glioma Stem Cells: Evidence and Limitation. Seminars in Cancer Biology. 2007; 17: 214–218.

- **Fidler IJ, Kripke ML.** Metastasis results from preexisting variant cells within a malignant tumor. Science. 1977; 197(4306):893-5.

- **Filatova A, Acker T, Garvalov BK.** The cancer stem cell niche(s): the crosstalk between glioma stem cells and their microenvironment. Biochim Biophys Acta. 2013;1830(2):2496-508.

- **Finkelstein SD, Black P, Nowak TP, Hand CM, Christensen S, Finch PW**. Histological characteristics and expression of acidic and basic fibroblast growth factor genes in intracerebral xenogeneic transplants of human glioma cells. Neurosurgery. 1994; 34(1):136-43.

- **Folkins C, Shaked Y, Man S, Tang T, Lee CR, Zhu Z, Hoffman RM, Kerbel RS.** Glioma tumor stem-like cells promote tumor angiogenesis and vasculogenesis via vascular endothelial growth factor and stromal-derived factor 1. Cancer Res. 2009; 69(18):7243-51.

- **Fomchenko EI, Holland EC.** Mouse models of brain tumors and their applications in preclinical trials. Clin Cancer Res. 2006; 12(18):5288-97.

- **Frank NY, Schatton T, Frank MH.** The therapeutic promise of the cancer stem cell concept. J Clin Invest. 2010; 120(1):41-50.

- **Galli R, Binda E, Orfanelli U, Cipelletti B, Gritti A, De Vitis S, Fiocco R, Foroni C, Dimeco F, Vescovi A.** Isolation and characterization of tumorigenic, stem-like neural precursors from human glioblastoma. Cancer Res. 2004; 64(19):7011-21.

- **Gangemi RM, Griffero F, Marubbi D, Perera M, Capra MC, Malatesta P, Ravetti GL, Zona GL, Daga A, Corte G.** SOX2 silencing in glioblastoma tumor-initiating cells causes stop of proliferation and loss of tumorigenicity. Stem Cells. 2009; 27(1):40-8

- **Garcia-Barros M, Paris F, Cordon-Cardo C, Lyden D, Rafii S, Haimovitz-Friedman A, Fuks Z, Kolesnick R**. Tumor response to radiotherapy regulated by endothelial cell apoptosis. Science. 2003; 300(5622):1155-9.

- **Germano IV, Swiss V, Casaccia P.** Primary Brain Tumors, Neural Stem Cell, and Brain Tumor Cancer Cells: Where Is the Link? Neuropharmacology. 2010. 58.

- **Gil-Perotin S, Marin-Husstege M, Li J, Soriano-Navarro M, Zindy F, Roussel MF, Garcia-Verdugo JM, Casaccia-Bonnefil P.** Loss of p53 induces changes in the behavior of subventricular zone cells: implication for the genesis of glial tumors. J Neurosci. 2006;26(4):1107-16.

- **Gil-Ranedo J, Mendiburu-Eliçabe M, García-Villanueva M, Medina D**, **del Álamo M, Izquierdo M.** An off-target nucleostemin RNAi inhibits growth in human glioblastoma-derived cancer stem cells. PLoS One. 2011;6(12):e28753.

- **Girolamo F, Dallatomasina A, Rizzi M, Errede M, Wälchli T, Mucignat MT, Frei K, Roncali L, Perris R, Virgintino D.** Diversified expression of

NG2/CSPG4 isoforms in glioblastoma and human foetal brain identifies pericyte subsets. PLoS One. 2013 ;8(12):e84883.

- **Gómez-Gaviro MV, Lovell-Badge R, Fernández-Avilés F, Lara-Pezzi E.** The vascular stem cell niche. J Cardiovasc Transl Res. 2012;5(5):618-30.

- **Gondo Y, Fukumura R.** ENU-induced mutant mice for a next-generation gene-targeting system. Prog Brain Res. 2009;179:29-34.

- **Gondo Y, Fukumura R, Murata T, Makino S.** ENU-based gene-driven mutagenesis in the mouse: a next-generation gene-targeting system. Exp Anim. 2010;59(5):537-48.

- **Greenfield, Jeffrey P, William S Cobb, David Lyden.** Resisting Arrest: a Switch from Angiogenesis to Vasculogenesis in Recurrent Malignant Gliomas. Cancer. 2010; 120 (3).

- **Griguer CE, Oliva CR, Gobin E, Marcorelles P, Benos DJ, Lancaster JR Jr, Gillespie GY.** CD133 is a marker of bioenergetic stress in human glioma. PLoS One. 2008;3(11):e3655.

- **Gustafsson MV, Zheng X, Pereira T, Gradin K, Jin S, Lundkvist J, Ruas JL, Poellinger L, Lendahl U, Bondesson M.** Hypoxia requires notch signaling to maintain the undifferentiated cell state. Dev Cell. 2005; 9(5):617-28.

- **Hadjipanayis, Costas G, and Erwin G Van Meir.** Tumor Initiating Cells in Malignant Gliomas: Biology and Implications for Therapy. Journal of Molecular Medicine. 2009; 363–374.

- **Hadjipanayis CG, Van Meir EG.** Brain cancer propagating cells: biology, genetics and targeted therapies. Trends in Molecular Medicine 2009; 15:519-530.

- **Hardee ME, Zagzag D**. Mechanisms of glioma-associated neovascularization. Am J Pathol. 2012 Oct;181(4):1126-41.

- **Hawkins P.** Progress in assessing animal welfare in relation to new legislation: opportunities for behavioural researchers. J Neurosci Methods. 2014; 34:135-8.

- **He H, Niu CS, Li MW.** Correlation between glioblastoma stem-like cells and tumor vascularization. Oncol Rep. 2012; 27(1):45-50.

- **Heddleston JM, John M, Zhizhong Li, Roger E Mclendon, Anita B Hjelmeland,Jeremy N Rich.** The Hypoxic Microenvironment Maintains Glioblastoma Stem Cells and Promotes Reprogramming Towards a Cancer Stem Cell Phenotype. Cell Cycle 2009; 8 (20): 3274–3284.

- **Heddleston JM, Li Z, Lathia JD, Bao S, Hjelmeland AB, Rich JN.** Hypoxia inducible factors in cancer stem cells. Br J Cancer. 2010**;** 102(5):789-95.

- **Holmberg Olausson K, Maire CL, Haidar S, Ling J, Learner E, Nistér M, Ligon KL.** Prominin-1 (CD133) Defines Both Stem and Non-Stem Cell Populations in CNS Development and Gliomas. PLoS One. 2014 ;9(9):e106694.

- **Holland EC**. Progenitor cells and glioma formation. Curr Opin Neurol. 2001; 14(6):683-8.

- **Holmin S, Almqvist P, Lendahl U, Mathiesen T.** Adult nestin-expressing subependymal cells differentiate to astrocytes in response to brain injury. Eur J Neurosci. 1997; 9(1):65-75.

- **Hu YY, Zheng MH, Cheng G, Li L, Liang L, Gao F, Wei YN, Fu LA, Han H.** Notch signaling contributes to the maintenance of both normal neural stem cells and patient-derived glioma stem cells. BMC Cancer. 2011; 11:82.

- **Huang G, Ashton C, Kumbhani DS, Ying QL**. Genetic manipulations in the rat: progress and prospects. Curr Opin Nephrol Hypertens. 2011; 20(4):391-9.

- **Janbazian L, Karamchandani J, Das S.** Mouse models of glioblastoma: lessons learned and questions to be answered. J Neurooncol. 2014 ;118(1):1-8.

- **Jang MS, Zlobin A, Kast WM, Miele L.** Notch signaling as a target in multimodality cancer therapy. Curr Opin Mol Ther. 2000; 2(1):55-65.

- **Jang T, Litofsky NS, Smith TW, Ross AH, Recht LD.** Aberrant nestin expression during ethylnitrosourea-(ENU)-induced neurocarcinogenesis. Neurobiol Dis. 2004; 15(3):544-52.

- **Jang T, Savarese T, Low HP, Kim S, Vogel H, Lapointe D, Duong T, Litofsky NS, Weimann JM, Ross AH, Recht L.** Osteopontin expression in intratumoral astrocytes marks tumor progression in gliomas induced by prenatal exposure to N-ethyl-N-nitrosourea. Am J Pathol 2006; 168: 1676-1685.

- **Jansen AS, Nguyen XV, Karpitskiy V, Mettenleiter TC, Loewy AD.** Central command neurons of the sympathetic nervous system: basis of the fight-or-flight response. Science. 1995; 270(5236):644-6.

- **Jensen RL, Ragel BT, Whang K, Gillespie D.** Inhibition of hypoxia inducible factor-1alpha (HIF-1alpha) decreases vascular endothelial growth factor (VEGF) secretion and tumor growth in malignant gliomas. J Neurooncol. 2006; 78(3):233-47.

- **Jensen JB, Parmar M.** Strengths and limitations of the neurosphere culture system. Mol Neurobiol. 2006; 34: 153-161

- **Jensen, Randy L.** 2009. Brain Tumor Hypoxia: Tumorigenesis, Angiogenesis, Imaging, Pseudoprogression, and as a Therapeutic Target. Chemotherapy: 317–335.

- **Jovčevska I, Kočevar N, Komel R.** Glioma and glioblastoma - how much do we (not) know? Mol Clin Oncol. 2013 ;1(6):935-941.

- **Kalluri HS, Dempsey RJ.** Osteopontin increases the proliferation of neural progenitor cells. Int J Dev Neurosci. 2012 ; 30(5):359-62.
- **Kang SH, Fukaya M, Yang JK, Rothstein JD, Bergles DE.** NG2+ CNS glial progenitors remain committed to the oligodendrocyte lineage in postnatal life and following neurodegeneration. Neuron.;68(4):668-81.
- **Katayama K, Ueno M, Yamauchi H, Nakayama H, Doi K.** Microarray analysis of genes in fetal central nervous system after ethylnitrosourea administration. Birth Defects Res B Dev Reprod Toxicol. 2005; 74(3):255-60.
- **Kennedy CL, O'Bryan MK.** N-ethyl-N-nitrosourea (ENU) mutagenesis and male fertility research. Hum Reprod Update. 2006; 12(3):293-301.
- **King GD, Curtin JF, Candolfi M, Kroeger K, Lowenstein PR, Castro MG.** Gene therapy and targeted toxins for glioma. Curr Gene Ther. 2005; 5(6):535-57.
- **Kleihues P, Louis DN, Scheithauer BW, Rorke LB, Reifenberger G, Burger PC, Cavenee WK.** The WHO classification of tumors of the nervous system. J Neuropathol Exp Neurol. 2002; 61(3):215-25; discussion 226-9.
- **Kolenda J, Jensen SS, Aaberg-Jessen C, Christensen K, Andersen C, Brünner N, Kristensen BW.** Effects of hypoxia on expression of a panel of stem cell and chemoresistance markers in glioblastoma-derived spheroids. J Neurooncol. 2011; 103(1):43-58.
- **Lantos PL, Louis DN, Rosenblum MK, Kleihues P.** Tumours of the Nervous System. Oxford University Press: London. 2002.
- **Li JL , Sainson RC, Shi W, Leek R, Harrington LS, Preusser M, Biswas S, Turley H, Heikamp E, Hainfellner JA, Harris AL**. Delta-like 4 Notch ligand regulates tumour angiogenesis, improves tumor vascular function, and promotes tumour growth in vivo. Cancer Res. 2007 ;67(23):11244-53.

- **Li JL, Harris AL.** Crosstalk of VEGF and Notch pathways in tumour angiogenesis: therapeutic implications. Front Biosci (Landmark Ed). 2009 1;14:3094-110.

- **Li Z, Bao S, Wu Q, Wang H, Eyler C, Sathornsumetee S, Shi Q, Cao Y, Lathia J, McLendon RE, Hjelmeland AB, Rich JN.** Hypoxia-inducible factors regulate tumorigenic capacity of glioma stem cells. Cancer Cell. 2009; 15(6):501-13.

- **Llaguno SA, Chen J, Kwon CH, Parada LF.** Neural and cancer stem cells in tumor suppressor mouse models of malignant astrocytoma. Cold Spring Harb Symp Quant Biol. 2008;73:421-6.

- **Lois C, Alvarez-Buylla A.** Long-distance neuronal migration in the adult mammalian brain. Science. 1994; 264(5162):1145-8.

- **Lu DY, Yeh WL, Huang SM, Tang CH, Lin HY, Chou SJ.** Osteopontin increases heme oxygenase-1 expression and subsequently induces cell migration and invasion in glioma cells. Neuro Oncol. 2012; 14(11):1367-78.

- **Mandillo S, Tucci V, Hölter SM, Meziane H, Banchaabouchi MA, Kallnik M, Lad HV, Nolan PM, Ouagazzal AM, Coghill EL, Gale K, Golini E, Jacquot S, Krezel W,Parker A, Riet F, Schneider I, Marazziti D, Auwerx J, Brown SD, Chambon P, Rosenthal N, Tocchini-Valentini G, Wurst W.** Reliability, robustness, and reproducibility in mouse behavioral phenotyping: a cross-laboratory study. Physiol Genomics. 2008; 34(3):243-55.

- **Martin P, Bateson P.** Measuring behaviour. An introductory guide. American Journal of Physical Anthropology. 1986; 74: 3.

- **Matsuda Y, Hagio M, Ishiwata T.** Nestin: a novel angiogenesis marker and possible target for tumor angiogenesis. World J Gastroenterol. 2013; 19(1):42-8.

- **Mennel HD, Kosse N, Heverhagen JT, Alfke H.** Primary and transplanted ENU induced rat tumors in neurooncology. Exp Toxicol Pathol. 2004; 56(1-2):25-35.

- **Michalczyk K, Ziman M.** Nestin structure and predicted function in cellular cytoskeletal organisation. Histol Histopathol. 2005; 20(2):665-71.

- **Mori H, Ninomiya K, Kino-oka M, Shofuda T, Islam MO, Yamasaki M, Okano H, Taya M, Kanemura Y.** Effect of neurosphere size on the growth rate of human neural stem/progenitor cells. J Neurosci Res. 2006; 84(8):1682-91.

- **Morton DB, Griffiths PH**. Guidelines on the recognition of pain, distress and discomfort in experimental animals and an hypothesis for assessment. Vet Rec. 1985; 116(16):431-6.

- **Nadig RR.** Stem cell therapy - Hype or hope? A review. J Conserv Dent. 2009; 12(4):131-8.

- **Najbauer J, Huszthy PC, Barish ME, Garcia E, Metz MZ, Myers SM, Gutova M, Frank RT, Miletic H, Kendall SE, Glackin CA, Bjerkvig R, Aboody KS.** Cellular host responses to gliomas. PLoS One. 2012;7(4):e35150.

- **Nogueira AB, Sogayar MC, Colquhoun A, Siqueira SA, Nogueira AB, Marchiori PE, Teixeira MJ.** Existence of a potential neurogenic system in the adult human brain. J Transl Med. 2014; 12:75.

- **O'Brien CA , Pollett A, Gallinger S, Dick JE.** A human colon cancer cell capable of initiating tumour growth in immunodeficient mice. Nature. 2007, 4;445(7123):106-10.

- **Ogden AT, Waziri AE, Lochhead RA, Fusco D, Lopez K, Ellis JA, Kang J, Assanah M, McKhann GM, Sisti MB, McCormick PC, Canoll P, Bruce JN.** Identification of A2B5+CD133- tumor-initiating cells in adult human gliomas. Neurosurgery. 2008; 62(2):505-14.

- **Ohgaki H, Dessen P, Jourde B, Horstmann S, Nishikawa T, Di Patre PL, Burkhard C, Schüler D, Probst-Hensch NM, Maiorka PC, Baeza N, Pisani P,Yonekawa Y, Yasargil MG, Lütolf UM, Kleihues P.** Genetic pathways to glioblastoma: a population-based study. Cancer Res. 2004 1;64(19):6892-9.

- **Ohgaki H, Kleihues P.** Epidemiology and etiology of gliomas. Acta Neuropathol. 2005. 109; 1, 93-108.

- **Ohgaki H, Kleihues P**. Genetic pathways to primary and secondary glioblastoma. Am J Pathol. 2007; 170(5):1445-53.

- **Omuro A, DeAngelis LM.** Glioblastoma and other malignant gliomas: a clinical review. JAMA. 2013 ;310(17):1842-50.

- **Ostrom QT, Bauchet L, Davis FG, Deltour I, Fisher JL, Langer CE, Pekmezci M, Schwartzbaum JA, Turner MC, Walsh KM, Wrensch MR, Barnholtz-Sloan JS.** The epidemiology of glioma in adults: a "state of the science" review. Neuro Oncol. 2014.

- **Ostrom QT, Gittleman H, Farah P, Ondracek A, Chen Y, Wolinsky Y, Stroup NE, Kruchko C, Barnholtz-Sloan JS.** CBTRUS statistical report: Primary brain and central nervous system tumors diagnosed in the United States in 2006-2010. Neuro Oncol. 2013; 15 Suppl 2:ii1-56.

- **Pastrana E, Silva-Vargas V, Doetsch F.** Eyes wide open: a critical review of sphere-formation as an assay for stem cells. Cell Stem Cell 2011; 8:486-498.

- **Pavon LF, Marti LC, Sibov TT, Malheiros SM, Brandt RA, Cavalheiro S, Gamarra LF**. In vitro Analysis of Neurospheres Derived from Glioblastoma Primary Culture: A Novel Methodology Paradigm. Front Neurol. 2014; 4:214.

- **Pistollato F, Abbadi S, Rampazzo E, Persano L, Della Puppa A, Frasson C, Sarto E, Scienza R, D'avella D, Basso G.** Intratumoral hypoxic

gradient drives stem cells distribution and MGMT expression in glioblastoma. Stem Cells. 2010; 28(5):851-62.

- **Purow BW, Haque RM, Noel MW, Su Q, Burdick MJ, Lee J, Sundaresan T**, **Pastorino S, Park JK, Mikolaenko I, Maric D, Eberhart CG, Fine HA.** Expression of Notch-1 and its ligands, Delta-like-1 and Jagged-1, is critical for glioma cell survival and proliferation. Cancer Res.2005 15;65(6):2353-63.

- **Rafat N, Beck GCh, Schulte J, Tuettenberg J, Vajkoczy P.** Circulating endothelial progenitor cells in malignant gliomas. J Neurosurg. 2010 ;112(1):43-9

- **Reya T, Morrison SJ, Clarke MF, Weissman IL.** Stem cells, cancer, and cancer stem cells. Nature. 2001; 414(6859):105-11.

- **Reynolds BA, Weiss S.** Generation of neurons and astrocytes from isolated cells of the adult mammalian central nervous system. Science. 1992; 255(5052):1707-10.

- **Rich, Jeremy N. 2007.** Cancer Stem Cells in Radiation Resistance. Cancer Research (19): 8980–8984.

- **Sadahiro H, Yoshikawa K, Ideguchi M, Kajiwara K, Ishii A, Ikeda E, Owada Y, Yasumoto Y, Suzuki M**. Pathological features of highly invasive glioma stem cells in a mouse xenograft model. Brain Tumor Pathol. 2013; 31:77-84.

- **Saibaba P, Sales GD, Stodulski G, Hau J.** Behaviour of rats in their home cages: daytime variations and effects of routine husbandry procedures analysed by time sampling techniques. Lab Anim. 1996; 30(1):13-21.

- **Schiffer D, Annovazzi L, Caldera V, Mellai M.** On the origin and growth of gliomas. Anticancer Res. 2010; 30(6):1977-98.

- **Schiffer D, Mellai M, Annovazzi L, Caldera V, Piazzi A, Denysenko T, Melcarne A**. Stem cell niches in glioblastoma: a neuropathological view. Biomed Res Int.;2014:725921.

- **Schittenhelm J, Simon P, Harter PN, Zachskorn C, Schlaszus H, Röttger F, Winkels M, Weller M, Meyermann R, Mittelbronn M.** CD133 expression is associated with small round blue cell tumour morphology in human central nervous system neoplasms. Histopathology. 2011; 58(5):739-49.

- **Scully S, Francescone R, Faibish M, Bentley B, Taylor SL, Oh D, Schapiro R, Moral L, Yan W, Shao R.** Transdifferentiation of glioblastoma stem-like cells into mural cells drives vasculogenic mimicry in glioblastomas. J Neurosci. 2012; 32(37):12950-60.

- **Seidel S, Garvalov BK, Wirta V, von Stechow L, Schänzer A, Meletis K, Wolter M, Sommerlad D, Henze AT, Nistér M, Reifenberger G, Lundeberg J, Frisén J,Acker T.** A hypoxic niche regulates glioblastoma stem cells through hypoxia inducible factor 2 alpha. Brain. 2010; 133(Pt 4):983-95.

- **Selkirk SM, Morrow J, Barone TA, Hoffer A, Lock J, DeChant A, Mangla S, Plunkett RJ, Miller RH.** Elevation of osteopontin levels in brain tumor cells reduces burden and promotes survival through the inhibition of cell dispersal. J Neurooncol. 2008; 86(3):285-96.

- **Selye H.** The general adaptation syndrome and the diseases of adaptation. J Allergy. 1946; 17(6):231; 289; 358.

- **Shen G, Shen F, Shi Z, Liu W, Hu W, Zheng X, Wen L, Yang X.** Identification of cancer stem-like cells in the C6 glioma cell line and the limitation of current identification methods. In Vitro Cell Dev Biol Anim. 2008; 44(7):280-9.

- **Shih AH, Holland EC.** Developmental neurobiology and the origin of brain tumors. J Neurooncol. 2004, 70(2):125-36.

- **Shin JH, Lee YS, Hong YK, Kang CS.** Correlation between the prognostic value and the expression of the stem cell marker CD133 and isocitrate dehydrogenase1 in glioblastomas. J Neurooncol. 2013; 115(3):333-41.

- **Shiras A, Bhosale A, Shepal V, Shukla R, Baburao VS, Prabhakara K, Shastry P**. A unique model system for tumor progression in GBM comprising two developed human neuro-epithelial cell lines with differential transforming potential and coexpressing neuronal and glial markers. Neoplasia. 2003; 5(6):520-32.

- **Schmidt-Kastner R, Humpel C.** Nestin expression persists in astrocytes of organotypic slice cultures from rat cortex. Int J Dev Neurosci. 2002; 20(1):29-38.

- **Singh SK, Clarke ID, Terasaki M, Bonn VE, Hawkins C, Squire J, Dirks PB.** Identification of a cancer stem cell in human brain tumors. Cancer Res. 2003; 63(18):5821-8.

- **Slikker W, Mei N, Chen T.** N-ethyl-N-nitrosourea (ENU) increased brain mutations in prenatal and neonatal mice but not in the adults. Toxicol Sci. 2004; 81(1):112-20.

- **Soda Y, Marumoto T, Friedmann-Morvinski D, Soda M, Liu F, Michiue H, Pastorino S, Yang M, Hoffman RM, Kesari S, Verma IM.** Transdifferentiation of glioblastoma cells into vascular endothelial cells. Proc Natl Acad Sci U S A. 2011; 108(11):4274-80.

- **Starkweather AR, Sherwood P, Lyon DE, McCain NL, Bovbjerg DH, Broaddus WC.** A biobehavioral perspective on depressive symptoms in patients with cerebral astrocytoma. J Neurosci Nurs. 2011; 43(1):17-28.

- **Stojanovich L.** Stress and autoimmunity. Autoimmun Rev. 2010; 9(5):A271-6.

- **Suslov ON, Kukekov VG, Ignatova TN, Steindler DA.** Neural stem cell heterogeneity demonstrated by molecular phenotyping of clonal neurospheres. Proc Natl Acad Sci U S A. 2002;99(22):14506-11.

- **Takebe N, Ivy SP.** Controversies in cancer stem cells: targeting embryonic signaling pathways. Clin Cancer Res. 2010; 16(12):3106-12.

- **Tamaki S, Eckert K, He D, Sutton R, Doshe M, Jain G, Tushinski R, Reitsma M, Harris B, Tsukamoto A, Gage F, Weissman I, Uchida N.** Engraftment of sorted/expanded human central nervous system stem cells from fetal brain. J Neurosci Res. 2002 Sep 15;69(6):976-86.

- **Taylor MD, Poppleton H, Fuller C, Su X, Liu Y, Jensen P, Magdaleno S, Dalton J, Calabrese C, Board J, Macdonald T, Rutka J, Guha A, Gajjar A, Curran T, Gilbertson RJ.** Radial glia cells are candidate stem cells of ependymoma. Cancer Cell. 2005;8: 323-335.

- **Vik-Mo EO, Sandberg C, Joel M, Stangeland B, Watanabe Y, Mackay-Sim A, Moe MC, Murrell W, Langmoen IA.** A comparative study of the structural organization of spheres derived from the adult human subventricular zone and glioblastoma biopsies. Exp Cell Res. 2011 ;317(7):1049-59.

- **Vincent K.Y. Ho, Jaap C. Reijneveld, Roelien H. Enting, Henri P. Bienfait, Pierre Robe, Brigitta G. Baumert, Otto Visser.** Changing incidence and improved survival of gliomas. European Journal of Cancer, Available online 24 June 2014.

- **Wang J, Sakariassen PØ, Tsinkalovsky O, Immervoll H, Bøe SO, Svendsen A, Prestegarden L, Røsland G, Thorsen F, Stuhr L, Molven A, Bjerkvig R, Enger PØ**. CD133 negative glioma cells form tumors in nude rats and give rise to CD133 positive cells. Int J Cancer. 2008; 122(4):761-8.

- **Wang R, Chadalavada K, Wilshire J, Kowalik U, Hovinga KE, Geber A, Fligelman B, Leversha M, Brennan C, Tabar V.** Glioblastoma stem-like cells give rise to tumour endothelium. Nature. 2010; 468(7325):829-33.

- **Wang J, Wakeman TP, Lathia JD, Hjelmeland AB, Wang XF, White RR, Rich JN, Sullenger BA.** Notch promotes radioresistance of glioma stem cells. Stem Cells. 2010; 28(1):17-28.

- **Wang Y, Yan W, Lu X, Qian C, Zhang J, Li P, Shi L, Zhao P, Fu Z, Pu P, Kang C, Jiang T, Liu N, You Y.** Overexpression of osteopontin induces angiogenesis of endothelial progenitor cells via the avβ3/PI3K/AKT/eNOS/NO signaling pathway in glioma cells. Eur J Cell Biol. 2011; 90(8):642-8.

- **Wharton SB, Chan KK, Whittle IR.** Microtubule-associated protein 2 (MAP-2) is expressed in low and high grade diffuse astrocytomas. J Clin Neurosci. 2002; 9(2):165-9.

- **Whitman MC, Greer CA.** Adult neurogenesis and the olfactory system. Prog Neurobiol. 2009; 89(2):162-75.

- **Xiao-Qin HA, Man Zhao, Xiao-Yun Li, Jun-Hua Peng, Ju-Zi Dong, Zhi-Yun Deng, Hong-Bin Zhao, Yong Zhao, Yuan-Yuan Zhang.** Distribution of endothelial progenitor cells in tissues from patients with gastric cancer. Oncol Lett. 2014; 7(5): 1695–1700.

- **Yan YP, Lang BT, Vemuganti R, Dempsey RJ**. Osteopontin is a mediator of the lateral migration of neuroblasts from the subventricular zone after focal cerebral ischemia. Neurochem Int. 2009;55(8):826-32.

- **Yang ZJ, Wechsler-Reya RJ.** Hit 'em where they live: targeting the cancer stem cell niche. Cancer Cell. 2007; 11(1):3-5.

- **Yasenkov R, Deboer T.** Chapter 12-Circadian modulation of sleep in rodents, in: Progress in Brain Research, Elsevier, 2012, Volume 199, Pages 203-218, ISSN 0079-6123, ISBN 9780444594273.

- **Yu SP, Yang XJ, Zhang B, Ming HL, Chen C, Ren BC, Liu ZF, Liu B.** Enhanced invasion in vitro and the distribution patterns in vivo of CD133+ glioma stem cells. Chin Med J (Engl). 2011; 124(17):2599-604.

- **Zeppernick F, Ahmadi R, Campos B, Dictus C, Helmke BM, Becker N, Lichter P, Unterberg A, Radlwimmer B, Herold-Mende CC.** Stem cell marker CD133 affects clinical outcome in glioma patients. Clin Cancer Res. 2008; 14(1):123-9.

- **Zhang M, Song T, Yang L, Chen R, Wu L, Yang Z, Fang J.** Nestin and CD133: valuable stem cell-specific markers for determining clinical outcome of glioma patients. J Exp Clin Cancer Res. 2008; 27:85.

- **Zhang XP, Zheng G, Zou L, Liu HL, Hou LH, Zhou P, Yin DD, Zheng QJ, Liang L, Zhang SZ, Feng L, Yao LB, Yang AG, Han H, Chen JY.** Notch activation promotes cell proliferation and the formation of neural stem cell-like colonies in human glioma cells. Mol Cell Biochem. 2008; 307(1-2):101-8.

- **Zhao Y, Dong J, Huang Q, Lou M, Wang A, Lan Q.** Endothelial cell transdifferentiation of human glioma stem progenitor cells in vitro. Brain Res Bull. 2010; 82(5-6):308-12.

- **Zook BC, Simmens SJ, Jones RV.** Evaluation of ENU-induced gliomas in rats: nomenclature, immunochemistry, and malignancy. Toxicol Pathol. 2000; 28(1):193-201.

- **Zook BC, Simmens SJ.** Neurogenic tumors in rats induced by ethylnitrosourea. Exp Toxicol Pathol. 2005; 57(1):7-14.